UNIVERSITÀ DI SIENA

Department of Biotechnology, Chemistry and Pharmacy

DOCTORAL THESIS IN BIOCHEMISTRY AND MOLECULAR BIOLOGY

XXXIII CYCLE

Coordinator: Prof. Lorenza Trabalzini

Vascular Endothelial Growth Factors and Endothelial Cells Behaviour

SSD: BIO/14

PhD candidate:

Emma Ristori

Supervisor:

Prof. Sandra Donnini

Academic year 2019/2020

TABLE OF CONTENTS

Abstract

The vascular endothelium is an important tissue often underestimated for its role in health and disease. Endothelial cells dysfunction is at the base of many if not all diseases. The inaccessibility of this tissue made difficult its assessment for many years.

Vascular dysfunction can occur at different levels of vascular development and maintenance: during initial vasculogenesis, angiogenesis and late vascular remodelling. Vasculogenesis denotes the early developmental process of artery-veins specification. Angiogenesis refers to the formation of new blood vessels from pre-existing quiescent vessels. The angiogenic process is initiated by pro-angiogenic factors that induce endothelial cell sprouting, migration and vascular anastomosis. Newly formed vascular networks undergo extensive vascular remodelling, that includes distinct processes of vascular pruning and regression of selected vascular branches, to form a functional and mature quiescent vasculature.

Vascular endothelial growth factors (VEGFs) are critical players in artery specification during development, in angiogenesis and in vascular maintenance. VEGFs bind to transmembrane VEGFRs receptors to initiate the intracellular response. The VEGF-VEGFR signalling pathway activation and regulation are very complex. In fact, the binding of the ligand VEGF to the VEGFRs receptor is not the only event involved in the activation and regulation of the signalling cascade. Co-receptors, kinases, phosphatases, and other proteins involved in the intracellular trafficking of the VEGF-VEGFR complex modulate the signal specificity, amplitude and duration.

Angiogenesis and vessels stability are tightly regulated physiological processes. Indeed, excessive angiogenesis and increased permeability lead to vascular dysfunction and the progression of several diseases. In the recent years, neurodegenerative diseases such as Alzheimer's disease have been strongly associated to vascular dysfunction (Review I) and to VEGF/VEGFR2 aberrant signalling. Recent studies suggest an important role of the AD-related β-amyloid precursor protein (APP) in maintaining cellular homeostasis in the brain, however the role of this protein in endothelial cells and its interactions with the VEGF signalling is still unknown (Review II).

In this thesis work, I have examined the role of APP in regulating VEGF/VEGFR2 signalling and endothelial cells stability (Paper I).

Furthermore, I have investigated the *in vivo* role of VEGF mediated signalling in artery specification during zebrafish vascular development (Paper II).

In conclusion, VEGF mediated signalling is regulated by a multifactor system and each individual regulatory mechanism leads to a specific outcome in angiogenesis and vessel stability.

Riassunto

L'endotelio vascolare è un importante tessuto il cui ruolo sia in fisiologia, che in patologia è stato a lungo sottovalutato. Per molti anni, l'inaccessibilità di questo tessuto ha reso difficoltoso valutarne il ruolo fisio-patologico.

La disfunzione delle cellule endoteliali è alla base di molti se non tutti gli stati patologici e può manifestarsi a diversi livelli dello sviluppo vascolare: durante la vasculogenesi, durante il processo di angiogenesi oppure durante il rimodellamento vascolare. Il processo di vasculogenesi consiste nella specializzazione di precursori vascolari in arterie e vene. Il termine angiogenesi si riferisce invece alla formazione di nuovi vasi sanguigni a partire da vasi preesistenti. Il processo è attivato da fattori pro-angiogenici che promuovono la migrazione e proliferazione delle cellule endoteliali e l'anastomosi dei vasi neoformati. In seguito, i nuovi vasi subiranno rimodellamenti secondari, come la regressione di particolari capillari, per formare un network vascolare maturo e funzionale.

I fattori di crescita endoteliali vascolari (VEGFs) svolgono un ruolo cruciale, sia durante il processo di vasculogenesi e angiogenesi, che nel mantenimento della funzionalità vascolare. La trasduzione del segnale attivata dai VEGFs è complessa. La risposta intracellulare è attivata dal legame dei VEGFs con specifici recettori di membrana (VEGFRs). L'intensità e la durata del segnale sono invece modulate dal legame dei VEGFs con co-recettori e dall'interazione del complesso VEGF/recettore con chinasi, fosfatasi e altre proteine coinvolte nel trasporto del complesso all'interno della cellula.

L'angiogenesi e l'integrità dei vasi sono processi fisiologici strettamente controllati. Infatti, un'angiogenesi non controllata e la perdita d'integrità di membrana con l'aumento di permeabilità portano a disfunzione vascolare e conseguenze patologiche.

Negli ultimi anni, la disfunzione vascolare e l'alterazione del signalling del VEGF nel tessuto vascolare sono state associate all'insorgenza di numerose malattie neurodegenerative, incluso l'Alzheimer (Review I).

Recenti studi suggeriscono un importante ruolo della β-amyloid precursor protein (APP), proteina chiave nello sviluppo della malattia di Alzheimer, nel mantenimento dell'omeostasi cellulare nel cervello, tuttavia la funzione di questa proteina a livello vascolare e la sua interazione con il signalling del VEGF sono tuttora ignote (Review II).

In questo lavoro di tesi ho esaminato il ruolo di APP nella regolazione e modulazione del signalling VEGFA/VEGFR2 e nel mantenimento della funzionalità vascolare (Paper I).

Ho inoltre studiato il ruolo del signalling di VEGF nel differenziamento di arterie e vene durante lo sviluppo vascolare embrionale utilizzando il modello *in vivo* di zebrafish (Paper II).

Il mio lavoro di ricerca ha contribuito ad ampliare la conoscenza sulla complessa modulazione del signalling di VEGF nel tessuto vascolare, sia durante lo sviluppo embrionale, che durante l'omeostasi vascolare.

PREFACE

During my Ph.D. (XXXIII cycle) I deeply investigated different aspects of vascular biology.

I spent part of the first year of my PhD at the Yale University (USA) in the laboratory of Stefania Nicoli. Under her supervision I became familiar with the zebrafish model and with the study of vascular development. During this period I deepened my knowledge in microscopy imaging techniques and I learned how to experimentally approach developmental biology questions using an *in vivo* model.

In the second part of my PhD I focused on the study of the β-Amyloid Precursor Protein in the endothelial cells under the supervision of Prof. Marina Ziche and Prof. Sandra Donnini. Still focusing on the vascular tissue, I became familiar with several *in vitro* cell biology techniques.

I spent the last part of my PhD back to Yale University (USA), this time in the laboratory of Prof. Michael Simons, where I deepened my knowledge in angiogenic growth factors signalling and trafficking.

This thesis focuses on one of the most important regulators of endothelial cells behaviour, the vascular endothelial growth factors (VEGFs).

VEGFs have a central role in all aspects of vascular biology and therefore represent the link between all my projects.

PUBLICATIONS

This thesis is based on the following publications, which are referred to in the text by their Roman numerals.

Reviews:

I. Hrelia, P., Sita, G., Ziche, M., **Ristori, E.,** Marino, A., Cordaro, M., Molteni, R., Spero, V., Malaguti, M., Morroni, F., & Hrelia, S. (2020). Common Protective Strategies in Neurodegenerative Disease: Focusing on Risk Factors to Target the Cellular Redox System. *Oxidative medicine and cellular longevity*, 2020, 8363245. https://doi.org/10.1155/2020/8363245 ***All authors equally contributed to this work.**

II. **Ristori, E.**, Donnini, S., & Ziche, M. (2020). New Insights Into Blood-Brain Barrier Maintenance: The Homeostatic Role of β-Amyloid Precursor Protein in Cerebral Vasculature. *Frontiers in physiology*, 11, 1056. https://doi.org/10.3389/fphys.2020.01056

Papers:

I. **Ristori, E.**, Cicaloni, V., Salvini, L., Tinti, L., Tinti C., Simons, M., Corti, F., Donnini, S, Ziche, M. Amyloid-β Precursor Protein APP Down-Regulation Alters Actin Cytoskeleton-Interacting Proteins in Endothelial Cells. *Cells,* 2020, 9, 2506. https://doi.org/10.3390/cells9112506

II. Zhou, W., **Ristori, E.**, He, L., Ghersi, J.J., Mehta, S., Zhang, R., Betsholtz, C., Nicoli, S., Sessa, W.C. Akt is required for artery formation during embryonic vascular development. *(In revision).*

Other papers by the author:

Dionna M. Kasper, Albertomaria Moro, **Emma Ristori**, Anand Narayanan, Guillermina Hill-Teran, Elizabeth Fleming, Miguel Moreno-Mateos, Charles Vejnar, Jing Zhang, Donghoon Lee, Mengting Gu, Mark Gerstein, Antonio Giraldez, Stefania Nicoli (2017). *microRNAs Establish Uniform Traits during the Architecture of Vertebrate Embryos.* Developmental Cell 03/2017; 40(6). DOI: 10.1016/j.devcel.2017.02.021.

Emma Ristori, Stefania Nicoli (2017). *Chapter 15: Comparative functions of miRNAs in embryonic neurogenesis and neuronal network formation*. Essentials of Noncoding RNA in Neuroscience: Ontogenetics, Plasticity of the Vertebrate Brain, 1st edited by Davide De Pietri Tonelli, 06/2017: chapter 15; Elsevier, Imprint Academic press. ISBN: 9780128044025

Anand Narayanan, Guillermina Hill-Teran, Albertomaria Moro, **Emma Ristori**, Dionna M. Kasper, Christine A. Roden, Jun Lu, Stefania Nicoli (2016). *In vivo mutagenesis of miRNA gene families using a scalable multiplexed CRISPR/Cas9 nuclease system*. Scientific Reports 08/2016; 6. DOI:10.1038/srep32386

Miguel A. Lopez-Ramirez, Charles-Félix Calvo, **Emma Ristori**, Jean-Léon Thomas, Stefania Nicoli (2016). *Isolation and Culture of Adult Zebrafish Brain-derived Neurospheres*. Journal of Visualized Experiments 02/2016; 2016(108). DOI: 10.3791/53617

Emma Ristori, Sandra Donnini, Marina Ziche (2016). *Studying Vascular Angiogenesis and Senescence in Zebrafish Embryos*. Angiogenesis Protocols, 01/2016; ISBN: 978-1-4939-3626-7. DOI: 10.1007/978-1-4939-3628-1_27

Vitor Fortuna, Luc Pardanaud, Isabelle Brunet, Roxana Ola, **Emma Ristori**, Massimo M Santoro, Stefania Nicoli, Anne Eichmann (2016). *Vascular Mural Cells Promote Noradrenergic Differentiation of Embryonic Sympathetic Neurons*. Cell Reports 06/2015;11(11). DOI:10.1016/j.celrep.2015.05.028

Emma Ristori, Miguel Alejandro Lopez-Ramirez, Anand Narayanan, Guillermina Hill-Teran, Albertomaria Moro, Charles-Félix Calvo, Jean-Léon Thomas, Stefania Nicoli (2015). *A Dicer-miR- 107 Interaction Regulates Biogenesis of Specific miRNAs Crucial for Neurogenesis*. Developmental Cell 02/2015; 32(5). DOI: 10.1016/j.devcel.2014.12.013

Emma Ristori, Stefania Nicoli (2015). *miRNAs Expression Profile in Zebrafish*

Developing Vessels. Methods in molecular biology (Clifton, N.J.) 01/2015; 1214. DOI:10.1007/978-1-4939-1462- 3_7

PARTECIPATION TO CONGRESSES

National conferences

- 39° Congresso Nazionale della Società Italiana di Farmacologia (SIF). Oral Communication: Role of amyloid-β precursor protein in maintaining vascular stability and blood brain barrier integrity in response to stress factors. **Ristori E.,** Ziche M. and Donnini S. (Firenze, 20th -23th November 2019).

AWARDS

- Mention to **Best Oral Communication** at the 39° Congresso Nazionale della Società Italiana di Farmacologia (SIF). Firenze, 20th -23th November 2019.

- **Research travel grant recipient** SIF (Società Italiana di Farmacologia) to carry out research in the Laboratory of Professor Michael Simons at the Yale University. New Haven, USA.

1. LIST OF ABBREVIATIONS

AD	Alzheimer's Disease
ADAM10	Disintegrin and metalloproteinase domain-containing protein 10
AICD	APP Intracellular Domain
Akt	RAC-alpha serine/threonine-protein Kinase
Alk	Activin-receptor-Like Kinase
APLP1	APP-like Proteins 1
APLP2	APP-like Proteins 2
APP	Amyloid-β Precursor Protein
Aβ	Amyloid-β peptide
BACE1	β-secretase 1
BBB	Blood Brain Barrier
BM	Basement Membrane
BMP	Bone Morphogenetic Protein
C-terminal	Carboxy-terminal
C83 (βCTF)	APP C-terminal fragment beta
C89 (αCTF)	APP C-terminal fragment alpha
CA	Caudal Aorta
CAA	Cerebral Amyloid Angiopathy
CAMs	Cell Adhesion Molecules
CCV	Common Cardinal Vein
COUP-TFII	COUP Transcription Factor 2
CV	Caudal Vein
DA	Dorsal Aorta
Dab2	Disabled 2
DEP1	Density Enhanced Phosphatase 1
Depp	Decidual protein induced by progesterone
DLAV	Dorsal Longitudinal Anastomotic Vessel
Dll4	Delta-like 4
EC	Endothelial Cell
ECM	Extracellular Matrix
eNOS	endothelial Nitric Oxide Synthase
EPAS1	Endothelial PAS domain protein 1
ERK1/2	Extracellular Regulated Kinase 1/2
FAK	Focal Adhesion Kinase
Flk1	Fetal liver kinase 1 (VEGFR2)
Flt1	Fms-like tyrosine kinase 1 (VEGFR1)
Flt4	Fms-related tyrosine kinase 4 (VEGFR3)
FOXO	Forkhead box O
GSK3b	Glycogen Synthase Kinase 3b
HEY	HES-related with YRPW motif protein
HIF	hypoxia inducible factor
hpf	hours post fertilization
HS	Heparan Sulfate
HSPG	Heparan Sulfate Proteoglycan

HUVECs	human umbilical vein endothelial cells
KDR	Kinase insert Domain Receptor (VEGFR2)
LDLs	Low-Density Lipoproteins
MMP	Matrix metalloproteinase
Nck	SH2 domain adaptor Nck
NICD	Notch Intracellular Domain
NO	Nitric Oxide
NRP	Neuropilin
NRP1	Neuropilin 1
NRP2	Neuropilin 2
p3	APP non-amyloidogenic extracellular fragment
p38MAPK	p38 Mitogen-Activated Protein Kinase
PAR-3	Proteinase-Activated Receptor 3
PAK	p21-Activated protein Kinase
PCV	Posterior Cardinal Vein
PDGF	Platelet-Derived Growth Factor
PDK	Phosphoinositide– Dependent protein Kinase 1
PECAM-1	Platelet endothelial cell adhesion molecule-1
PI3K	Phosphatidylinositol-3 Kinase
PKB	Protein Kinase B (Akt)
PKC	Ca2+-dependent protein kinase C
PLCγ	Phospholipase Cγ
PlGF	Placenta Growth Factor
PTP	Phosphotyrosine Phosphatase
RTK	Receptor Tyrosin Kinase
sAPPα	soluble Amyloid Precursor Protein cleaved by α-secretase
sAPPβ	soluble Amyloid Precursor Protein cleaved by β-secretase
SCK	SHC-related adaptor protein
Se/ISV	Intersegmental Vessels
SeA	Intersegmental Arteries
SeV	Intersegmental Veins
SH2	Src Homology 2
SHB	Src homology 2 domain containing adaptor protein B
SHP2	Src Homology 2 domain PTP
SMC	Smooth Muscle Cell
Src	proto-oncogene tyrosine-protein kinase Sr
sVEGFR	soluble Vascular Endothelial Growth Factor Receptor
TSAd	T-cell-Specific Adapter protein
Y	Tyrosine
VEGF	Vascular Endothelial Growth Factor
VEGFR	Vascular Endothelial Growth Factor Receptor
VEPTP	Vascular Endothelial PTP
VPF	Vascular Permeability Factor (VEGF)

2. INTRODUCTION

2.1 THE VASCULAR ENDOTHELIUM

Blood vessels form the largest surface of the human body and their main function is to deliver oxygen and nutrients to tissues and organs. A single layer of endothelial cells (ECs) lines the inner bed of arteries, capillaries and veins to form the vascular endothelium, a semi-permeable barrier separating blood cells from the surrounding tissues.

For many years, this monolayer was regarded as a mere inert barrier, however, it is now well established that ECs are highly metabolically active and play critical role in many physiological processes including, the trafficking of blood cells between blood and underlying tissues, the control of vascular tone, the maintenance of blood fluidity, permeability, angiogenesis and both innate and adaptive immunity.

It is also well established that the endothelium is involved in most if not all disease states.

The vascular endothelium is a very heterogeneous tissue that changes in space and time, in structure and function, and in health and disease (Aird, 2007a; Aird, 2007b). In fact, ECs phenotypes vary between different organs, between different segments of the vascular loop within the same organ, and between neighbouring endothelial cells of the same organ and blood vessel type (Potente & Mäkinen, 2017).

Arteries and veins represent the first level of heterogeneity. Although both function as conduits and are characterized by a continuous non-fenestrated lining of ECs, basement membrane (BM) and layers of smooth muscle cells (SMCs), they differ in fundamental ways. First, arteries carry oxygenated blood, whereas veins contain deoxygenated blood (except for pulmonary circulation, where the oxygenation status is reversed). Compared with arteries, large veins have a greater capacity to mediate an inflammatory response (Eriksson et al., 2005). At a morphological level, arteries show thicker walls and tighter cell-junctions compared to veins. Furthermore arteries pulsate, whereas vein do not. At a molecular level, arteries and veins express unique markers (Torres-Vázquez et al., 2003). Arterial ECs preferentially express ephrinB2, Delta-like 4 (Dll4), Hey1 and Hey2, neuropilin 1 (NRP1), endothelial PAS domain protein 1 (EPAS1), activin-receptor-like kinase 1 (Alk1), and decidual protein induced by progesterone (Depp). Venous ECs preferentially express EphB4, neuropilin 2 (NRP2) and COUP-TFII (Torres-Vázquez et al., 2003).

From the main arteries and veins a network of arteriole and post-capillary venules depart to meet in the capillaries, the major exchange vessels in the circulation. Differently from the continuous monolayer of arteries and veins, the endothelium of capillaries may be continuous, fenestrated, or discontinuous, according to the needs of the underlying tissue, and they have a varying extent of BM and pericyte coverage (**Figure 1**).

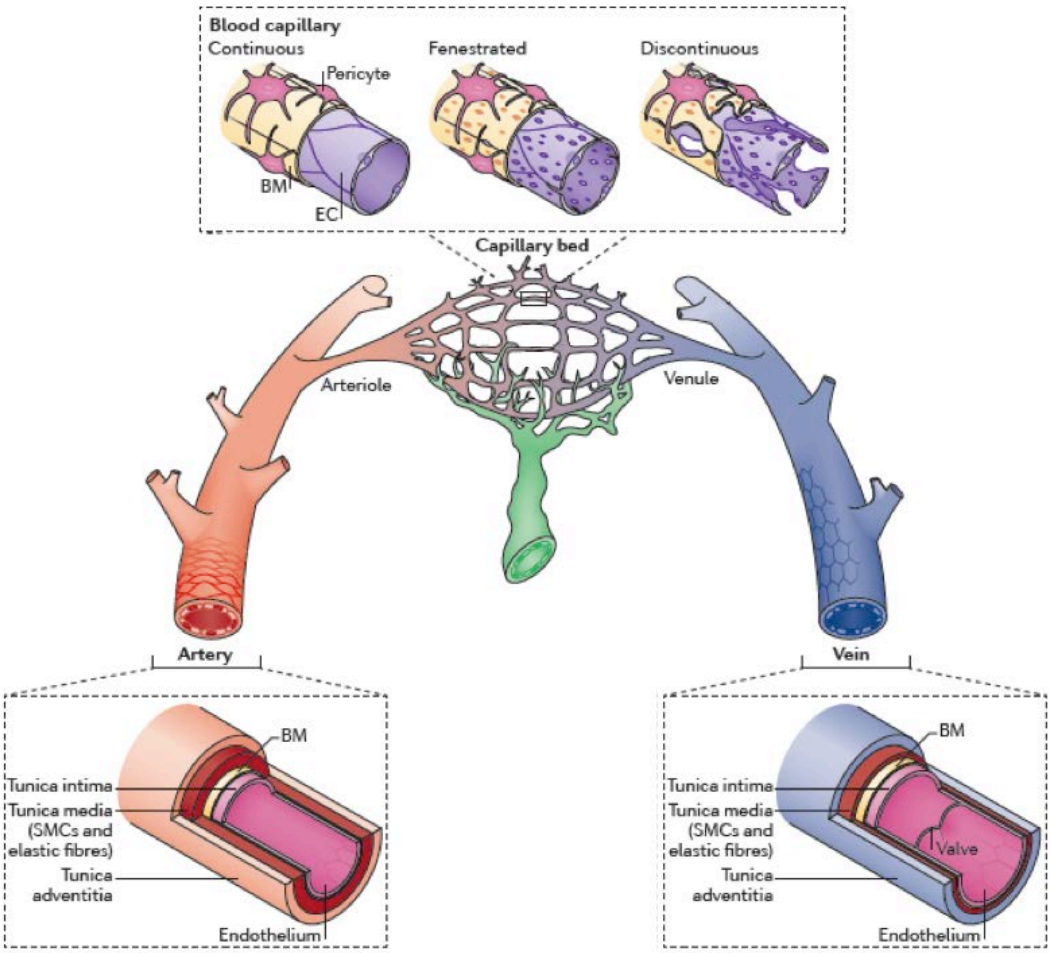

Figure 1: Hierarchical organization of the vasculature. In red, arteries and in blue the veins interconnect through a network of capillaries. In green blind-ended lymphatic capillaries and collecting vessels drain fluid into the venous circulation. At the top of the figure is shown the anatomy of capillary vessels and at the bottom the anatomy of larger vessels (modified from Potente & Mäkinen, 2017).

In general, vascular ECs are polarized cells, with a luminal membrane that is directly exposed to blood constituents and circulating cells, and a basolateral surface that is

separated from surrounding tissues by a glycoprotein basement membrane, which is secreted and anchored to their cell membrane by ECs themselves.

In healthy adults ECs are quiescent and their main function is to deliver oxygen and nutrients to tissues and organs. However, ECs can sense and respond to space- and time-dependent changes of the surrounding microenvironment and can be rapidly activated in response to signals from tissues in need of vascularization. When activated, ECs undergo dynamic and complex morphological and biochemical changes and assume a permeable, pro-thrombotic, and pro-inflammatory phenotype that allow them to invade and expand in avascularised tissues.

This unique plasticity of endothelium to respond, adapt and rearrange requires rigorous regulatory mechanisms, which prevent from a detrimental uncontrolled and persistent vascular growth. Alteration of these regulatory mechanisms is often the cause of pathological situation frequently occurring in diseases (e.g. tumour growth, vascular eye disease or overgrowth syndromes) (Adams & Alitalo, 2007; Potente et al., 2011).

Among the different signalling processes, the Vascular Endothelial Growth Factors (VEGFs) act as critical players in endothelial development and plasticity.

2.2 VASCULAR ENDOTHELIAL GROWTH FACTORS (VEGFS)

Vascular endothelial growth factors (VEGFs) are the strongest pro-angiogenic factors and master regulators of vascular development and of blood and lymphatic vessels function in adult vasculature during both health and disease.

In mammals, the VEGF family is composed of 5 related factors, VEGF-A (originally named vascular permeability factor, VPF) (Senger et al., 1983), VEGF-B, VEGF-C, VEGF-D and the placenta growth factor (PlGF). In addition, a number of nonvertebrate polypeptides show structural and functional similarities with the mammalian VEGFs, including the snake venom-derived polypeptides VEGFF (Yamazaki et al., 2005) and the parapox virus open reading frame VEGFE (Ogawa et al., 1998).

VEGFs are homodimeric polypeptides and their ability to bind to receptors and co-receptors is regulated by alternative splicing (Grunewald et al., 2010). VEGFA alternative splicing generates several splice variants. These include VEGF121, VEGF165, VEGF189, and VEGF206, and the less common isoforms VEGF145 and VEGF183. VEGF165 (VEGF164 in mice) is the most frequently expressed isoform in tissues, and is also the most physiologically relevant isoform (Ferrara, 2010).

In addition to the "conventional" VEGFA variants, a series of VEGFA splice variants denoted VEGFA(121,145,165,183,189)b have been described as anti-angiogenic, since their bind to VEGF receptors fails to promote an efficient activation of the receptors (Harper & Bates 2008; Grunewald et al., 2010).

Different VEGFs specifically bind to different receptors, and different properties of the VEGF family members modulate their biological impact. For instance, the different heparan sulfate (HS) binding affinities result in specific spatial distribution of the different VEGFA isoforms. The lack of binding sites for HS allows the VEGFA121 isoform to freely diffuse in the extracellular space, while the high affinity for HS of VEGFA165 and VEGFA189 causes the retention of these isoforms on the cell surface or in the extracellular matrix.

2.2.1 VEGFS RECEPTORS AND CO-RECEPTORS

Mammalian VEGFs bind with high affinity to homodimers or heterodimers of three receptor tyrosine kinases (RTKs): VEGFR1 (Flt1), VEGFR2 (Flk1; KDR) and VEGFR3 (Flt4). The three cell surface receptors show an overall similar structure, characterized by an extracellular domain containing immunoglobulin-like loops, a transmembrane domain, a juxtamembrane domain, and a cytoplasmatic domain composed by a tyrosine kinase domain and a C-terminal tail (Koch et al., 2011). However, VEGFRs strongly differ in mode of activation, signalling and biological effects.

The VEGFR1 (Flt1 (Fms-like tyrosine kinase 1) in mouse) is expressed in vascular ECs, macrophages, and monocytes and in a wide range of other cell types including neuronal cells (Selvaraj et al., 2015). VEGFR1 behaves as a negative regulator in endothelial biology, and its signalling and biology appears more elusive than that of other VEGFRs. The binding of VEGFR1 to its ligands, VEGFA, VEGFB or PlGF, activates only a weak tyrosine kinase activity. VEGFR1 can exist as a homodimer or a heterodimer with VEGFR2 (VEGFR1/VEGFR2), depending on the ligand (Mac Gabhann & Popel, 2007). Alternative splicing of VEGFR1 results in the production of a soluble form, sVEGFR1. VEGFA binding to sVEGFR1, to full length VEGFR1 homodimers and VEGFR1/VEGFR2 heterodimers decreases the amount of VEGFA available to bind to VEGFR2, implicating VEGFR1 in negative regulation of VEGFR2 signalling and function (Cudmore et al., 2012; Kappas et al., 2008). Thus, both VEGFR1 and sVEGFR1 are largely viewed as decoys that control the VEGFA available to bind to and activate VEGFR2. Supporting this hypothesis, Flt1-/- mice embryos die at E9 from excessive ECs

proliferation and subsequent disorganization and dysfunction of the vascular network. This is due to an increase of the amount of VEGFA available for VEGFR2 binding and the consequent excessive activation of VEGFA-VEGFR2 signalling (Fong et al., 1995). In addition, expression of VEGFR1 in non-ECs may also directly influence angiogenesis. For example, expression of VEGFR1 in retinal myeloid cells suppresses angiogenesis during mouse embryonic development (Stefater et al., 2011).

The VEGFR2 (KDR (Kinase insert domain receptor) or Flk1 (Fetal liver kinase 1) in mouse) is expressed in ECs and their precursors, but it is also found in other cell types, such as neuronal cells and tumor cells. VEGFA, VEGFC and VEGFD binding induces VEGFR2 activation (McColl et al., 2003). Alternative splicing of this receptor results in the production of the soluble form, sVEGFR2 that is involved in modulation of lymphatic vessels growth by competing with VEGFR3 for the binding of VEGFC (Albuquerque et al., 2009). VEGFA is the major ligand of VEGFR2, and their interaction is necessary to maintain vascular network homeostasis (Ando & Yamamoto, 2009; Potente et al., 2011). Flk-/- mice die at E8.5 as a result of an early defect in ECs and hematopoietic cells development (Shalaby et al., 1995). A similar phenotype was observed in VEGFA-/- mice (Carmeliet et al., 1996; Ferrara et al., 1996). Furthermore, VEGFR2 serves a critical function in pathological processes associated with neovascularization such as tumor angiogenesis (Plate et al., 1993; Millauer et al., 1994). The VEGFA-VEGFR2 signalling and its regulation will be discussed in detail in the next paragraph.

The VEGFR3 (Flt4 (Fms-related tyrosine kinase 4) in mouse) is known to be preferentially expressed in lymphatic endothelium, however several vascular endothelial cell types such as venous and capillary, and neuronal progenitors, macrophages and osteoblasts also express this receptor (Orlandini et al., 2006; Schmeisser et al., 2006; Han et al., 2015). During early development both blood and lymphatic endothelial cells express VEGFR3 (Alitalo, 2011), and its expression becomes restricted to the lymphatic system in the adult. However, VEGFR3 expression is reintroduced in ECs during specific processes of active angiogenesis such as during retinal development and tumor neovascularization (Benedito et al., 2012; Tammela et al., 2008). VEGFR3 binding to its ligands, VEGFC and VEGFD, promotes lymphendothelial cell migration (Mäkinen et al., 2001) and lumen formation during lymphangiogenesis (Goldman et al., 2007). VEGFR3 binding to proteolytically processed VEGFC and VEGFD, promotes VEGFR3/VEGFR2 heterodimerization (Dixelius et al., 2003). VEGFR3/VEGFR2 heterodimers are involved in both pathological and physiological angiogenic sprouting of vascular endothelium (Nilsson et al., 2010; Tvorogov et al., 2010), implying an important role of VEGFR3 also

blood vessel formation. Indeed, VEGFR3 gene targeted inactivation results in mouse embryonic death at E10.5 due to cardiovascular failure and impaired vascular organization (Dumont et al., 1998). *In vitro* studies showed differential downstream signalling of VEGFR3 homodimers and heterodimers. In fact, while VEGFR3/VEGFR2 heterodimerization mediates VEGFC-induced Akt signalling, VEGFR3 homodimers drive VEGFC-induced ERK1/2 activation in lymphatic endothelial cells (Deng et al., 2015). However, the *in vivo* role of VEGFR2/VEGFR3 still remains to be clarified.

VEGFs also bind with high affinity to so-called "co-receptors", such as the neuropilin (NRP) family members NRP1 and NRP2 and to heparan sulfate proteoglycans (HSPGs) (**Figure 2**). Moreover, their ability to bind to various transmembrane proteins allows the formation of multiprotein complexes that include several VEGF-non binding proteins such as integrins and ephrinB2 (Shibuya, 2013). The interactions of VEGF ligands with and co-receptors and accessory molecules influence VEGF biology by stabilizing ligand–receptor complexes, leading to prolonged signalling duration.

NRP family includes NRP-1 and NRP-2 and consists in transmembrane glycoproteins that bind to VEGFs and semaphorins, which are axon guidance proteins. VEGFs show specific affinity for NRP-1 and NRP-2: VEGFA165 binds both NRPs, while VEGFA145, VEGFC and VEGFD bind only to NRP2, and VEGFB and PlGF bind only to NRP1 (Soker et al., 1998). The simultaneous binding of VEGFs to NRPs and VEGFRs induces the formation of NRPs/VEGFRs complexes. The VEGFC-induced NRP2/VEGFR3 complex is important in lymphatic vessel sprouting (Xu et al., 2010). NRPs are involved in VEGFR2 trafficking. In fact, the binding of the protein synectin to their cytoplasmatic domains directs NRP1/VEGFR2 internalization and endosomal trafficking (Lanahan et al., 2010). Moreover, NRP1 is able to bind VEGF independently from VEGFR2, thus sequestering the ligand and affecting VEGFR2 signalling (Cackowski et al., 2004).

HSPGs are cell-surface and secreted proteins that carry heparan sulfate (HS) chains. HSPGs can bind to various heparin-binding growth factors found on the extracellular matrix (ECM) or the cell membrane. HSPGs such as syndecans and glypicans bind all VEGF isoforms and family members except for VEGFA121, which lacks HS binding sites. Furthermore, HS chains can directly bind both VEGFR1 and VEGFR2 (Park & Lee, 1999; Xu et al., 2011; Corti et al., 2019); HS also binds to NRP1 but not to NRP2 (Vander Kooi et al., 2007). Binding of VEGFR2 to HSPGs expressed in adjacent cells leads to increased and prolonged VEGF-induced signal, due to HS-dependent trapping of the active VEGF/VEGFR2 signalling complex (Jakobsson et al., 2006). Furthermore, HS

shapes the spatial distribution of VEGFA isoforms influencing blood vessel branching patterns (Ruhrberg et al., 2002). The simultaneous binding of VEGFA to VEGFR2, NRP1 and HSPGs induces the formation of a complex that is crucial for ECs survival, sprouting and migration, and vascular permeability (Simons et al., 2016).

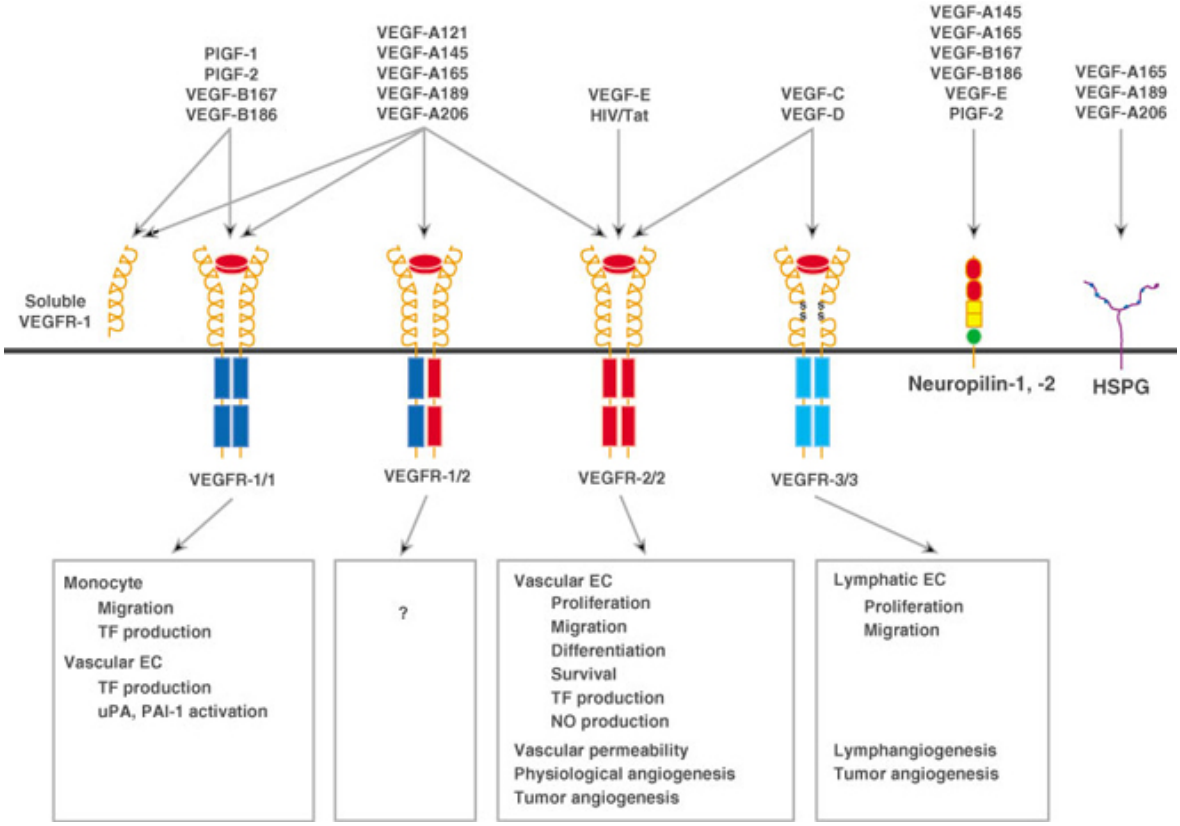

Figure 2: Interactions between VEGF and VEGF receptors and co-receptors, and their biological function (from Matsumoto & Claesson-Welsh, 2001)

Integrins are heterodimeric transmembrane receptors composed of one alpha (α) and one beta (β) subunit that link the intracellular actin cytoskeleton to ECM proteins and transmit bidirectional signals "outside-in" and "inside-out" across the membrane. Integrin β1 and integrin β3 binding to VEGFR2 is important for VEGF signalling. In particular, ECM-binding VEGFA induces integrin β3-VEGFR2 association, which is required for full VEGFR2 activation. The reciprocal activation of integrin αVβ3 and VEGFR2 regulates cellular activities involved in angiogenesis, including ECs migration, survival and anastomosis (Byzova, et al., 2000; West et al., 2012). Additional partners such as Src and syndecan-1 can activate both VEGFR2 and integrin αVβ3-VEGFR2 (Rapraeger et al.,

2013). ECM-binding VEGFA also induce integrin β1-VEGFR2 association, shifting VEGFR2 localization at the focal adhesion, which is accompanied with increased activation of VEGFR2 (Chen et al., 2010).

EphrinB2 is the transmembrane ligand for Eph receptors and is required for early angiogenesis remodelling (Adams et al., 2001). The early expression of ephrinB2 in arteries and of EphB4 in veins contributes to establish borders between these two compartments during vascular development. Most importantly, ephrinB2 is required for internalization and full signalling activity of VEGFR2 (Wang et al., 2010). At the molecular level, ephrinB2 interacts with the clathrin-associated sorting protein Dab-2 and the cell polarity regulator PAR-3. The ephrinB2/Dab2/PAR-3 complex promotes the movement of the activated VEGFR2 from the plasma membrane into the cell, and thereby activating the downstream signal transduction cascades that control ECs sprouting (Nakayama et al., 2013). Moreover, C-terminal ephrinB2 PDZ motif is required for VEGFR2 localization in tip filopodia (Sawamiphak et al., 2010).

VEGFRs bind *in cis* to freely diffusible VEGFs or to VEGFs presented by co-receptor on the same cells. VEGFRs bind *in trans* to VEGFs presented by co-receptors expressed on adjacent cells (Koch et al., 2011).

In the canonical VEGFRs signalling, all RTKs are activated by VEGF ligand binding, to induce homodimerization or heterodimerization of the receptor, leading to conformational changes and consequent activation of the tyrosin kinase and autophosphorylation of the tyrosine residues in the receptor intracellular domains. Adaptor molecules bind to the intracellular phosphotyrosine residues and surrounding amino acids to initiate various intracellular signalling pathways. VEGFRs activation is strictly regulated by receptor trafficking, including internalization and degradation, and by the activity of phosphotyrosine phosphatases (PTPs), such as DEP1, VEPTP, SHP2, and PTP1B that dephosphorylate the activated phosphotyrosine sites (Kappert et al., 2005).

On the contrary, non-canonical VEGFRs activation doesn't depend on VEGF ligand binding with the receptor and includes shear-stress-mediated VEGFR2 phosphorylation and VEGFR2 binding to non-VEGF ligands (Shibuya, 2013; Simons et al., 2016).

Canonical and non-canonical pathways can mediate immediate responses, such as vascular permeability, as well as longer-term responses that require gene regulation, such as EC survival, proliferation and migration.

2.2.2 VEGFA-VEGFR2 SIGNALLING

The VEGFR2 is the main VEGF receptor on ECs, and the VEGFA-VEGFR2 signalling is essential for ECs differentiation, proliferation, migration, and formation of the vascular tube during development and in the adult, in physiology and pathology.

Ligand binding to VEGFR2 *in cis* or *in trans* induces conformational changes in the receptor that allows the intracellular protein kinase domain activation and the auto- or trans-phosphorylation of tyrosine residues on the receptor dimer itself as well as on downstream signal transducers. VEGFR2 has five major tyrosine (Y) phosphorylation sites: Y951 (Y949 in mouse), Y1054 (Y1152 in mouse), Y1059 (Y1157 in mouse), Y1175 (1173 in mouse) and Y1214 (Y1212 in mouse), and each of these activates different signalling pathways with consequent induction of a specialized function of the receptor (**Figure 3**).

The Y1054 and Y1059 sites are located within the kinase domain and their phosphorylation is critical for the receptor kinase activity (Kendall et al. 1999).

Phosphorylation at Y951 site has an important role in VEGF-induced permeability. This phosphorylation site is not usually activated in quiescent ECs, but is phosphorylated during active angiogenesis in certain ECs during development as well as in tumor vasculature (Matsumoto et al. 2005). Y951 serves as a binding site for the SH2 domain of T-cell-specific adapter molecule (TSAd, also known as VRAP), which in turn binds and activates Src protein kinase. Src interacts with major cytoskeletal components, such as actin and cell–cell adhesion proteins. In response to VEGFA, Src regulates adherens junctions by phosphorylating VE-cadherin and β-catenin and inducing rearrangement of cell junctions and subsequent increased vascular permeability (Gordon et al., 2016; Matsumoto et al., 2005). Furthermore, Src phosphorylation can induce the PI3K/Akt pathway and the consequent activation of endothelial nitric oxide synthase (eNOS). Activation of eNOS can also occur through the direct association between eNOS and Ca2+/calmodulin in a phospholipase Cγ (PLCγ)-Ca2+ dependent manner (Dimmeler et al., 1999; Fulton et al., 1999). eNOS-mediated generation of nitric oxide (NO) is involved in VEGF-induced vessel dilatation, increased vascular permeability, and angiogenesis (Fukumura et al., 2001).

Activation of the Y1175 phosphorylation site regulates endothelial progenitor differentiation during embryonic development, as well as ECs survival during adulthood (Sakurai et al., 2005). Phosphorylated Y1175 (pY1175) binds several signalling mediators such as PLCγ, and several adapters such as SHB and SCK. How the interaction between pY1175 and each of its mediators contributes to the downstream signalling is still under

investigation. pY1175-PLCγ binding mediates the activation of the Ca2+-dependent protein kinase C (PKC), and the downstream activation of ERK1/2 pathway, which is crucial for many aspects of ECs biology including ECs proliferation, migration and cell fate specification (Takahashi et al., 2001; Simons et al., 2016). pY1175-SHB binding promotes VEGF-induced FAK activation and contributes to focal adhesion turnover and ECs migration (Holmqvist et al., 2003).

Phosphorylation of Y1214 is implicated in ECs actin cytoskeleton remodelling and migration (Lamalice et al., 2004). Phosphorylated Y1214 (pY1214) binds to Nck. pY1214-Nck interaction recruits and activates the tyrosine kinase Fyn, which initiates the cascade of phosphorylation events that lead to activation of the p38 mitogen-activated protein kinase (p38MAPK) pathway (Lamalice et al., 2006).

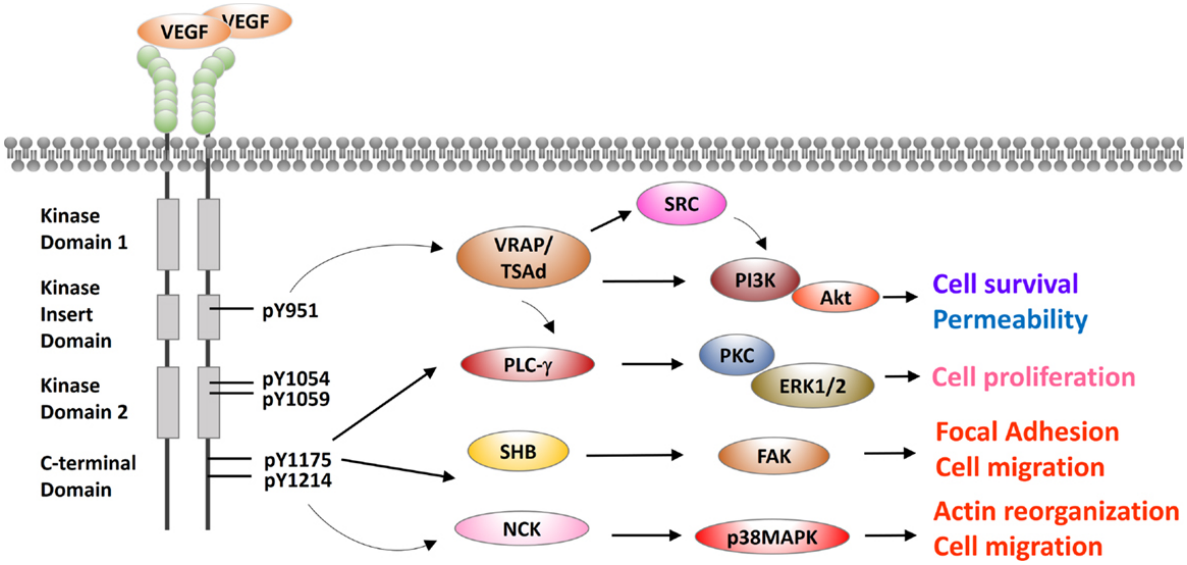

Figure 3: VEGF-activated VEGFR2 phosphorylation sites and downstream signalling pathways in ECs (from Zhu & Zhou, 2015).

VEGFR2 signalling can also be initiated in a non-VEGF-dependent manner through non-canonical pathways. For example mechanical forces, such as shear stress, are able to induce VEGFR2 activation independently from VEGF ligand binding. This non-canonical VEGFR2 activation is mediated by sheer-stress-dependent activation of cytoplasmatic Src that in turn phosphorylates VEGFR2 and mediates the formation of a mechanosensory complex within VEGFR2, VEGFR3, VE-cadherin and PECAM-1 initiating the downstream signalling (Jin et al., 2003; Tzima et al., 2005; Coon et al.,

2015). Shear stress can also promote angiogenesis through p38MAPK signalling activation (Gee et al., 2010). In addition, sheer stress can induce matrix metalloproteinase-dependent (MMP) release of VEGFA ligands from ECM, enhancing VEGFR2 activation (dela Paz et al., 2013). Another example of non-canonical pathway is VEGFR2 activation mediated by non-VEGF ligands. In fact, VEGFR2 can bind to a number of ligands such as galectins, gremlin, lactate and LDLs and mediate ECs sprouting, migration and VEGFR2 trafficking and recycling (Mitola et al., 2010; Markowska et al., 2011; Jin et al., 2013; Ruan & Kazlauskas, 2013).

VEGFR2 signalling is tightly controlled by several regulatory mechanisms acting at different levels. Receptor expression levels, VEGF ligands availability and their different binding affinity, the presence of non-VEGF ligands and VEGF-binding co-receptors modulate the receptor/ligand interaction. The activity of inactivating tyrosine phosphatases plays a crucial role in modulating VEGFR2 downstream signalling. Moreover, VEGFR2 endocytosis and intracellular trafficking are key regulators of the specificity as well as the strength and duration of the signalling output (Lanahan et al., 2010; Simons, 2012; Nakayama et al., 2013). Indeed, the activation of VEGFR2 downstream signalling continues during internalization, and VEGFR2 internalization is required for Akt and ERK1/2 signalling activation. After exerting its function, internalized VEGFR2 is either sent to lysosome for degradation or recycled back to the cell membrane via slow or fast recycling pathways (Simons, 2012). In addition, VEGFR2 signalling output is directly or indirectly regulated by crosstalk between VEGFR2 and others VEGFRs or co-receptors, as well as the interplay with other receptors intracellular signalling pathways, thus creating complex positive and negative feedback loops (Simons et al., 2016).

2.2.3 VEGF SIGNALLING IN VASCULOGENESIS, ANGIOGENESIS AND VASCULAR REMODELLING.

The cardiovascular system is one of the first to develop during vertebrate embryogenesis. The first major vessels of the vertebrate embryo are generated via a process known as vasculogenesis. Vasculogenesis is the mechanism by which mesoderm-derived cells called angioblasts coalesce to form vascular cords. Following the vasculogenic formation of primary vessels, the initial vascular network is expanded by the complex secondary process of angiogenesis, which remodels pre-existing vessels either by sprouting and elongation or by the division or fusion of existing vessels. Vessels subsequently recruit supportive smooth muscle cells and pericytes to protect the

endothelium and maintain vascular integrity. The majority of vessels develop by sprouting angiogenesis from pre-existing vessels (Potente et al 2011; Adams et al., 2007). In the adult, angiogenesis occurs physiologically during cyclic reproductive changes in women, in skeletal muscle remodelling during exercise, and during tissue repair and regeneration (Wietecha et al., 2012). Adult angiogenesis can also accompany pathologic processes such as tumor growth, diabetic retinopathy, and rheumatoid arthritis (Folkman, 1995; Bhadada et al. 2011).

The VEGF signalling is one of the most important regulators of these processes, however, the precise genetic programming required to shape the cardiovascular system is still only partially understood due to the complexity of multiple cellular interactions.

Vasculogenesis is divided into three stages: first, the induction of endothelial progenitors (angioblasts) and hematopoietic progenitors (hemangioblasts) and their commitment to vasculogenesis; second, the assembly of endothelial precursor cells into blood vessels; and third, the transition from vasculogenesis to angiogenesis.

During this process, vessels become specified as arteries and veins. The mediators of arterial-venous identity are still under investigation. Experimental evidence indicates that signalling by Eph and ephrin genes between arteries and veins, and between blood vessels and adjacent tissues, is required for the demarcation of arterial-venous domains, vascular morphogenesis, and the guidance of angiogenic sprouts. Upstream to Eph/ephrin signalling, the VEGFs and Notch signalling promote arterial fate by positively controlling ephrin-B2 expression (Torres-Vázquez et al., 2003). In pre-arterial angioblasts, VEGFA promotes the activation of Notch signalling through the VEGFA/VEGFR2/NRP1 complex. Notch activity suppresses the venous and promotes the arterial fate in these ECs progenitors, orchestrating the arterial-venous specification program (Wythe et al., 2013). In pre-venous endothelial precursors, the nuclear orphan receptor transcription factor COUP-TFII and the PI3K-Akt signalling repress arterial differentiation by suppressing Notch and NRP1 signalling (Lin et al., 2007). Down-regulation of Notch promotes venous fate by reducing ephrin-B2 and upregulating EphB4 expression (You et al., 2005)

Angiogenesis, which serves to expand the vascular network, also occurs in three major phases: first, the activation of a specific EC, called tip cell, in the pre-existing, quiescent blood vessel. This cell acquires migratory properties and specifies to lead the sprouting process; second, the induction of stalk cell phenotype in cells neighbouring the tip cells. Stack cells undergo proliferation, elongation and lumenization in order to shape the nascent vessel; third, fusion of the newly formed sprouts to the pre-existing vasculature

via anastomosis, allowing perfusion of blood and stabilization of the developing vascular network.

The specification of tip and stalk cells is mainly controlled by crosstalk between VEGFs and Notch signalling (Geudens & Gerhardt, 2011).

During initial tip cell activation, VEGF promotes Dll4 expression in tip cells, Dll4 activates its Notch receptor in the neighbouring stalk cells, which further represses VEGF receptor expression in these cells and inhibit sprouting. The invasive and motile tip cells behaviour that drives angiogenesis is induced by VEGFA and VEGFC signalling via VEGFR2 and VEGFR3. Stalk cell behaviour suppression in tip cells is induced by NRP1-mediated inhibition of BMP/ALK signalling (**Figure 4**).

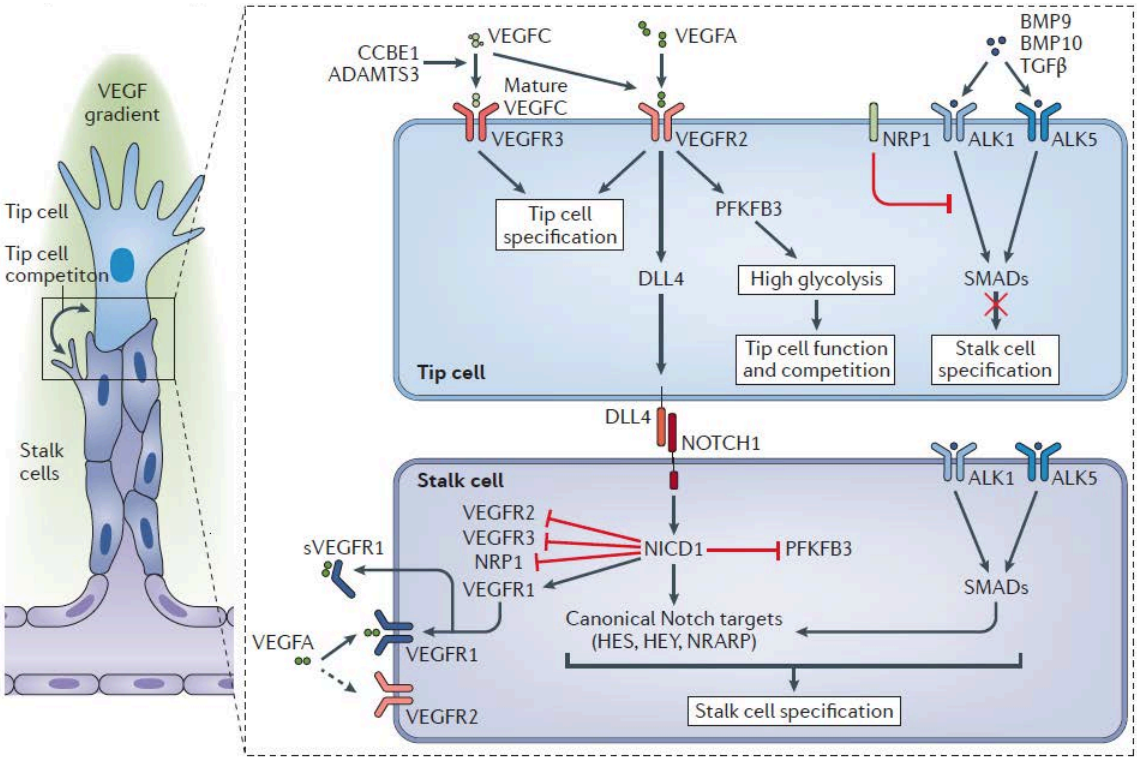

Figure 4: Molecular mechanisms of endothelial tip cell selection. Activation of VEGFRs in tip cells induces downstream Dll4 expression that activates receptor Notch in neighbouring cells that assume stalk cell behaviour (from Potente & Mäkinen, 2017).

Tip cells inhibit adjacent cells to acquire the same fate by a process called lateral inhibition, mediated by Notch signalling. Inhibition of tip fate promotes stalk cell specification and acquisition of a proliferative phenotype.

Once formed, the nascent vessel are stabilized by recruitment of mural cells from the surrounding stroma, mediated by PDGF secretion from the nearby ECs. Mural cells provide support and guidance for vascular remodelling and are subdivided into pericytes in the microvasculature and vascular SMCs in larger vessels.

Newly formed vascular networks undergo extensive vascular remodelling to form a functional and mature vasculature. Vascular pruning and vascular regression are triggered by the down-regulation of VEGF, and can occur in embryonic development, as well as in adult vasculature during luteolysis (Goede at al., 1998).

The correct regulation VEGF signalling is critical for vascular development and remodelling. Alteration of this regulatory signalling can cause pathological angiogenesis and uncontrolled vascular permeability observed in many diseases such as cancer, retinopathies and neurovascular disorders.

2.2.4 VEGF SIGNALLING AND VASCULAR DYSFUNCTION

Endothelial dysfunction contributes to the pathogenesis of a variety of diseases and syndromes, including neurodegenerative diseases. ECs disease state is closely connected to the physiological state. During physiological remodelling, ECs of different beds are activated by local signals, and the initiating stimulus disappears once adaptation is completed and normalcy is restored. By contrast, in pathological remodelling, the initial triggers generally persist creating further instability, and even when initiating triggers are removed, the vasculature does not return to its normal state. In this feedforward loop, instability leads to detrimental ECs activation characterized by matrix remodelling, leukocyte recruitment, inflammation and ECs transformation (**Figure 5**). This implies that persistent instability is central to multiple vascular disorders (Schwartz et al., 2018).

Ageing and cardiovascular risk factors such as hypertension, diabetes and vasculopathy are the main cause of vascular dysfunction. Persistent oxidative stress, abnormal protein deposition and hypoxia promote ECs permeable, prothrombotic, and pro-inflammatory phenotype.

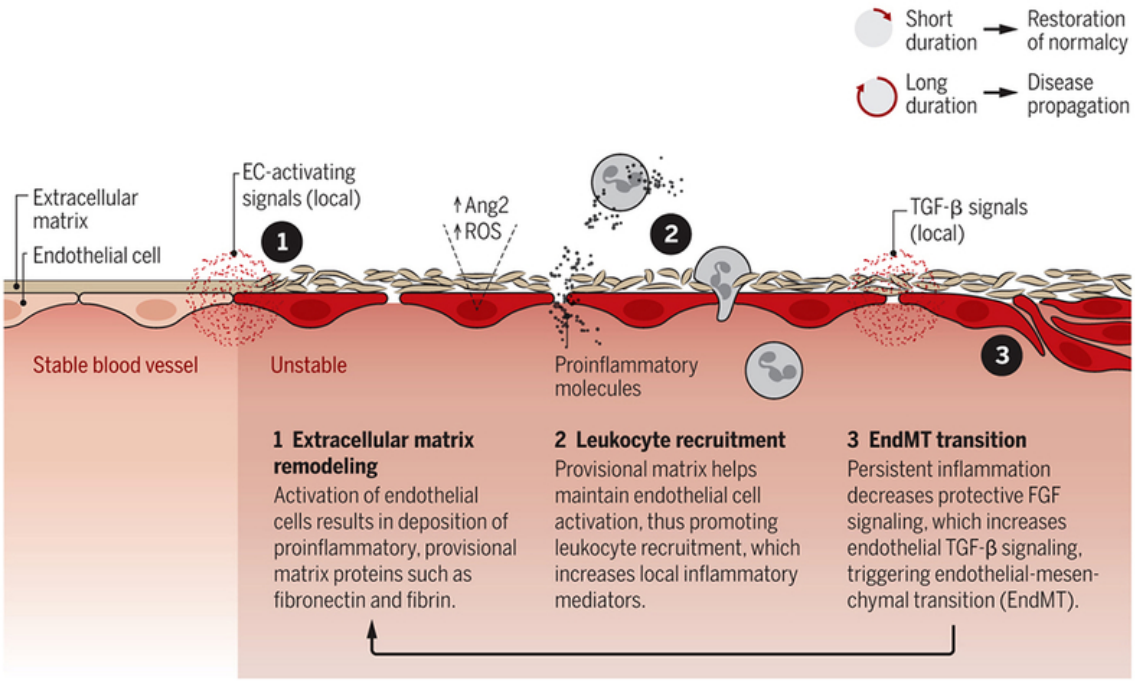

Figure 5: **Persistent Instability and disease** (From Schwartz et al., 2018).

Evidence suggests that VEGF/VEGFR signalling has been implicated in pathogenesis of several diseases. VEGF primarily exerts its effect through the production of vasodilatatory mediators, and VEGF-mediated pathogenic effects are primarily due to its effects on vascular permeability and neo-angiogenesis.

Aberrant VEGF signalling has been linked to a number of eye diseases, such as age-related macular degeneration, diabetic retinopathy, diabetic macular edema and retinopathy of prematurity (Ferrara & Adamis, 2016).

Deregulation of VEGFR1 and soluble sVEGFR1 also participate in pathological processes, by acting as endogenous inhibitors of VEGFA/VEGFR2 signalling. sVEGFR1 expression has been linked to corneal avascularity in the eye (Ambati et al., 2006), and to the pathogenesis of pre-eclampsia during pregnancy (Koga et al., 2003).

VEGFs and VEGF receptors are also expressed in non-ECs, including cancer cells. Since hypoxia is a major regulator of VEGF expression via hypoxia inducible factor (HIF), VEGF is dramatically upregulated in cancer. VEGF secreted by tumor cells induces ECs activation and tumor angiogenesis, which promotes tumor progression and expansion (Ferrara & Adamis, 2016). The efficacy of anti-VEGF therapies confirms the key role of VEGF-mediate angiogenesis in tumor growth (Kim et al., 1993).

Furthermore, VEGF is associated with the clinical manifestation of

neurodegenerative diseases. In particular, VEGFA appears to protect against cognitive impairment in Alzheimer's disease (AD) (Garcia et al., 2014). However, mixed evidences report both up- and down-regulation of VEGFA gene and protein expression in blood, brain and cerebrovascular fluid of AD patients, suggesting a complex role of this signalling in neurodegenerative diseases (Mahoney et al., 2019). AD is characterized by an excessive deposition of amyloid-β (Aβ) peptides that destabilizes vascular integrity, promoting vascular leakage. The vascular damage induced by Aβ includes alteration of vascular tone, impairment of vascular remodelling, and loss of barrier functions, as well as suppression of the intrinsic angiogenic properties of the endothelium and the promotion of a premature senescence phenotype in *in vivo* and *in vitro* models (Donnini et al., 2010; Nannelli et al., 2018). The molecular mechanisms of these multiple Aβ-induced effects on ECs are complex and include direct and indirect interaction with angiogenic growth factors, including VEGF. Treatment with $A\beta_{1\text{-}40}$ significantly decreases VEGFR2 expression levels both in ECs and in the brains of AD mouse models (Cho et al., 2017). Moreover, cell culture studies revealed that Aβ at pathological concentrations acts as a VEGF antagonist, inhibiting VEGF-induced tyrosine phosphorylation of VEGFR2, as well as VEGF-stimulated phosphorylation of Akt and eNOS in ECs (Patel et al., 2010; Cifuentes et al., 2015). On the contrary, overexpression of VEGF signalling driving hyper-vascularization was also observed in brains of AD patients and of murine AD models (Tarkowski et al., 2002; Biron et al., 2011). Interestingly, physiological levels of Aβ are also required for the endothelial homeostasis, and increasing evidence highlights the importance of amyloid-β precursor protein (APP) in supporting the function of the vascular tissue (Cantara et al., 2004; Müller et al 2017; Ristori et al., 2020). To date, the exact role of APP and its metabolites in the vascular endothelium still remains elusive.

3. VEGF SIGNALLING AND AMYLOID-β PRECURSOR PROTEIN (APP): ROLE OF ENDOTHELIAL APP IN VEGFR2 ACTIVATION

(PAPER I AND REVIEW I - II)

3.1 THE AMYLOID-β PRECURSOR PROTEIN (APP)

The amyloid-β precursor protein (APP) is a ubiquitous type-1 integral membrane protein often associated to Alzheimer's disease (AD) and Cerebral amyloid angiopathy (CAA). Despite its role in the development of the pathogenesis, APP exerts several physiological roles that have been mainly investigated in neuronal tissue and, to date, the role of APP in vasculature and endothelial cells has not been fully elucidated.

APP belongs to a conserved gene family that includes two mammalian homologues, the APP-like proteins (APLPs) APLP1 and APLP2. These proteins are type I integral membrane proteins that share similar structural organization and partially overlapping functions, and this may explain why single-gene-knockout animal models have failed to show any major phenotype (Shariati & De Strooper, 2013). Structurally, APP and APLPs share conserved regions, although APP is the only family member containing the sequence encoding Aβ peptides (d'Uscio et al., 2017). APP presents three major isoforms, generated by alternative splicing: APP695, APP751 and APP770. The APP695 isoform is mainly expressed in neurons, whereas APP751 and APP770 are the predominant forms expressed in non-neuronal cells, including endothelial cells and platelets (Van Nostrand et al., 1994). Under physiological conditions, APP is cleaved by different secretases through two main proteolytic pathways: the amyloidogenic and non-amyloidogenic processing (**Figure 6**). The latter leads to the release in the extracellular space of the soluble form sAPP-α generated by α-secretase (ADAM10) cleavage, and the p3 peptide, through cleavage of α-secretase and the γ-secretase complex (composed of four subunits: presenilins, nicastrin, Aph-1 and Pen-2). By contrast, in the amyloidogenic processing, β-secretase (BACE1) cleavage releases sAPP-β (another soluble form with different structure and physiological properties), and subsequent cleavage of β-secretase and γ-secretase generates different Aβ isoforms of various lengths. Moreover, γ-secretase cleavage in the APP transmembrane region yields the biologically active APP intracellular domain (AICD) in both the proteolytic pathways. The main species of Aβ peptides involved in CAA and AD are Aβ1–40 and Aβ1–42. The Aβ1–42 peptides are the predominant form in AD neuronal plaques, whereas deposition of Aβ1–40 peptides on the

cerebral vasculature contributes to the onset of CAA (Stakos et al., 2020). While it is well established the neuronal origin of amyloid deposits observed in AD and CAA, evidences show that activated endothelial cells and platelets are also able to release Aβ1–40 peptides (Kitazume et al., 2012; Canobbio et al., 2015). Under normal physiological conditions, APP is predominantly processed through the non-amyloidogenic pathway and the Aβ peptide is constitutively generated at relatively low levels. In addition, several mechanisms of Aβ clearance involving the cerebrovasculature contribute to maintain the concentrations of these peptides to physiological levels in the brain. Some of these mechanisms include Aβ degradation by proteolytic enzymes, phagocytosis by macrophages, intramural periarterial drainage, and receptor mediated Aβ transport across the BBB in which the main transport proteins are: the P-glycoprotein (P-gp), the low-density lipoprotein receptor related protein-1 (LRP-1), and the receptor for advanced glycation end products (RAGE).

Interestingly, APP processing is influenced by its cellular distribution: the cell-surface accumulation of APP favours non-amyloidogenic processing (Jiang et al., 2014). On the contrary, the retention of APP in acidic compartments, such as early endosomes, promotes amyloidogenic processing (O'Brien and Wong, 2011).

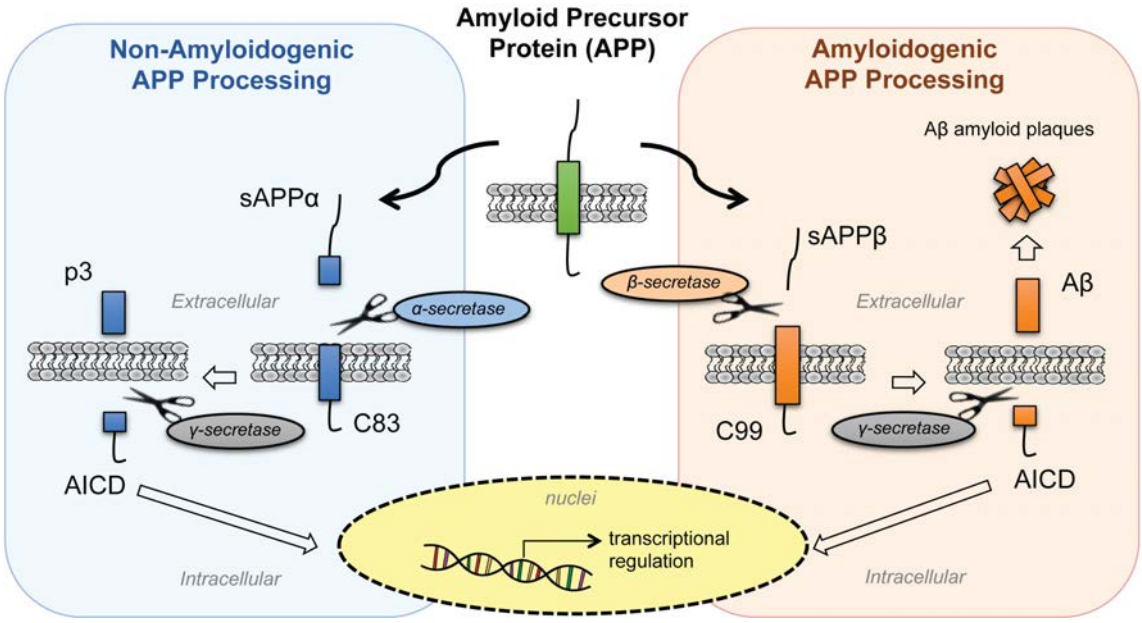

Figure 6: **Proteolytic pathways of Amyloid Precursor Protein (APP).** APP can be processed through a non-amyloidogenic proteolytic pathway (in blue), or an amyloidogenic proteolytic pathway (in orange). The amyloidogenic proteolytic pathway releases Aβ peptides and it is involved in AD pathogenesis (From Ristori et. al., 2020).

3.2 APP AND VASCULAR ENDOTHELIUM

Several physiological roles have been attributed to APP and its processing products, some of which impact neurovascular development and function. Even if APP is notoriously known for its contribution to pathogenesis of neurodegenerative diseases, and many physiological roles have been identified in neural cells (Perez et al., 1997; Nicolas and Hassan, 2014; Nhan et al., 2015; Habib et al., 2017; Coronel et al., 2018), little is known on its function on endothelial cells and cerebral vasculature.

APP is highly expressed in embryonic endothelium, suggesting an important role of this macromolecule and its metabolites in early angiogenesis (Ott & Bullock, 2001). A strong correlation between APP loss-of-function models and vascular dysfunction has been reported, supporting the importance of this protein and its metabolites on vascular homeostasis. In the zebrafish embryo, knockdown of APP by morpholino causes diffuse angiogenic defects especially in the brain. This phenotype can be rescued by reintroducing Aβ peptides supporting the hypothesis that these peptides have an essential role in angiogenesis during embryonic development (Luna et al., 2013). Indeed, blocking Aβ production by inhibition of β- or γ-secretase activity causes reduced angiogenesis both *in vitro* and *in vivo* (Paris et al., 2005). Several studies showed that APP exerts vascular protective properties under physiological conditions. In fact, APP regulates expression and function of endothelial nitric oxide synthase (eNOS) in cerebrovascular endothelium (d'Uscio et al., 2018).

Moreover, evidences suggest that APP mediates endothelial cells' response to angiogenic growth factors and modulates angiogenesis.

Different APP metabolites have been shown to have different roles in angiogenesis and vascular maintenance. Aβ peptides, for example, show both anti-angiogenic and pro-angiogenic effects in a dose-dependent manner *in vitro*. In fact, high micromolar concentrations of different Aβ variants impair angiogenesis, while low nanomolar concentrations of either Aβ1–40 or Aβ1–42 promote angiogenesis in cultured cerebral and peripheral endothelial cells by promoting cell proliferation, migration, and tube formation (Cantara et al., 2004; Cameron et al., 2012). However, the role of Aβ on angiogenesis *in vivo* is still controversial since cerebral hyper-vascularization was observed in human AD brains and transgenic animals overexpressing APP (Biron et al., 2011). To note, the majority of neo-formed vessels observed in AD are so called "string vessels", non-functional capillaries composed by connecting tissue and lacking endothelial cells (Brown, 2010; Forsberg et al., 2018). It has been proposed that the Aβ-induced aberrant angiogenesis may be the basis for BBB disruption in AD (Biron et al., 2011).

Aβ peptides can modulate angiogenesis by functionally interacting with important angiogenic signalling pathways, such as the FGF-2, the VEGF and the notch signalling (Cantara et al., 2004; Patel et al., 2010; Cameron et al., 2012), however *in vivo* and *in vitro* studies showed once again controversial results. While brains of patients with AD show up-regulation of the vascular endothelial growth factor (VEGF) suggesting an interaction of VEGF with APP processing (Burger et al., 2009), *in vitro* studies revealed that high concentrations of Aβ act as a VEGF antagonist, inhibiting VEGR receptor (VEGFR2) activation as well as VEGF-stimulated activation of eNOS in endothelium (Patel et al., 2010; Lamoke et al., 2015; Cho et al., 2017).

Another APP metabolite, the secreted APP-α ectodomain, sAPP-α, has been proposed to modulate angiogenesis by binding to the FGF-2 receptor (FGFR-1). In particular, sAPP-α may counterbalance Aβ anti-angiogenic effect by competing with Aβ and FGF-2 for binding to FGFR-1 (Reinhard et al., 2013). More studies are needed to unravel the dichotomy of Aβ roles on angiogenesis and to establish the exact role of each APP metabolite on angiogenesis.

While the APP soluble metabolites act mostly as ligands, the APP full-length membrane protein function as a membrane receptor and interacts with cell-adhesion molecules and the extracellular matrix. APP extracellular domain binds a series of ECM molecules including collagen, spondin, laminin, reelin and heparan sulfate proteoglycans (glypican and syndecans), and to cell adhesion molecules (CAMs) expressed in neighbour cells, suggesting an important function of APP as an adhesion molecule (Sosa et al., 2017).

Finally, the APP intracellular domain (AICD) plays an important role as a transcriptional regulator and shares many structural and functional similarities with the receptor Notch (Cao & Sudhof, 2001; Kopan & Ilagan, 2004; Hamid et al., 2007; Deyts et al., 2016), suggesting that APP may contribute to the stability of endothelial phenotype by modulating various APP physiological functions including trafficking and signal transduction.

3.3 AIM PAPER 1

The amyloid-β precursor protein (APP) is ubiquitous transmembrane glycoprotein abundantly expressed in the cerebrovascular endothelium, mainly known for its cleavage product Aβ and its detrimental role in the pathogenesis of neurodegenerative disease such as Cerebral Amyloid Angiopathy (CAA) and Alzheimer's disease (AD). Increasing evidence supports the hypothesis that vascular dysfunction plays a major role in CAA and AD and several studies raise the possibility that vascular dysfunction could be an early step in these diseases and could even precede significant Aβ deposition (de la Torre, 2018). Accumulation of neuron-derived Aβ peptides is considered the primary influence driving AD and CAA pathogenesis, however recent studies highlighted the importance of the physiological role of its precursor APP in cell homeostasis, suggesting a potential role of this protein in maintaining tissue homeostasis (Ristori et al., 2020). APP is cleaved by different secretases through two main proteolytic pathways resulting in non-amyloidogenic and amyloidogenic processing, the latter being associated with the disease. Several research lines have focused on the amyloidogenic properties and toxicity of the Aβ peptide, with less regard for the normal cell biological roles of APP and its other cleavage products. In particular, the exact role of APP in cerebrovascular and cardiovascular homeostasis is still unknown.

In this study, we investigated the physiological role of APP full-length in endothelial cells. We showed that loss of APP impairs endothelial cells functionality *in vitro*, by reducing Human Umbilical Vein Endothelial Cells (HUVECs) proliferation, migration and adhesion. We used molecular and proteomic approaches to investigate major cellular targets of APP down-regulation in endothelial cells and we observed that loss of APP alters focal adhesion stability and cell-cell junctions' expression. Moreover, APP is necessary to mediate endothelial response to the VEGF-A growth factor. The data suggest that intact expression and processing of APP are required for normal endothelial function. We propose that APP regulates endothelial cells function by modulating actin-cytoskeleton interacting proteins such as integrins and the Src/FAK signalling.

Further research is needed to investigate the specific role of APP in different vascular beds. We believe that a deep understanding of APP function in maintaining vascular homeostasis might shed light on new therapeutic targets and provide a new perspective on treatment options of neurodegenerative diseases

Article

Amyloid-β Precursor Protein APP Down-Regulation Alters Actin Cytoskeleton-Interacting Proteins in Endothelial Cells

Emma Ristori [1,2], Vittoria Cicaloni [2], Laura Salvini [2], Laura Tinti [2], Cristina Tinti [2], Michael Simons [3,4], Federico Corti [3], Sandra Donnini [1,2,*] and Marina Ziche [2,5,*]

[1] Department of Life Science, University of Siena, 53100 Siena, Italy; emma.ristori@student.unisi.it
[2] Toscana Life Sciences Foundation, 53100 Siena, Italy; v.cicaloni@toscanalifesciences.org (V.C.); l.salvini@toscanalifesciences.org (L.S.); l.tinti@toscanalifesciences.org (L.T.); c.tinti@toscanalifesciences.org (C.T.)
[3] Yale Cardiovascular Research Center, 300 George Street, New Haven, CT 06511, USA; michael.simons@yale.edu (M.S.); federico.corti@yale.edu (F.C.)
[4] Departments of Medicine (Cardiology) and Cell Biology, Yale School of Medicine, New Haven, CT 06511, USA
[5] Department of Medicine, Surgery and Neurosciences, University of Siena, 53100 Siena, Italy
* Correspondence: sandra.donnini@unisi.it (S.D.); marina.ziche@unisi.it (M.Z.); Tel.: +39-0577-235382 (S.D.)

Received: 9 October 2020; Accepted: 17 November 2020; Published: date

Abstract: The amyloid-β precursor protein (APP) is a ubiquitous membrane protein often associated with Alzheimer's disease (AD) and cerebral amyloid angiopathy (CAA). Despite its role in the development of the pathogenesis, APP exerts several physiological roles that have been mainly investigated in neuronal tissue. To date, the role of APP in vasculature and endothelial cells has not been fully elucidated. In this study, we used molecular and proteomic approaches to identify and investigate major cellular targets of APP down-regulation in endothelial cells. We found that APP is necessary for endothelial cells proliferation, migration and adhesion. The loss of APP alters focal adhesion stability and cell–cell junctions' expression. Moreover, APP is necessary to mediate endothelial response to the VEGF-A growth factor. Finally, we document that APP propagates exogenous stimuli and mediates cellular response in endothelial cells by modulating the Scr/FAK signaling pathway. Thus, the intact expression and processing of APP is required for normal endothelial function. The identification of molecular mechanisms responsible for vasoprotective properties of endothelial APP may have an impact on clinical efforts to preserve and protect healthy vasculature in patients at risk of the development of cerebrovascular disease and dementia including AD and CAA.

Keywords: amyloid-β precursor protein; APP; vascular APP; endothelial homeostasis; actin cytoskeleton-interacting proteins; integrins; Src/FAK; VEGFR2/VEGF

1. Introduction

The amyloid-β precursor protein (APP) is a ubiquitous type-1 integral membrane protein that plays an important role in neurovascular degeneration [1]. APP is proteolytically cleaved by secretases, resulting in a series of biologically active fragments, including the amyloid-β peptide characterizing the pathogenesis of Alzheimer's disease (AD) and cerebral amyloid angiopathy (CAA). Despite its major role in AD and CAA, APP cleavage products play diverse physiological

roles that are important for neuronal development and function [2]. APP is involved in tissue repair after traumatic brain injury (TBI), exerting neuroprotective functions [3–5]. Furthermore, APP expression and processing are strongly increased in response to ischemic injury and stress exposure [6,7], suggesting a role in mediating tissue response to external perturbations.

At a cellular level, APP acts as a mechanical linker between the extracellular environment and the cellular cytoskeleton. Full-length APP functions as a membrane cell adhesion molecule in the developing nervous system by binding to several extracellular matrix components (HSPGs, reelin, laminin and F-spondin) and interacting with numerous adaptor proteins and other cell adhesion molecules (integrins, neural cell adhesion molecules) [8–13]. APP presents a conserved YENPTY cytoplasmatic domain similar to non-receptor tyrosine kinases; this motif interacts with scaffold proteins associated with the dynamics of the cytoskeleton and has been shown to regulate gene transcription. These features indicate that APP is involved in propagating extracellular responses [14]. Since neuronal damage is the main cause for cognitive decline in AD and CAA, much effort has been directed to understanding the role of APP in neuronal tissue; however, there is scarce information about its physiological role in other cell types including endothelial cells (ECs).

APP is highly expressed in the endothelium during embryogenesis, suggesting an important role for this macromolecule and its metabolites in vascular development and angiogenesis [15]. Genetic studies in zebrafish and mice revealed defects in vascular development and increased vulnerability to hypoxic injury upon APP gene inhibition [16,17]. More recently, APP was found to have protective properties in the vasculature by regulating expression of endothelial nitric oxide synthase (eNOS) in cerebrovascular endothelium [18].

Increasing evidence supports a hypothesis that vascular dysfunction precedes neuronal degeneration in AD and CAA development and that blood vessels are the origin for a variety of pathogenic pathways that lead to neuronal damage and dementia [19]. Thus, the understanding of the role of APP in ECs and in the vascular system homeostasis is critical to preservation of brain integrity.

Here, we investigated the biological role of APP in ECs homeostasis by generating an in vitro APP-knockdown model using human umbilical vein ECs (HUVECs). The loss of APP resulted in altered cellular morphology and reduction of cell migration and proliferation. We used a proteomic approach to identify biological pathways affected by APP silencing. This demonstrated altered protein expression of actin cytoskeleton-interacting proteins, mainly involved in actin organization, cell adhesion, cell–cell contact and VEGF-mediated angiogenesis in APP-deficient ECs. Integrins and other focal adhesion proteins also showed a reduced expression in ECs with reduced APP levels. Moreover, APP-silenced ECs lost barrier function due to altered expression of tight junctions proteins. Finally, we observed a reduced response to pro-angiogenic stimuli, due to a reduced activation of the VEGF signaling. Taken together, these results suggest that APP can regulate ECs responsiveness to extracellular environment by modulating cytoskeleton-interacting proteins.

2. Materials and Methods

2.1. Cell Cultures

Human umbilical vein endothelial cells (HUVECs) (Lonza, Basel, Switzerland) were used up to passage 7. Cells were cultured on 1% gelatin-coated dishes with endothelial growth medium (EGM-2) (Lonza) supplemented with antibiotics (100 U/mL penicillin and 100 µg/mL streptomycin, Euroclone, Milan, Italy), glutamine (2 mM, Euroclone), and 10% fetal bovine serum (FBS, Hyclone, GE Healthcare, Little Chalfont, UK).

2.2. Small interfering RNA Transfection

Transient knockdown experiments were performed following the Reverse-Transfection of adherence cells protocol adapted from Qiagen (Qiagen, Hilden, Germany). Briefly, siRNAs and Lipofectamine® 2000 (Invitrogen, Carlsbad, CA, USA) were diluted in Opti-MEM (Gibco, Thermo

Fisher Scientific, Waltham, MA, USA) and incubated for 20 min at room temperature to allow the formation of the transfection complex. Confluent cells were then harvested and seeded on top of silencing complexes in 60 mm (3.5×10^5 cells) or 100 mm (6.5×10^5 cells) or 6-well plate dishs (1.8×10^5 cells). Cells were transfected for 48 h under their normal growth conditions (EGM-2, 10% FBS) with 20 nM siRNA control (Negative Control siRNA, Qiagen #0001027310), or 20 nM siAPP-A (Hs_APP_8 FlexiTube® siRNA, Qiagen #SI02776893), or 10 nM siAPP-B (Hs_APP_10 FlexiTube® siRNA, Qiagen #SI02780288), or 20 nM siAPP-C (ON-TARGETplus Human APP (351) siRNA, Dharmacon #J-003731-06-0002). All results showed in main figures refer to HUVEC cells transfected with 20 nM of siAPP-C (Dharmacon Inc., Lafayette, CO, USA).

2.3. Real-time PCR

The RNeasy Plus Kit (Qiagen) was used according to the manufacturer's instructions to extract and prepare total RNA. A total amount of 1 μg RNA was transcribed, and quantitative RT-PCR was performed as previously reported [20]. The following primer sequences were used: APP forward 5′-TGGCCAACATGATTAGTGAACC-3′; APP reverse 5′-AAGATGGCATGAGAGCATCGT-3′; APLP1 forward 5′-CACCAGGTTGTGCCCTTCC-3′; APLP1 reverse 5′-GGCCTCACTCACAAATTCACC-3′; APLP2 forward 5′-CGACGGCACCATGTCAGAC-3′; APLP2 reverse 5′-CAACGAGGCATCACGGC-3′; ZO-1 forward 5′-GTGCCTAAAGCTATTCCTGTGAGTC-3′; ZO-1 reverse 5′-CTATGGAACTCAGCACGCCC-3′; claudin5 forward 5′-CTGCTGGTTCGCCAACATT-3′; claudin5 reverse 5′-TGCGACACGGGCACAG-3′; β-catenin forward 5′-GTCGAGGACGGTCGGACT-3′; β-catenin reverse 5′-CAAATCAGCTTGAGTAGCCATTGTC-3′; VE-cadherin forward 5′-GCACCAGTTTGGCCAATATA-3′; VE-cadherin reverse 5′-GGGTTTTTGCATAATAAGCAGG-3′; FAK forward 5′-ATCCCACACATCTTGCTGACTT-3′; FAK reverse 5′-GCATTCCTTTTCTGTCCTTGTC-3′; SRC forward 5′-CAGTGTCTGACTTCGACAACGC-3′; SRC reverse 5′-CCATCGGCGTGTTTGGAGTA-3′; VEGFR1, VEGFR2, VEGFR3 and ERK 1/2 (Qiagen); GAPDH forward 5′-GCCACATCGCTCAGACACC-3′; GAPDH reverse 5′-AATCCGTTGACTCCGACCTTC-3′. The fold change expression was determined using the comparative Ct method ($2^{-\Delta\Delta Ct}$) normalized to GAPDH housekeeping gene expression. Data are reported as fold change relative to siCtrl, which was set to 1.

2.4. Western Blot

Cells were silenced for 48 h, harvested and seeded (3×10^5 cells) in 6-cm plates. Media were then replaced with EGM-2; 10% FBS and lysate was collected after 24 h. For experiments with VEGF, cells were starved overnight in EBM-2, 0.1% FBS. After 24 h (60% of confluence), cells were treated or not with VEGFa (50 ng/mL, R&D Systems, Minneapolis, MN. USA #293-VE-025) for 5 min. Next, cells were washed and lysed, and an equal amount of proteins was used for Western analysis, as described [21]. The expression of APP (Cell Signaling, Danvers, MA, USA #2450, 1:1000), vinculin (Cell signaling #13901, 1:1000), paxillin (Millipore, Burlington, MA, USA #3794, 1:1000 and Abcam, Cambridge, United Kingdom #ab32084, 1:1000), Integrin β3 (Bioss, Woburn, MA, USA #bs0342R Rabbit, 1:1000), Integrin β1 (Santa Cruz, Dallas, TX, USA #SC6622, 1:1000), kindlin-3 (Cell Signaling #10459, 1:1000), ZO-1 (Thermo Fisher Scientific # 33-9100, 1:1000 and Life Technologies, Carlsbad, CA, USA #61-7300, 1:1000), VE-cadherin (Cell signaling #2500, 1:1000), β-catenin (Cell signaling #9562, 1:1000), claudin5 (Abcam, Cambridge, United Kingdom #ab53765, 1:300 and Thermo Fisher Scientific #35-250, 1:1000), p-VEGFR2 (Y1175, Cell Signaling #2478, 1:1000; Y951, Cell Signaling #4991, 1:1000; Y1059, Cell Signaling #3817, 1:1000), VEGFR2 (Cell Signaling #9698, 1:1000), p-ERK1/2 (T202/Y204, Cell Signaling #4370, 1:2000), ERK1/2 (Cell Signaling #9102, 1:1000), p-Src (Y416, Cell Signaling #6943, 1:1000), Src (Cell Signaling #2110, 1:1000), p-FAK (Y397, Sigma-Aldrich, St. Louis, MO, USA # 8556, 1:1000), FAK (Cell Signaling # 3285, 1:1000), β-actin (Sigma-Aldrich #A5316, 1:10000) and GAPDH (Cell Signaling #2118, 1:2000) were evaluated. Data are reported as fold change of arbitrary densitometry units (A.D.U.) of the target protein with respect to β-actin or GAPDH used as the loading control and normalized for siCtrl sample.

2.5. Immunoprecipitation (IP)

HUVEC cells were cultured in normal growth conditions until they reached confluence. Cells were quickly washed twice with ice-cold PBS, lysed in in 1% Triton lysis buffer and spun at 16,000× *g* for 20 min. 300 μg of cleared lysate was immunoprecipitated for 2 h at 4 °C under gentle rotation with 50 μL/sample of Protein-G DynaBeads (Thermo Fisher Scientific, Waltham, MA, USA), preincubated in 4 μg/sample of anti-VEGFR2 antibody (Cell Signaling #9698). Beads were washed 3 times with PBS, resuspended in 20 μL of 1× loading buffer and boiled for 10 min at 70 °C. Samples were analyzed by western blot as described above using anti-APP and anti-VEGF antibodies.

2.6. Immunofluorescence Microscopy

Cells were transfected with siRNA for 48 h as described above. Silenced HUVEC cells were then harvested and seeded (8×10^4 cells) on 10 mm ø on glass coverslips pre-coated with 1% gelatin in triplicate in EBM-2 10% FBS. After 24 h cells were fixed with fresh 4% PFA for 10 min, blocked with 3% BSA for 40 min and incubated at 4 °C overnight in primary antibody. The following primary antibodies were used: rabbit anti-APP (Cell Signaling #2452, 1:100), mouse anti-APP (Cell Signaling #2450, 1:100); rabbit anti-vinculin (Cell signaling #13901, 1:100), rabbit anti-ZO-1 (Life Technologies #61-7300, 1:50), mouse anti-VE-cadherin (Santa Cruz #sc-9989, 1:200), mouse anti-claudin5 (Thermo Fisher #35-2500, 1:200), mouse anti- β-catenin (Cell Signaling #2677 1:200). The day after, cells were washed 3 times, 5 min each with 0.5% BSA in PBS and incubated for one hour at room temperature in secondary antibody: Alexa Fluor 488-labeled anti-Mouse (Thermo Fisher #A-11001, 1:400) and anti-Rabbit (Thermo Fisher #A-11008, 1:400) or Alexa Fluor 555-labeled anti-Mouse (Thermo Fisher #A32727, 1:400) and anti-Rabbit (Thermo Fisher #A32732, 1:400). For actin cytoskeleton staining, cells were incubated with conjugated DyLight 488-Phalloidin (Thermo Fisher #12379, 1:50) for 30 min at room temperature. DAPI (Thermo Fisher Scientific #62248, 1:1000) was used to counterstain nuclei. Stained cells were mounted and viewed by confocal microscopy (Leica SP5 with 63× oil objective, Leica, Wetzlar, Germany).

2.7. Cell Proliferation Assay

Cell viability was determined by MTT test [22] HUVECs were first silenced for 48 h. Transfected cells were then harvested and seeded in a 96-mutiwell plate (3×10^3 cells/well) and incubated in EGM-2, 1% FBS for 18 h and 24 h. Cells were exposed for 4 h to 1.2 mM MTT (3-[4,5-dimethylthiazol-2-yl]-2,5-diphenyltetrazolium bromide; Sigma-Aldrich, St. Louis, MO, USA) in fresh PBS (without phenol red). After the solubilization of formazan crystals in DMSO, absorbance was measured with a microplate absorbance reader (Infinite 200 Pro SpectraFluor; Tecan, Männedorf, Switzerland) at 540 nm. Data are reported as the fold change of absorbance units (at 540 nm), taking as reference the siCtrl sample.

2.8. Wound Healing Scratch Assay

ECs migration was assessed using an in vitro wound healing assay as previously reported [20]. Briefly, cells were silenced for 48 h as previously described. Transfected cells were then harvested and seeded on a 24-mutiwell plate (1×10^5 cells/well) and incubated under their normal growth conditions (EGM-2, 10% FBS) until they reached complete confluence (18–24 h). A sterile 1000 μL micropipette tip was used to scrape the confluent monolayer and create the wound. Wells were washed twice with PBS and cells were exposed to EBM-2 and the indicated treatment (0.1% FBS; 10% FBS or 50 ng/mL VEGFa). 2.5 mg/mL ARA-C (Cytosine β-D-arabinofuranoside; Sigma-Aldrich) was added to the wells to suppress cell proliferation. Images of the wound in each well were acquired from 0 h to 8 h, 18 h and 24 h under a phase contrast microscope at 10x magnification. Finally, cells were fixed and stained with the PanReac kit. Results were quantified using ImageJ software, and data are reported as % of scratch closure normalized to siCtrl.

2.9. Cell Adhesion Assay

HUVEC were silenced as previously described; after 48 h, cells were harvested and seeded in triplicate in 96-well plates (2×10^4 cells/well) pre-coated with fibronectin (3 μg/mL) or collagen I (1 μg/mL) as previously described [23]. For short-term adhesion assays, attached cells were quantified after 1 h; for de-adhesion assays, cells were incubated for 18 h in normal growth conditions. At the end of the assay period, cultures were rinsed with two gentle washes with PBS (with Ca/Mg), fixed for 5 min with 4% paraformaldehyde and stained for 20 min with 0.5% Crystal Violet in distilled water for 20 min. Excess crystal violet was removed, and the cells were washed with water. The plates were dried and the stain extracted by 100 μL of methanol for 5 min. Absorbance was read at 540 nm in a plate reader (Infinite 200 Pro, SpectraFluor, Tecan, Männedorf, Switzerland).

2.10. In Vitro Permeability Assay

Cells were silenced for 48 h, harvested and seeded (2×10^5 cells/well) on gelatin-coated insert membranes (0.4 μm diameter pores, Corning, New York, USA), and the inserts were placed in 12-multiwell plates and incubated for 48 h in normal growth conditions (EGM-2, 10% FBS). Confluent monolayers were then starved with EBM-2 with 0.1% FBS for 4 h and treated with IL-1β (10 ng/mL) for 6 h [24]. FITC-Dextran (3 kDa, 10 μm) was used as a fluorescent marker of permeability, which was evaluated after 15 min by measuring the fluorescence in a plate reader (Infinite 200 Pro, SpectraFluor, Tecan, Männedorf, Switzerland) at 485/535 nm (excitation/emission). Data are reported as fold change of fluorescence units (RFU), taking as reference the siCtrl sample in the condition of medium EBM-2 with the addition of 0.1% serum (control condition).

2.11. Tube Formation Assay

HUVEC were silenced for 48 h, harvested and seeded (3×10^4 cells/well) on Corning® Matrigel®-coated 48-well plate in EBM-2, 0.1% FBS medium (control condition) or VEGFa (50 ng/mL, R&D Systems #293-VE-025). After 8 h of incubation, ECs were photographed and network formation on Matrigel was measured by means of the number of mashes per field (Nikon Eclipse E400 and camera Nikon DS-5MC, Nikon, Melville, NY, USA).

2.12. LC-MS/MS Proteomic and Bioinformatic Analysis

Control and silenced HUVEC were lysed in 2% Sodium deoxycholate (SDC)/100 mM ammonium bicarbonate, reduced with 5 mM tris-(2-carboxyethyl)-phosphine (TCEP) and alkylated in the dark with 10 mM iodoacetamide (IAA). Protein quantification was assessed using Pierce-BCA protein assay kit. 60 μg of proteins, for each sample, were processed adding trypsin (1:40) and incubated at 37 °C overnight. All reaction mixtures were acidified with 1% formic acid (FA) [25,26]. Digested samples were desalted using OASIS cartridges and reconstituted in 0.1% formic acid in water/acetonitrile (97/3, *v*/*v*). LC-MS/MS analyses were performed using a Q-Exactive Plus Orbitrap mass spectrometer (Thermo Fisher Scientific). These experiments were carried out using a DDA setting to select the "top twelve" most-abundant ions for MS/MS analysis. MS data analysis was conducted using a Proteome Discover 2.1 (Thermo Fisher Scientific). Functional annotation analysis was performed using DAVID 6.8 [27] and FunRich 3.1.3 [28]. The default peak-picking settings were used to process the raw MS files in MaxQuant (version 1.6.1.0), Perseus (version 1.6.1.1) and its integrated search engine Andromeda [29,30]. The protein quantification and calculation of statistical significance was carried out using two-way Student-t test and error correction (p value < 0.05) with the method of Benjamini–Hochberg. For further visualization, a Principle component analysis (PCA) [31], a heatmap graphic analysis with clustering tree and, to detect differentially expressed proteins, a volcano plot analysis were performed.

2.13. Statistical Analysis

Results are expressed as means ±SEM. Statistical analysis was generated by GraphPad software Prism 7 (San Diego, CA, USA). Student's *t*-test and Mann-Whitney U-test were applied to determined statistical differences between conditions. $p < 0.05$ was considered statistically significant.

3. Results

3.1. Loss of APP Affects Endothelial Cells Proliferation, Migration and Cytoskeleton Organization In Vitro

To study the physiological role of APP in ECs, we knocked down APP gene expression in HUVEC cells using an siRNA strategy. We started our experimental approach by selecting three different siRNAs, two targeting the 3'UTR region (siAPP-A and siAPP-B) and one targeting the APP mRNA coding sequence (siAPP-C). All three siRNAs (siAPP-A, siAPP-B and siAPP-C) knocked down significantly APP mRNA and protein expression after 48 h post transfection, as confirmed by RTqPCR analysis and western blot (WB) (Figures 1A,B and S1A,B). In mammals, the APP gene family includes, besides APP, two genes encoding the APP-like proteins (APLP1 and APLP2) that share similar structural organization and partially overlapping functions [32]. To confirm the specificity of APP knockdown, we checked relative mRNA expression levels of APP homologues genes APLP1 and APLP2 upon silencing with siAPP-A, -B or -C respectively, and observed that siAPP-C was the only siRNA that didn't show any off-target effect (Figures 1A and S1C,D). Moreover, the siAPP-C was the only siRNA with no effect on cell survival, as both siAPP-A and siAPP-B significantly induced caspase-3 activation after 48 h transfection (Figure S1E,F). Taking into account these findings, we therefore used siAPP-C as the specific siRNA to knockdown APP (hereinafter referred to as siAPP).

We then investigated the effect of APP silencing on cell proliferation and migration of HUVEC cells. The MTT assay showed a reduction of cell proliferation 24 h after siRNA transfection in ECs silenced for APP (siAPP) compared to control siRNA treated cells (siCtrl) (Figure 1C). The wound healing scratch assay showed normal migration at 8 h after scratch and a significant reduction of migration rate at 18 and 24 h after scratch (Figure 1D).

To understand if the migratory defect was due to cytoskeletal disorganization, we labeled control cells (siCtrl) and APP-silenced cells (siAPP) with an anti-APP antibody and F-actin stress fibers marker (Phalloidin). APP immunoreactivity was observed at the cell membrane, in the cytoplasm and in the Golgi of siCtrl HUVEC, and was expectedly lost in siAPP cells. APP-silenced cells appeared bigger and flatter and the phalloidin staining showed an altered organization characterized by shorter and thicker actin stress fibers, suggesting a potential role of APP in controlling assembly, disassembly or rearrangement of cytoskeletal structures (Figure 1E).

Altogether, our data suggest that APP is involved in ECs migration, proliferation and a correct cytoskeleton organization.

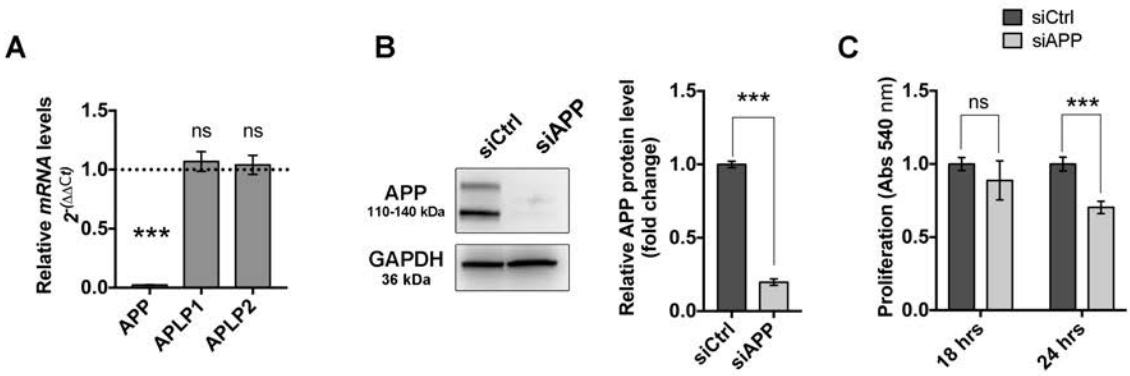

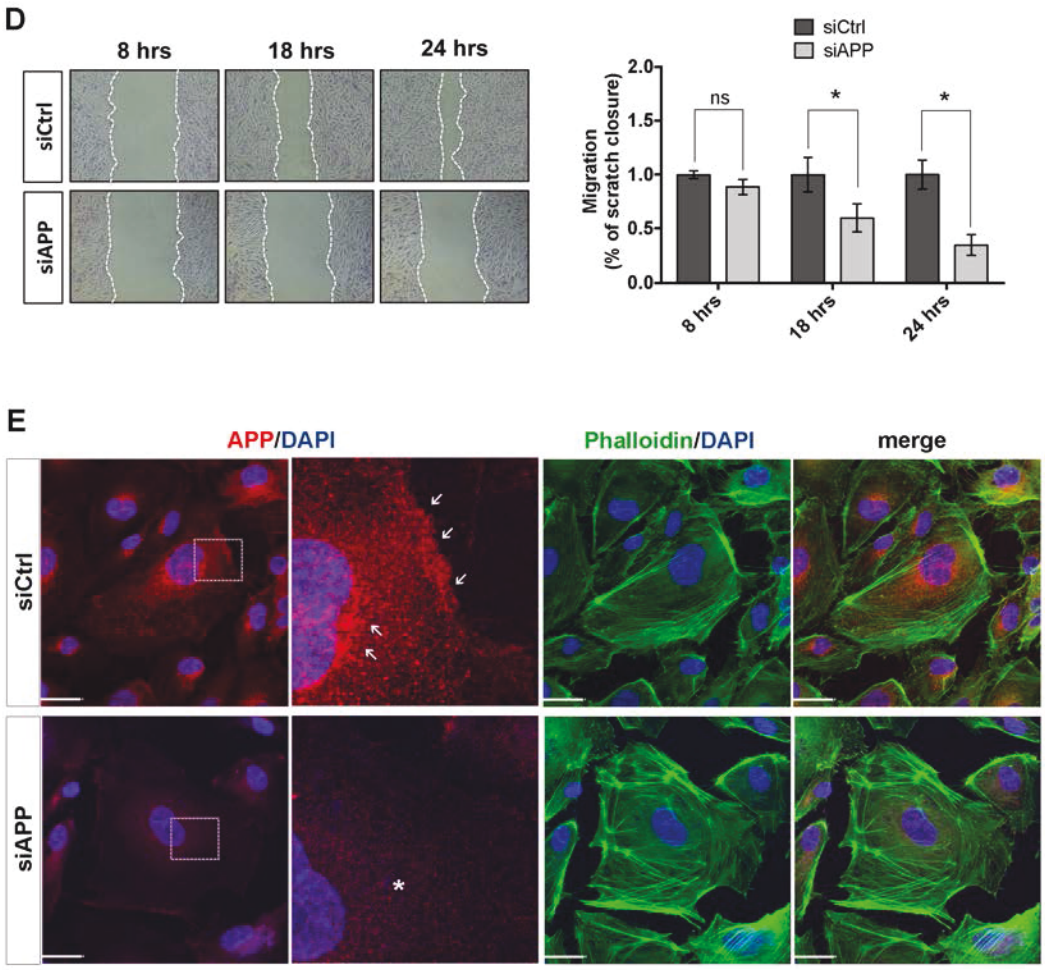

Figure 1. Amyloid precursor protein (APP) silencing reduces human umbilical vein EC (HUVEC) cell survival, migratory response and affects cytoskeleton organization: (**A**) mRNA expression levels are assessed by RTqPCR, relative mRNA levels of APP are significantly reduced upon silencing with siAPP for 48 h, while expression of homologues genes APLP1 and APLP2 is not affected, demonstrating the specificity of siRNA silencing with selected siAPP. GAPDH was used as housekeeping gene. Values are normalized to siCtrl (mean ± SEM; n 3 replicates; *** $p < 0.001$, ns not significant); (**B**) Western blot showing protein expression levels of APP following APP knockdown. Silencing of APP with siAPP-C for 48 h reduces APP protein levels. GAPDH was used as the internal control for western blotting. Data are presented as the means ± standard error of the mean (SEM); n 5 replicates; *** $p < 0.001$; (**C**) MTT assay at 18 h and 24 h post transfection showing a reduction of cell proliferation of silenced cells compared to siCtrl starting from 24 h after transfection (mean ± SEM; n 5 replicates; *** $p < 0.001$, ns not significant); (**D**) Wound healing scratch assay at 8 h, 18 h and 24 h post transfection, showing a reduction of migration rate in HUVEC silenced for APP starting from 18 h after transfection (mean ± SEM, n 5 replicates, * $p < 0.05$); (**E**) Immunofluorescence staining of control (siCtrl) and silenced (siAPP) HUVEC cells showing in red APP protein expression and in green F-actin stress fibers (Phalloidin-488), nuclei were stained with DAPI (blue). White arrows show APP high expression at the cell membrane and in the Golgi of siCtrl HUVEC; white asterisk show loss of APP expression in siAPP cells. Scale bar 25 μm.

3.2. Proteomic Analysis Confirms the Cytoskeleton Organization Defect and Reveals Alteration of Vascular Specific Pathways in APP-Silenced Cells

To investigate further the effect of APP on ECs biology, we performed a proteomic analysis to gain a comprehensive and quantitative description of changes in protein expression that occur in HUVEC cells upon APP silencing. We used a free-label quantification (LFQ) approach to directly compare relative abundance of proteins obtaining an unbiased insight into protein expression changes. To identify and quantify proteins, liquid chromatography followed by mass spectrometry (LC-MS) was performed on control HUVEC (siCtrl) and HUVEC silenced for APP (siAPP). Cells were silenced for APP for 48 h and samples were collected 24 h after siRNA transfection, maintaining the same experimental conditions of the results previously described.

Protein identification and quantification was performed with MaxQuant using the Uniprot_Homo sapiens (proteome:up000005640) database (search parameters were 20 ppm tolerance on peptides, 0.02 Da on fragments, and less than 1% false discovery rate, FDR). We identified 1225 and 1396 proteins for three biological replicates of siCtrl and siAPP, respectively (Figure S2A). To gain insight into the global similarities and differences between the six groups (siCtrl1, siCtrl2, siCtrl3 and siAPP1, siAPP2, siAPP3), we first performed an unsupervised clustering analysis that showed a differential clustering between siCtrl (siCtrl1, siCtrl2, siCtrl3) and siAPP (siAPP1, siAPP2, siAPP3) samples (Figure S2B). The principle component analysis (PCA) of all replicates of siCtrl and siAPP samples confirmed the clear proteomic differentiation between the two datasets (Figure S2C).

We then performed a functional comparison between the siCtrl common dataset and siAPP common dataset using FunRich software to analyze differences (p value < 0.001) in cellular components and biological processes (Figures 2A,B and S2D). We observed a reduction, in the expression of proteins involved in membrane (GO:0016020) and cytoskeleton (GO:0005856) cellular components (Figure S2D). In line with the previously described functional data, we observed a decrease of proteins associated with cell proliferation (GO:0008283) in the siAPP sample compared to the control (Figure 2B). We also found an evident reduction of proteins involved in cytoskeleton organization (GO:0030036) in the silenced sample (Figure 2B), confirming the defect in actin cytoskeleton of siAPP HUVEC cells previously described (Figure 1E).

The differential abundance of the 1158 common proteins was illustrated by volcano plot. A two-way Student-t test (p value < 0.05) was employed using Perseus software (v 1.6.1.1) to define the proteins that were differentially regulated in siAPP and siCtrl samples. The following criteria were applied: siCtrl–siAPP ≥ ±1.5, permutation-based FDR value set at 0.05. Proteins with a p-value less than 0.05 were considered statistically significant. We quantified 68 up-regulated and 105 down-regulated proteins in the siAPP HUVEC compared to the control group (siCtrl) (Figure 2C, Table S1). We identified a significant differential expression of proteins mainly involved in actin cytoskeleton organization (GO:0030036), in cell adhesion (GO:0007155) and in cell–cell junction organization (GO:0045216). In particular, we observed a down-regulation of actin-binding proteins involved in cytoskeleton regulation and dynamics such as radixin (RADI), α-actinin1 (ACTN1) and DPLI-1 and of proteins involved in promoting endothelial cell adhesion and migration such as integrins (ITGA2; ITGB1), and the integrin-activator kindlin3 (FERMT3) (Figure 2C,D).

We finally assessed differential expression of proteins involved in angiogenesis and vascular development and observed that endothelial markers such as VEGFR-2 (KDR) and VE-cadherin (CADH5) were not affected by the APP knockdown (Figure 2E). However, therefore was an up-regulation of endothelial activation markers such as ICAM-1, s-100 (S100), stabilin-1 (STAB1) and Fibronectin (FINC), indicating a role of APP in vascular inflammation (Figure 2E).

Collectively, these data confirm the presence of proliferation, migration and cytoskeleton organization defects observed in siAPP HUVEC and identify a significative change in ECs anchoring to the extracellular matrix, as well as in the interaction between adjacent ECs. This suggests the involvement of APP in vascular stability, integrity, and responsiveness to exogenous stimuli.

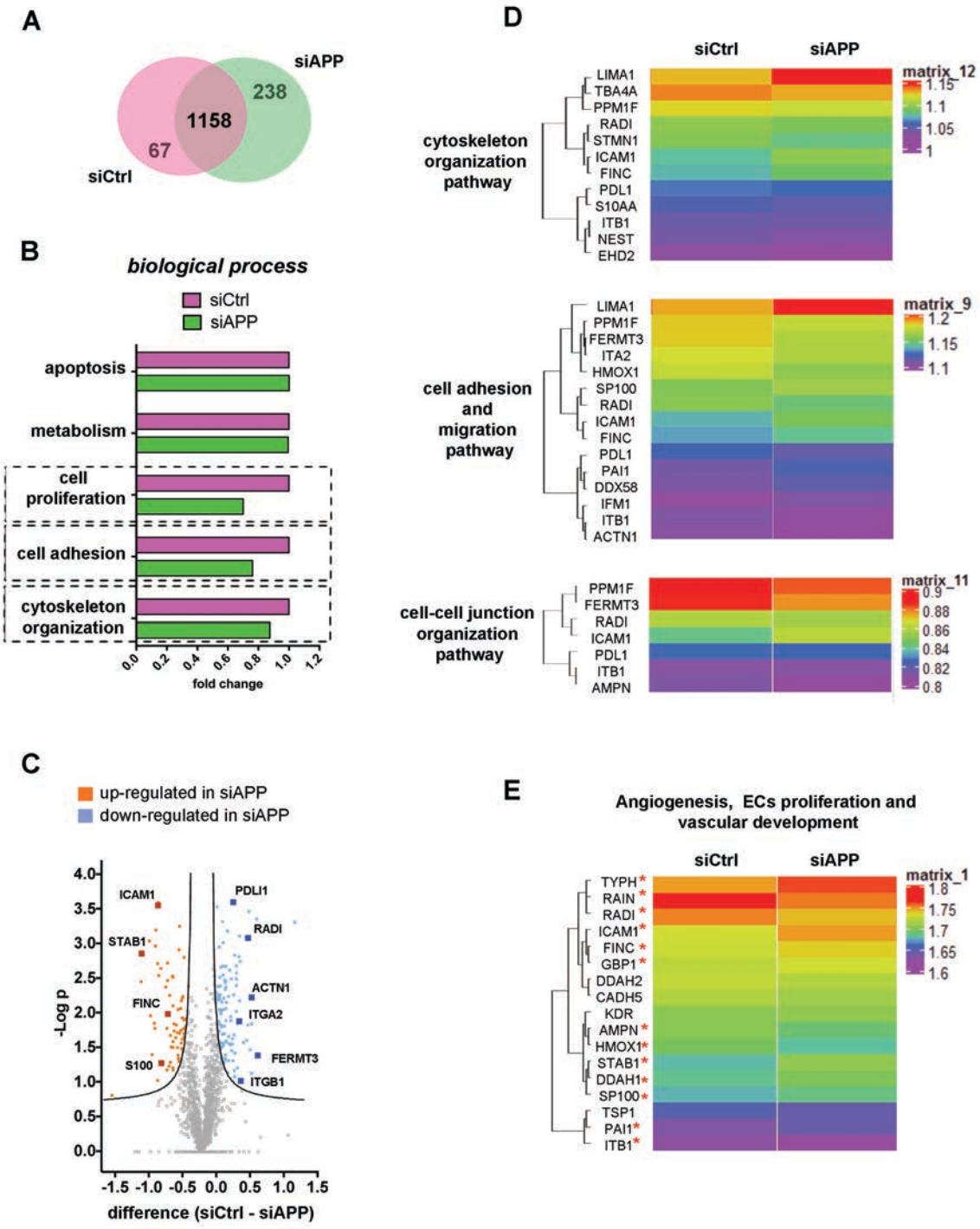

Figure 2. Proteomic analysis reveals a reduction of cytoskeleton and cell–cell, cell–extracellular matrix interaction proteins: (**A**) Venn diagram representing the number of common proteins in siCtrl and siAPP common datasets; (**B**) Functional comparison between siCtrl common dataset and siAPP common dataset using FunRich software reveals differences in cell proliferation, cell adhesion and cytoskeleton organization (p-value < 0.001). A fold change is calculated to show a functional comparison and reveals a reduction in the percentage of proteins involved in different biological processes; (**C**) The Volcano plot was constructed to show the significantly differentially expressed proteins between two datasets. Proteins with statistically significant differential expression (siCtrl–siAPP ≥ ±1.5, FDR < 0.05) are located in the top right and left quadrants. The orange points represent significantly upregulated proteins in siAPP and the blue points represent significantly downregulated proteins in siAPP; (**D**) The heat maps show proteins with statistically

significant differential expression; (**E**) The heat map shows the differential expression of proteins present in siAPP and siCtrl common database and specifically involved in vascular development, angiogenesis and ECs proliferation. Only proteins with red asterisk show statistical significance.

3.3. APP Silencing Affects Endothelial Cells Adhesion and Promotes a Reorganization of Focal Adhesions Complex

To confirm our proteomics results, we further investigated the role of APP on HUVEC cell-matrix adhesion and focal adhesions organization. We first assessed siAPP cell-matrix adhesion by investigating cell attachment on two different integrin's substrates, collagen I and fibronectin. HUVECs use predominantly α1β1 and α2β1 to adhere to collagen I and α5β1, α4β1 and αVβ3 to adhere to fibronectin [33]. Loss of APP prevented HUVEC cell attachment on both substrates (Figure 3A,B).

Moreover, loss of APP led to a reduction of protein expression of integrin β1, integrin β3 and the integrin activator kindlin-3 (FERMT3) in siAPP cells, validating our proteomic results (Figure 3C).

Integrin-dependent cell adhesion is predominantly mediated by focal adhesion proteins that link the integrins domains to the actin cytoskeleton to form the adhesion complex [34]. Thus, the down-regulation of integrin β expression might result in an altered organization of other focal adhesion components. To test this, we analyzed the expression levels of paxillin and vinculin, important components of focal adhesions [35]. Western blot analysis showed reduced protein expression levels of paxillin, but not vinculin in siAPP HUVEC (Figures 3D and S4). However, while siCtrl cells showed a clear localization of vinculin to the cell membrane, siAPP cells presented a less organized expression (Figure 3E, arrows).

Taken together these results demonstrate that loss of APP interferes with the integrin β-mediated cell adhesion by modulating focal adhesion proteins expression and organization.

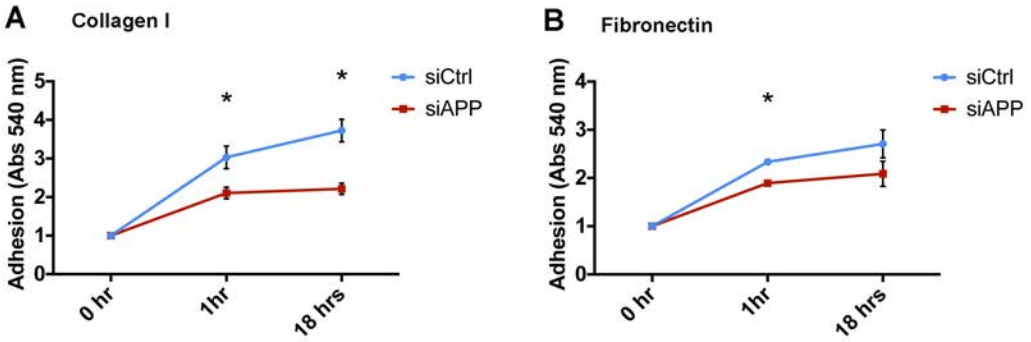

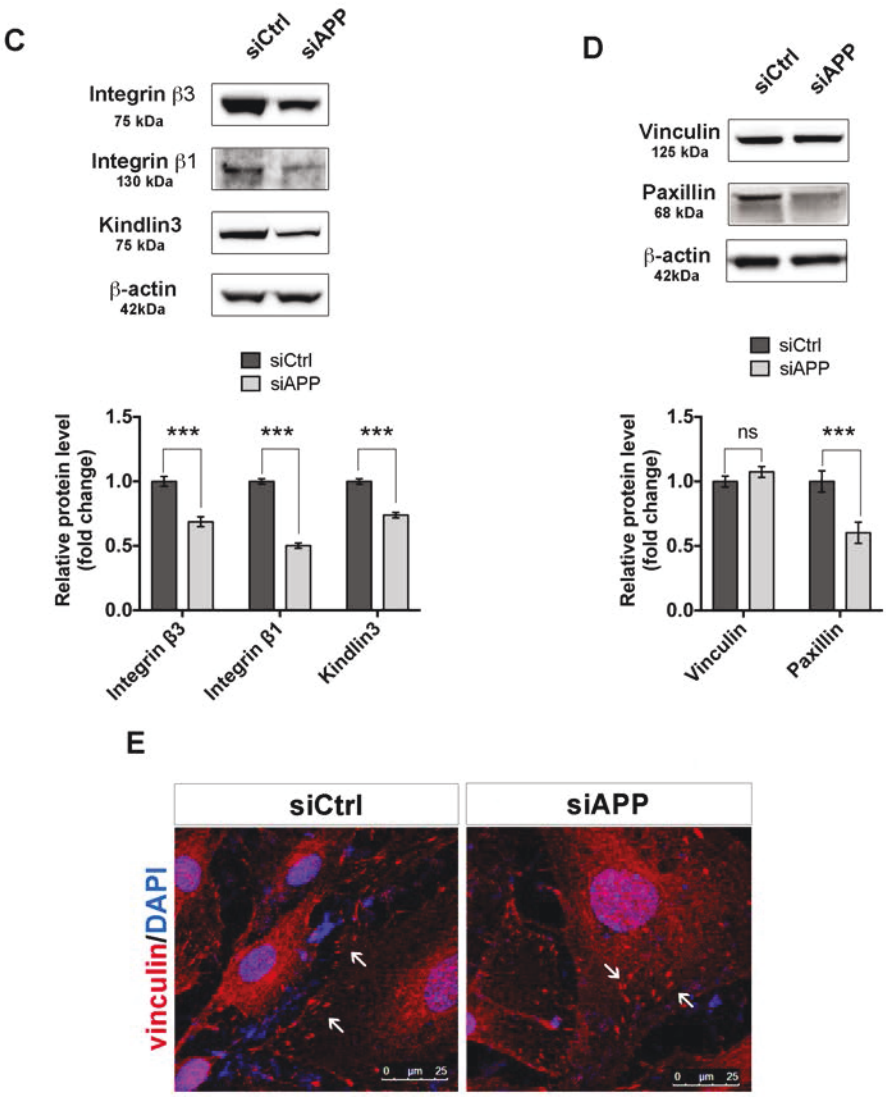

Figure 3. APP silencing affects HUVEC cell adhesion and focal adhesion organization and expression: Adhesion assay performed on collagen I (1 µg/mL) (**A**), and fibronectin (3 µg/mL) (**B**) coatings at different time-points (1 h, "short term adhesion", and 18 h "de-adhesion") (triplicate wells, n 3). Attached cells were quantified by Crystal Violet staining and absorbance (Abs) measured at 540 nm wavelength. Values are represented as mean ± SEM; * $p < 0.05$; (**C**) Western blot analysis of integrin β1, integrin β3 and kindlin3 protein expression in control and silenced HUVEC cells. The bar graph shows quantification of 4 replicates (n 4). β-actin was used as the internal control. Data are presented as the means ± SEM, *** $p < 0.001$; (**D**) Western blot analysis of focal adhesion proteins in control and silenced HUVEC cells. The bar graph represents the fold changes of the relative levels of focal adhesion proteins normalized to siCtrl. β-actin was used as the internal control. Data are presented as the means ± SEM, n 4 replicates, *** $p < 0.001$, ns not significant; (**E**) Subconfluent siCtrl and siAPP HUVEC cells stained for vinculin. White arrows indicate abnormal vinculin localization in siAPP cells compared to siCtrl. Scale bar 25 µm.

3.4. APP Controls Endothelial Barrier Function

Integrin-mediated cell-matrix adhesion, as well as endothelial cell junctions-mediated cell–cell adhesion, is essential for maintenance of endothelial monolayer barrier function [36–38].

Our proteomic data showed a reduced abundance of proteins involved in cell–cell junction organization, indicating a possible defect in permeability in HUVEC cells lacking APP. To test this,

we performed an in vitro permeability assay using confluent monolayers of siCtrl and siAPP HUVECs. We observed a significant increase of cellular permeability in HUVECs lacking APP under basal conditions (CTRL). To stress the system, we treated cells with interleukin-1 beta (IL-1 β), a pleotropic cytokine known to induce endothelial permeability [39]. IL-1β (10 ng/mL, 6 h) induced a significant increase in paracellular flux of FITCH-dextran in both siCtrl and siAPP cells; however, siAPP HUVEC cells showed an almost 4 fold-change increase when compared to siCtrl (Figure 4A). These results suggest a higher susceptibility to pro-inflammatory stimuli of ECs in the absence of APP.

Endothelial cell junctions, such as adherens junctions and tight junctions, have a critical role in maintaining vascular integrity. Modifications in the expression and organization of these cellular components increase endothelial permeability and vascular fragility in vivo [40,41]. We, therefore, assessed the expression and organization of the tight junction proteins ZO-1 and claudin5 and of the adherens junction proteins VE-cadherin and β-catenin in siAPP confluent HUVEC.

Immunostaining for ZO-1 and claudin5 revealed a reduction in tight junctions and ZO-1 localization at cell–cell contacts of siAPP HUVEC (Figure 4B, asterisk and white arrows). We also observed a reduction in the intensity of β-catenin staining, but no obvious defect in VE-cadherin expression and distribution (Figure 4B, white arrows). The reduction in the total amount of ZO-1, claudin5 and β-catenin protein levels was further confirmed by western blot analysis (Figure 4C and S4). mRNA expression levels were not affected by loss of APP, suggesting a defect in proteins stability (Figure 4D). Although VE-cadherin expression was unaffected by the silencing, the reduction of β-catenin protein levels indicated a defect in VE-cadherin activity. Altogether these data suggest that APP is involved in modulating the stability and localization of endothelial cell junctions.

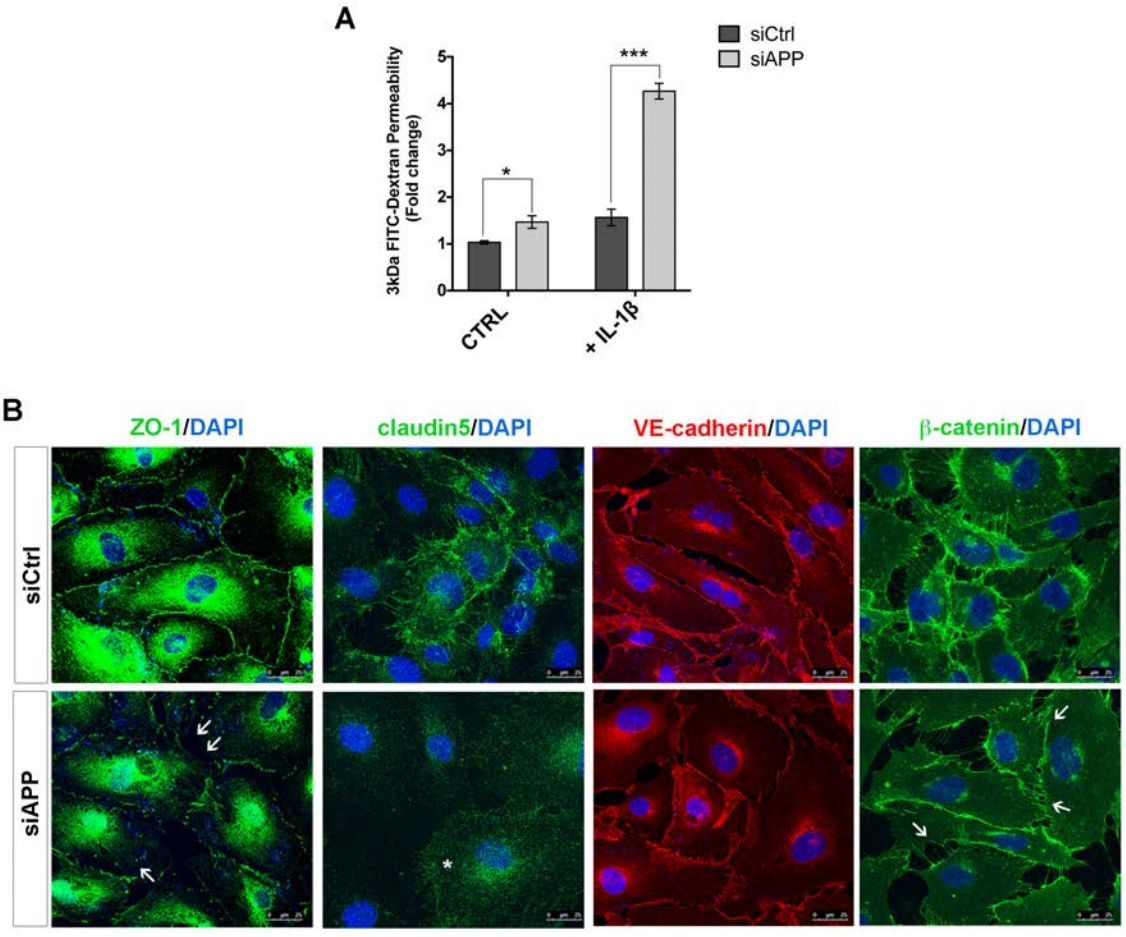

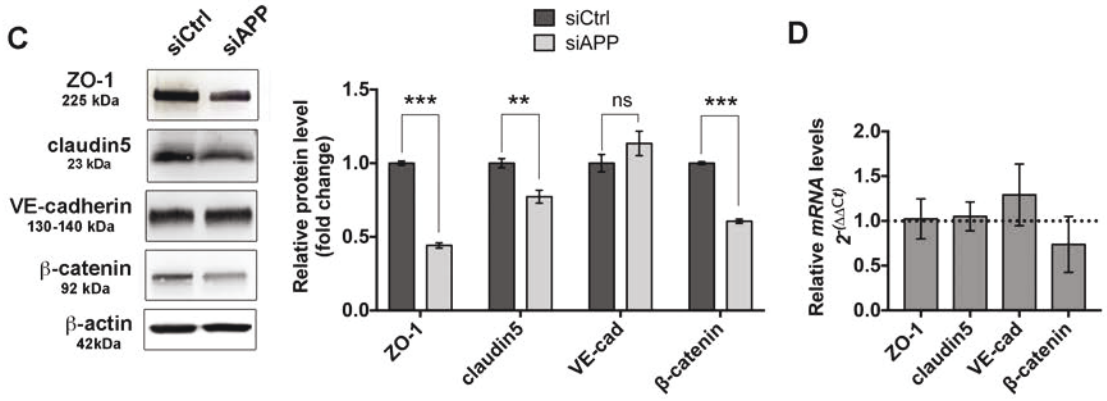

Figure 4. Loss of APP affects HUVEC monolayer barrier function: (**A**) Silenced and control HUVEC were grown on gelatin-coated insert membranes for 48 h after transfection to ensure confluence and treated with or without IL-1β (10 ng/mL) for 6 h. Permeability was measured using the tracer molecule FITC-dextran (3 kDa). Data are reported as fold change relative to siCtrl in basal conditions (mean ± SEM, n 3 replicates, * $p < 0.05$, *** $p < 0.001$); (**B**) Confluent silenced and control HUVEC were labeled for ZO-1 (green), claudin5 (green), VE-cadherin (red) and β-catenin (green). Staining shows a decreased claudin5 expression (asterisk) and reduced ZO-1 and β-catenin expression and organization at the cell–cell contact sites (white arrows) in cells silenced for APP. Scale bar 25 μm; (**C**) Western blot analysis of cell–cell junction proteins expression. The bar graph shows a significative reduction of ZO-1, claudin5 and β-catenin protein expression upon APP silencing (mean ± SEM, n 3 replicates, ** $p < 0.01$, *** $p < 0.001$, ns not significant); (**D**) RTqPCR showing unchanged mRNA expression.

3.5. APP Modulates Endothelial Response to Pro-Angiogenic Stimuli

Integrins and monolayer integrity are essential for vascular tissue homeostasis and endothelial responsiveness to angiogenic factors. We hypothesized that loss of APP, and the consequent deregulation of integrin expression would reduce endothelial cell ability to respond to extracellular stimuli including growth factors, thus negatively affecting angiogenesis.

To investigate the effect of APP silencing on angiogenesis we stimulated siCtrl and siAPP HUVECs with VEGF and measured VEGF-mediated cell migration and cell proliferation. The wound healing scratch assay showed that APP silencing significantly inhibited cell migration in response to VEGF at 8 h after scratch. Interestingly, silenced cells migrated normally in presence of 10% FBS, indicating that the defect observed was due to a dysregulation of VEGF-mediated signaling (Figure 5A). Moreover, silencing of APP also reduced the cell proliferation in response to VEGF treatment (Figure 5B).

We then investigated the ability of siAPP HUVEC seeded on Matrigel layer to form capillary-like tube structures in response to VEGF (50 ng/mL, 8 h). VEGF significantly promoted tube formation in siCtrl sample, while the formation of web/net-like structures was significantly inhibited in siAPP cells (Figure 5C).

To further support the hypothesis that the loss of APP affects the VEGF-mediated signaling, we analyzed activation of the VEGF_receptor-2 (VEGFR2) in response to VEGF. We observed that APP silencing significantly suppressed VEGFR2 phosphorylation following VEGF stimulation at its major phosphorylation sites, located, respectively, in the kinase insert domain (Y951), in catalytic domain (Y1054/1059), as well as in the carboxy-terminal domain (Y1175). Interestingly, we did not observe a decrease of VEGFR2 total protein and mRNA expression (Figure S3A,B). Notably, VEGFR2 was unable to immunoprecipitate APP, suggesting that VEGFR2 and APP do

not interact or form a complex (Figure S3C). Taken together, these results suggest that APP controls ECs response to VEGF by indirectly modulating VEGFR2 activation.

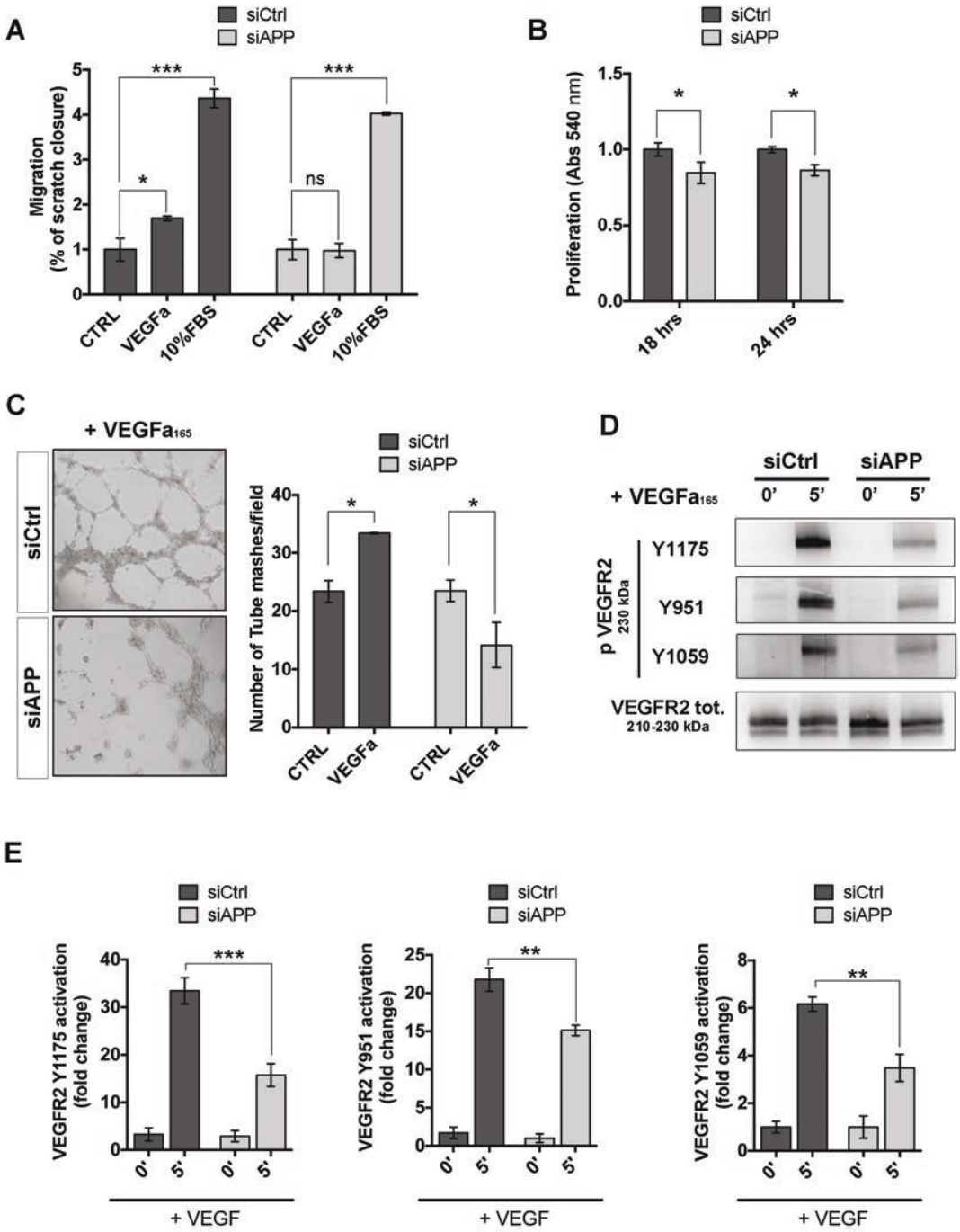

Figure 5. APP controls HUVEC response to angiogenic factors and modulates VEGFR2 activation: (**A**) Wound healing scratch assay at 8 h post transfection, showing a reduction of migration rate in HUVEC silenced for APP exposed to VEGFa (50 ng/mL) stimulation but not to 10% fetal bovine serum (FBS) (mean ± SEM, n 4 replicates, * $p < 0.05$, *** $p < 0.001$, ns not significant); (**B**) MTT assay at 18 h and 24 h post transfection of VEGFa treated cells (50 ng/mL, 18 and 24 h respectively) showing a reduction of cell proliferation of silenced cells with siAPP compared to siCtrl (mean ± SEM; n 3 replicates; * $p < 0.05$); (**C**) Tube formation assay showing a reduced angiogenic response

of siAPP cells. On the left, representative pictures of HUVEC network (10× magnification); On the right, quantification of number of mashes per picture (mashes/field) of silenced and control HUVEC seeded on Matrigel coating and treated with VEGFa (50 ng/mL) for 8 h. The results represent the mean ± SEM of 5 pictures (fields), * $p < 0.05$; (**D**) Western blot analysis showing evident reduction of VEGFR2 activation (phospho VEGFR2 Y1175, Y951 and Y1059) in APP-silenced cells stimulated with VEGFa (50 ng/mL) for 5 min; (**E**) Quantification of the immunoblots in c), The bar graphs represent the relative level of p-VEGFR2 Y1175, Y951 or Y1059 over total VEGFR2 in siCtrl and siAPP samples as determined by band density analysis (mean ± SEM, n 4 replicates, ** $p < 0.01$, *** $p < 0.001$).

3.6. APP Modulates Src/FAK Signaling

We next investigated the activation of VEGF–VEGFR2 downstream signaling in APP-silenced cells. HUVEC cells were transfected with siCtrl or siAPP for 48 h and then stimulated with VEGF (50 ng/mL). VEGFR2 phosphorylation at Y1175 site promotes ECs proliferation and migration through ERK pathway activation. Consistently with VEGFR2 Y1175 reduced activation, we found a significant reduction in p-ERK in siAPP HUVEC treated with VEGF, while total ERK protein and mRNA levels were unchanged (Figures 6A,B and S3B).

VEGFR2 phosphorylation by VEGF also activates the Src/FAK pathway to promote ECs migration and adhesion. However, Src can be also activated by integrins binding to extracellular matrix, making the Src/FAK pathway a meeting point between growth factors-mediated and integrins-mediated ECs proliferation, migration and survival.

We found that phosphorylation of Src at Y416 site, as well as phosphorylation of FAK at one of the Src-target sites (Y396) were significantly reduced in APP-silenced HUVEC when exposed to VEGF (Figure 6C,E). Total Src protein levels, but not mRNA levels were reduced by APP knockdown (Figures 6D and S3B). FAK total protein expression was unchanged, while mRNA levels were slightly up regulated by APP silencing, probably due to a compensatory mechanism (Figures 6F and S3B).

Notably, phosphorylation of ERK, Src and FAK was significantly reduced also at basal conditions in siAPP HUVEC, suggesting that APP regulates focal adhesion components phosphorylation independently of VEGFR2 activation (Figure 6G).

Taken together these data strongly indicate that APP controls Src/FAK pathway.

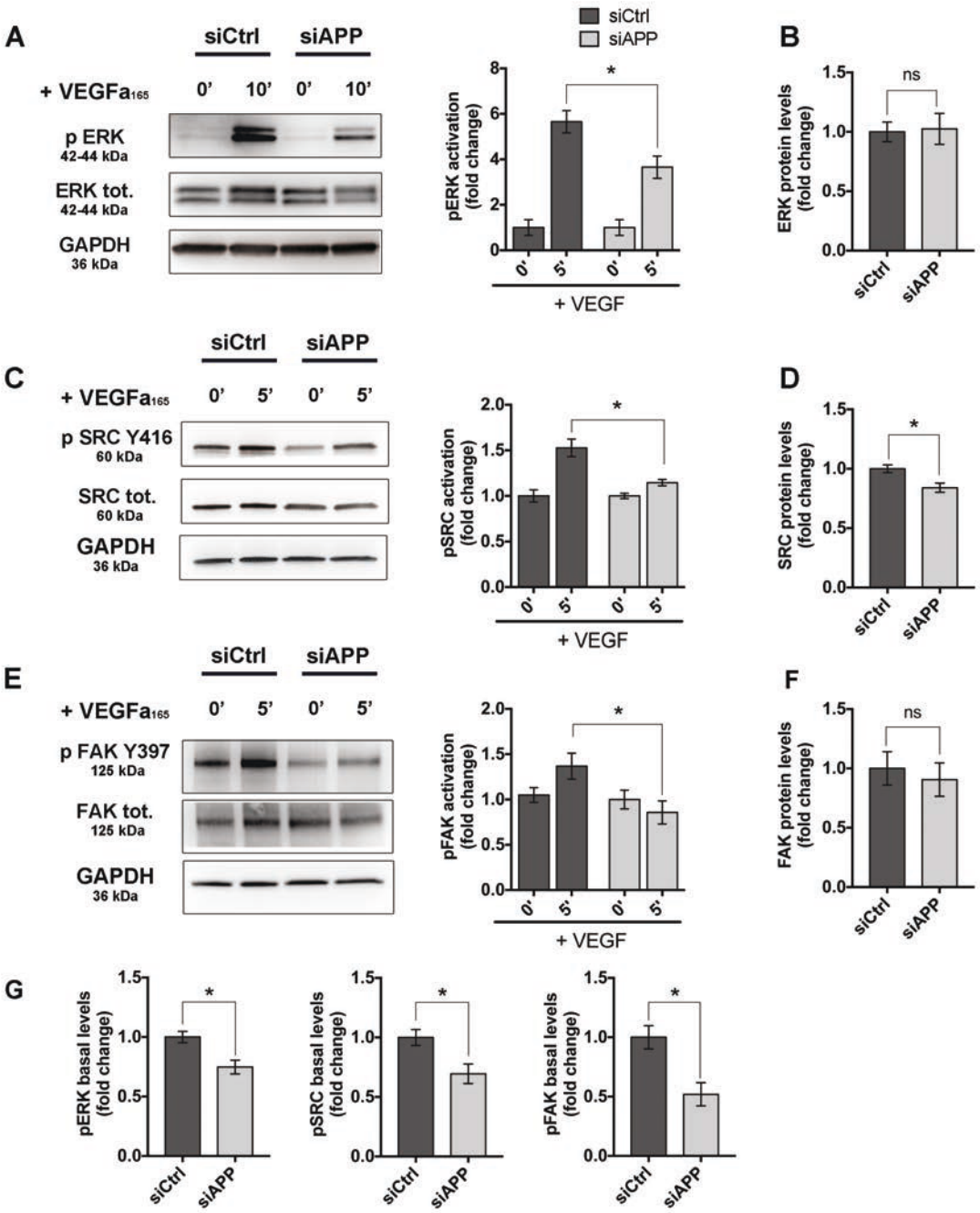

Figure 6. APP knockdown suppresses Src/FAK signaling: (**A**) Western blot analysis of ERK activation (p-ERK) shows reduced ERK phosphorylation in siAPP HUVEC treated with VEGF (50 ng/mL, 10 min) (**B**) Quantification showing unchanged ERK total levels upon APP silencing; (**C**) Western blot analysis of Src activation (p-Src) after VEGF treatment (50 ng/mL, 5 min) shows a significative reduction of p-Src-Y416 phosphorylation; (**D**) Quantification showing significative reduction of Src total levels in siAPP HUVEC; (**E**) Western blot analysis of FAK activation (p-FAK) after VEGF treatment (50 ng/mL, 5 min) showing down-regulation of FAK Y397 phosphorylation; (**F**) Quantification showing unchanged FAK total protein levels; (**G**) Quantification showing reduction of basal levels of p-ERK, p-SRC (Y416) and p-FAK (Y397) in siAPP HUVEC. All data are represented as mean ± SEM, n 4 replicates; * $p < 0.05$, ns not significant.

4. Discussion

The amyloid precursor protein (APP) is a membrane bound protein present in multiple cell types, including ECs. However, its functional role in the vasculature is still unknown. Previous studies suggest that APP may exert a protective role by regulating eNOS expression in cerebral vasculature. Yet, the phenotype of ECs lacking this protein is poorly known [42]. In the present study, we show that APP has an important role in endothelial cell function by modulating expression of cytoskeleton-interacting proteins and mediating endothelial cell responses to extracellular stimulation. Indeed, the loss of APP in ECs resulted in a defective actin cytoskeleton organization with a consequent reduction of cell adhesion, migration, proliferation and barrier function, and in inhibition of response to the pro-angiogenic growth factor VEGF-A.

Proteomic results showed that cellular compartments most strongly affected by the loss of APP are the plasma membrane and cytoskeleton. In particular, proteins involved in cell adhesion (FERMT3; ITGA2; ITGB1) and actin cytoskeleton organization (RADI; DPLI-1; ACTN1) were downregulated, suggesting that APP acts in ECs to maintain cellular functionality. Furthermore, protein markers of endothelial activation and dysfunction were upregulated (ICAM-1, S100, STAB1 and FINC), indicating that APP is instrumental for physiological endothelial-dependent vascular homeostasis.

We further demonstrated that the loss of APP resulted in a reduced expression of integrin-β1 and integrin-β3. Moreover, both proteomic and molecular results showed a down-regulation of the integrin-activator kindlin3 (FERMT3), indicating that APP not only controls expression and/or the stability of integrins in ECs expression, but also their activation.

Integrins activity is essential for ECs homeostasis [33,43,44]. As part of the focal adhesion complex, integrins provide not only a mechanical linkage between the intracellular actin cytoskeleton and extracellular matrix, but also mediate bidirectional signaling "outside-in" and "inside-out" through the cell membrane. Kindlins participate in linking integrins to the actin cytoskeleton, mediating the "inside-out" signal from the cytoplasm to the extracellular integrin domain [45,46]. Interestingly, kindlins have been shown to modulate APP metabolism and a genome-wide study on Alzheimer's related genes identified kindlins as a genetic risk factors [47].

Dysfunction of integrin-mediated signaling was confirmed by reduction of paxillin expression and loss of Src and FAK activation in siAPP cells. Paxillin and Src/FAK mediate the "outside-in" signal and their activation is critical for the stabilization of cell adhesion and the promotion of cell migration, proliferation and survival. In response to ligand-integrin binding, FAK auto-phosphorylates (Y397) and promotes Src activation that, in turn, phosphorylates FAK (Y576/577), promoting its kinase activity and its interaction with paxillin. Paxillin regulates gene expression through MAPK cascade and it is responsible to changes in shape and reorganization of the actin cytoskeleton by binding to downstream kinases and adaptors including the actin-binding protein vinculin [48]. Accordingly, in our study the reduction of paxillin expression coincides with an altered distribution of vinculin in siAPP cells.

Deregulation of the integrin-mediated signaling can also be responsible for the loss of endothelial barrier function. A recent study showed that the loss of integrin β1 and the consequent disruption of integrin β1-matrix interaction increase cerebral microvascular endothelial cell monolayer permeability in vivo and in vitro through reorganization of tight junction proteins via altered F-actin conformation [43]. Accordingly, in siAPP HUVECs we observed a decreased ZO-1 and claudin5 expression, associated with a reduction of integrin β1 expression and a consequent increase of endothelial permeability. Furthermore, in agreement with the notion that ZO-1 works as a major cytoskeleton organizer in ECs by controlling F-actin fiber distributions and regulating the tensile force acting on VE-cadherin [41], we also observed a decreased β catenin expression and altered VE-cadherin localization

Finally, we showed that the reduced expression of the focal adhesion complex and its altered interaction with actin-cytoskeleton, affects the ability of ECs to respond to the VEGF growth factor. We observed a reduced activation of VEGR2 receptor in response to exogenous VEGF in siAPP HUVEC and consequent inhibition of VEGF-induced endothelial cell migration and proliferation and loss of ECs angiogenic potential. We speculate that APP modulation of VEGF/VEGFR2

signaling is mediated by APP-integrin interaction since APP can interact with integrin-β1 [13,49], however further investigations are needed to elucidate this mechanism.

Here, we observed that siAPP HUVEC express lower levels of integrin-β3 and this coincides with lower levels of activation of the receptor. It is well known that integrin-β3 promotes VEGF/VEGFR2 signaling and that integrin KO models result in inhibition of angiogenesis and endothelial dysfunction [44,50,51]. However, the reduced response to VEGF might also be due to the alteration of shape and disorganization of the actin cytoskeleton in absence of APP. Indeed, the correct phosphorylation and stability at the cell membrane of the VEGF2 receptor is mediated by the correct interaction with cytoskeleton and cell surface proteins [52–54].

The downstream signaling of integrins and growth factors converge on the Src/FAK pathway. We showed that Src/FAK signaling was suppressed upon VEGF treatment in absence of APP. However, we also observed an inhibition of p-Src, and p-FAK in siAPP cells in basal condition, suggesting that the effect of APP on Src/FAK signaling is VEGF-independent.

Similarly, the loss of APP inhibits ERK1/2 activation independently from VEGFR2 activation. Indeed, APP can directly activate ERK1/2 signaling through its intracellular domain (AICD), and ERK1/2 phosphorylation/activation is increased in AD [55–58].

Taken together, our results indicate that APP is necessary for the focal adhesion complex expression/stability. The interaction with cytoskeleton-interacting proteins such integrins, is essential to maintain ECs proliferation, adhesion and angiogenesis. Loss of APP expression results in altered cellular response to environmental stimuli and leads to endothelial dysfunction (Figure 7).

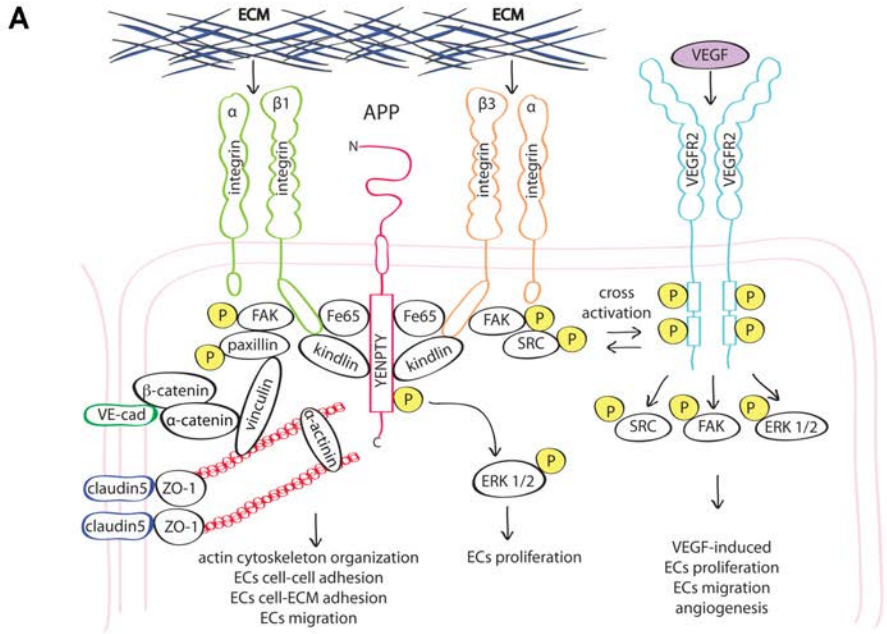

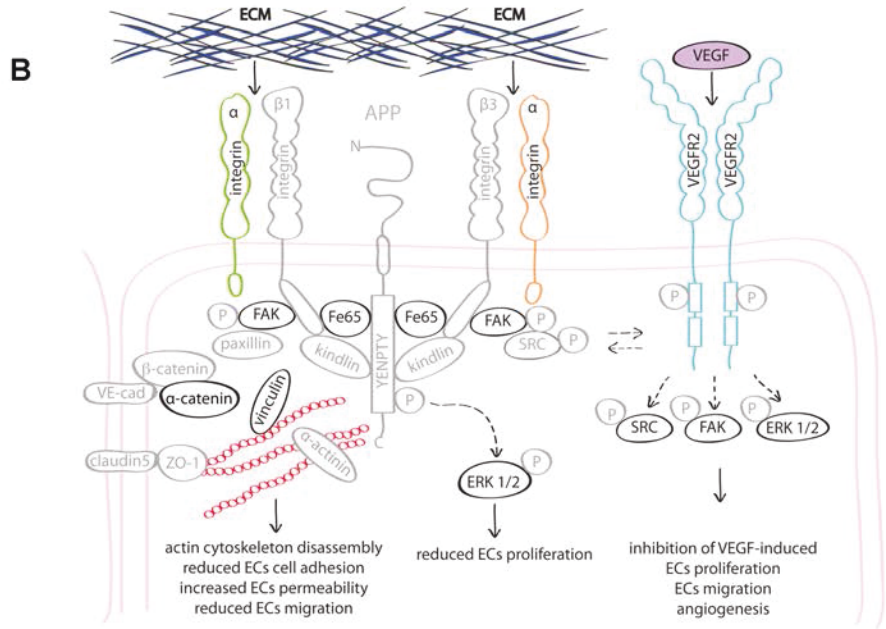

Figure 7. Proposed working model: (**A**) APP interacts with the integrin β-subunit. This interaction promotes the stability and functionality of focal adhesions and their correct localization at the cell membrane, and activation of VEGFR2; (**B**) Loss of APP leads to an altered expression and activation of actin cytoskeleton-interacting proteins (represented in grey) and to the reduced activity of several proteins at the cell membrane, included VEGFR2, ultimately causing endothelial dysfunction. Abbreviations: ECM extracellular matrix; (P) phosphorylation site.

5. Conclusions

While the pathological outcome of APP dysregulation is mainly associated to its overexpression, recent studies showed that APP expression levels tend to decrease with age [59,60], and APP-knockout mice show age-dependent cognitive deficit and impaired locomotor activity [61,62]. Moreover, senescent brains showed an increase of amyloidogenic processing mediated by BACE1 [63], indicating that amyloid-β peptides accumulation is not necessarily associated with APP overexpression. Furthermore, clinical trials targeting amyloid-β have failed to reverse the cognitive loss, and in some cases resulted in vascular severe adverse events (i.e., bapineuzumab), indicating the importance of physiological levels of amyloid-β peptides and highlighting the urgency to better understand the function of APP and its cleavage products in cell homeostasis.

In this study, we show that a correct expression level of APP may be necessary for the correct functionality of ECs. Although the use of HUVEC as model is not representative of all endothelial cell types found in an organism, they are an excellent model for the study of vascular endothelium properties and the main biological pathways involved in endothelium function. More studies addressing the APP function specifically in cerebrovascular endothelium will be needed.

A deep understanding of APP function in maintaining vascular homeostasis might shed light on new therapeutic targets and provide a new perspective on treatment options of neurodegenerative diseases.

Supplementary Materials: The following are available online at www.mdpi.com/xxx/s1, Figure S1: Selection of APP targeting siRNAs. Figure S2: Label free proteomic analysis of HUVEC following APP knockdown.

Figure S3: APP doesn't physically interact with VEGFR2 and APP knockdown doesn't reduce mRNA levels of VEGFR2-VEGF downstream signaling. Figure S4: Western Blot analysis with alternative antibodies. Table S1: List of up-regulated and down-regulated proteins.

Author Contributions: Conceptualization, M.Z., S.D. and E.R.; methodology, E.R.; proteomic analysis, V.C., L.T., L.S. and C.T.; validation, E.R.; writing—original draft preparation, E.R.; writing—review and editing, M.Z., F.C., S.D. and M.S.; all authors have read and agreed to the published version of the manuscript.

Funding: This research was funded by Italian Ministry of Education, University and Research (grant MIUR289 PRIN n. 20152HKF3Z to M.Z.), and by the Italian Society of Pharmacology (SIF) (travel fellowship to E.R.).

Conflicts of Interest: The authors declare no conflict of interest.

References

1. Selkoe, D.J.; Hardy, J. The amyloid hypothesis of Alzheimer's disease at 25 years. *EMBO Mol. Med.* **2016**, *8*, 595–608, doi:10.15252/emmm.201606210.
2. Dawkins, E.; Small, D.H. Insights into the physiological function of the beta-amyloid precursor protein: Beyond Alzheimer's disease. *J. Neurochem.* **2014**, *129*, 756–769, doi:10.1111/jnc.12675.
3. Corrigan, F.; Pham, C.L.; Vink, R.; Blumbergs, P.C.; Masters, C.L.; van den Heuvel, C.; Cappai, R. The neuroprotective domains of the amyloid precursor protein, in traumatic brain injury, are located in the two growth factor domains. *Brain Res.* **2011**, *1378*, 137–143, doi:10.1016/j.brainres.2010.12.077.
4. Corrigan, F.; Thornton, E.; Roisman, L.C.; Leonard, A.V.; Vink, R.; Blumbergs, P.C.; van den Heuvel, C.; Cappai, R. The neuroprotective activity of the amyloid precursor protein against traumatic brain injury is mediated via the heparin binding site in residues 96–110. *J. Neurochem.* **2014**, *128*, 196–204, doi:10.1111/jnc.12391.
5. Itoh, T.; Satou, T.; Nishida, S.; Tsubaki, M.; Hashimoto, S.; Ito, H. Expression of amyloid precursor protein after rat traumatic brain injury. *Neurol. Res.* **2009**, *31*, 103–109, doi:10.1179/016164108X323771.
6. Nihashi, T.; Inao, S.; Kajita, Y.; Kawai, T.; Sugimoto, T.; Niwa, M.; Kabeya, R.; Hata, N.; Hayashi, S.; Yoshida, J. Expression and distribution of beta amyloid precursor protein and beta amyloid peptide in reactive astrocytes after transient middle cerebral artery occlusion. *Acta Neurochir.* **2001**, *143*, 287–295, doi:10.1007/s007010170109.
7. Sayer, R.; Robertson, D.; Balfour, D.J.; Breen, K.C.; Stewart, C.A. The effect of stress on the expression of the amyloid precursor protein in rat brain. *Neurosci. Lett.* **2008**, *431*, 197–200, doi:10.1016/j.neulet.2007.11.032.
8. Ho, A.; Sudhof, T.C. Binding of F-spondin to amyloid-beta precursor protein: A candidate amyloid-beta precursor protein ligand that modulates amyloid-beta precursor protein cleavage. *Proc. Natl. Acad. Sci. USA* **2004**, *101*, 2548–2553, doi:10.1073/pnas.0308655100.
9. Hoe, H.S.; Lee, K.J.; Carney, R.S.; Lee, J.; Markova, A.; Lee, J.Y.; Howell, B.W.; Hyman, B.T.; Pak, D.T.; Bu, G.; et al. Interaction of reelin with amyloid precursor protein promotes neurite outgrowth. *J. Neurosci.* **2009**, *29*, 7459–7473, doi:10.1523/JNEUROSCI.4872-08.2009.
10. Reinhard, C.; Borgers, M.; David, G.; De Strooper, B. Soluble amyloid-beta precursor protein binds its cell surface receptor in a cooperative fashion with glypican and syndecan proteoglycans. *J. Cell Sci.* **2013**, *126*, 4856–4861, doi:10.1242/jcs.137919.
11. Sosa, L.J.; Bergman, J.; Estrada-Bernal, A.; Glorioso, T.J.; Kittelson, J.M.; Pfenninger, K.H. Amyloid precursor protein is an autonomous growth cone adhesion molecule engaged in contact guidance. *PLoS ONE* **2013**, *8*, e64521, doi:10.1371/journal.pone.0064521.
12. Chen, K.P.; Dou, F. Selective interaction of amyloid precursor protein with different isoforms of neural cell adhesion molecule. *J. Mol. Neurosci.* **2012**, *46*, 203–209, doi:10.1007/s12031-011-9578-3.
13. Young-Pearse, T.L.; Bai, J.; Chang, R.; Zheng, J.B.; LoTurco, J.J.; Selkoe, D.J. A critical function for beta-amyloid precursor protein in neuronal migration revealed by in utero RNA interference. *J. Neurosci.* **2007**, *27*, 14459–14469, doi:10.1523/JNEUROSCI.4701-07.2007.

14. Sosa, L.J.; Caceres, A.; Dupraz, S.; Oksdath, M.; Quiroga, S.; Lorenzo, A. The physiological role of the amyloid precursor protein as an adhesion molecule in the developing nervous system. *J. Neurochem.* **2017**, *143*, 11–29, doi:10.1111/jnc.14122.
15. Ott, M.O.; Bullock, S.L. A gene trap insertion reveals that amyloid precursor protein expression is a very early event in murine embryogenesis. *Dev. Genes Evol.* **2001**, *211*, 355–357, doi:10.1007/s004270100158.
16. Koike, M.A.; Lin, A.J.; Pham, J.; Nguyen, E.; Yeh, J.J.; Rahimian, R.; Tromberg, B.J.; Choi, B.; Green, K.N.; LaFerla, F.M. APP knockout mice experience acute mortality as the result of ischemia. *PLoS ONE* **2012**, *7*, e42665, doi:10.1371/journal.pone.0042665.
17. Luna, S.; Cameron, D.J.; Ethell, D.W. Amyloid-beta and APP deficiencies cause severe cerebrovascular defects: Important work for an old villain. *PLoS ONE* **2013**, *8*, e75052, doi:10.1371/journal.pone.0075052.
18. d'Uscio, L.V.; He, T.; Santhanam, A.V.; Katusic, Z.S. Endothelium-specific amyloid precursor protein deficiency causes endothelial dysfunction in cerebral arteries. *J. Cereb. Blood Flow Metab.* **2018**, *38*, 1715–1726, doi:10.1177/0271678X17735418.
19. de la Torre, J. The Vascular Hypothesis of Alzheimer's Disease: A Key to Preclinical Prediction of Dementia Using Neuroimaging. *J. Alzheimers Dis.* **2018**, *63*, 35–52, doi:10.3233/JAD-180004.
20. Nannelli, G.; Terzuoli, E.; Giorgio, V.; Donnini, S.; Lupetti, P.; Giachetti, A.; Bernardi, P.; Ziche, M. ALDH2 Activity Reduces Mitochondrial Oxygen Reserve Capacity in Endothelial Cells and Induces Senescence Properties. *Oxid. Med. Cell. Longev.* **2018**, *2018*, 9765027, doi:10.1155/2018/9765027.
21. Terzuoli, E.; Meini, S.; Cucchi, P.; Catalani, C.; Cialdai, C.; Maggi, C.A.; Giachetti, A.; Ziche, M.; Donnini, S. Antagonism of bradykinin B2 receptor prevents inflammatory responses in human endothelial cells by quenching the NF-kB pathway activation. *PLoS ONE* **2014**, *9*, e84358, doi:10.1371/journal.pone.0084358.
22. Pezzatini, S.; Morbidelli, L.; Solito, R.; Paccagnini, E.; Boanini, E.; Bigi, A.; Ziche, M. Nanostructured HA crystals up-regulate FGF-2 expression and activity in microvascular endothelium promoting angiogenesis. *Bone* **2007**, *41*, 523–534, doi:10.1016/j.bone.2007.06.016.
23. Alghisi, G.C.; Ponsonnet, L.; Ruegg, C. The integrin antagonist cilengitide activates alphaVbeta3, disrupts VE-cadherin localization at cell junctions and enhances permeability in endothelial cells. *PLoS ONE* **2009**, *4*, e4449, doi:10.1371/journal.pone.0004449.
24. Ciccone, V.; Monti, M.; Antonini, G.; Mattoli, L.; Burico, M.; Marini, F.; Maidecchi, A.; Morbidelli, L. Efficacy of AdipoDren(R) in Reducing Interleukin-1-Induced Lymphatic Endothelial Hyperpermeability. *J. Vasc. Res.* **2016**, *53*, 255–268, doi:10.1159/000452798.
25. Lin, Y.; Zhou, J.; Bi, D.; Chen, P.; Wang, X.; Liang, S. Sodium-deoxycholate-assisted tryptic digestion and identification of proteolytically resistant proteins. *Anal. Biochem.* **2008**, *377*, 259–266, doi:10.1016/j.ab.2008.03.009.
26. Zhou, J.; Zhou, T.; Cao, R.; Liu, Z.; Shen, J.; Chen, P.; Wang, X.; Liang, S. Evaluation of the application of sodium deoxycholate to proteomic analysis of rat hippocampal plasma membrane. *J. Proteome. Res.* **2006**, *5*, 2547–2553, doi:10.1021/pr060112a.
27. Huang da, W.; Sherman, B.T.; Lempicki, R.A. Bioinformatics enrichment tools: Paths toward the comprehensive functional analysis of large gene lists. *Nucleic Acids Res.* **2009**, *37*, 1–13, doi:10.1093/nar/gkn923.
28. Pathan, M.; Keerthikumar, S.; Chisanga, D.; Alessandro, R.; Ang, C.S.; Askenase, P.; Batagov, A.O.; Benito-Martin, A.; Camussi, G.; Clayton, A.; et al. A novel community driven software for functional enrichment analysis of extracellular vesicles data. *J. Extracell. Vesicles* **2017**, *6*, 1321455, doi:10.1080/20013078.2017.1321455.
29. Cox, J.; Mann, M. MaxQuant enables high peptide identification rates, individualized p.p.b.-range mass accuracies and proteome-wide protein quantification. *Nat. Biotechnol.* **2008**, *26*, 1367–1372, doi:10.1038/nbt.1511.
30. Cox, J.; Neuhauser, N.; Michalski, A.; Scheltema, R.A.; Olsen, J.V.; Mann, M. Andromeda: A peptide search engine integrated into the MaxQuant environment. *J. Proteome Res.* **2011**, *10*, 1794–1805, doi:10.1021/pr101065j.
31. Ringner, M. What is principal component analysis? *Nat. Biotechnol.* **2008**, *26*, 303–304, doi:10.1038/nbt0308-303.
32. Shariati, S.A.; De Strooper, B. Redundancy and divergence in the amyloid precursor protein family. *FEBS Lett.* **2013**, *587*, 2036–2045, doi:10.1016/j.febslet.2013.05.026.
33. Avraamides, C.J.; Garmy-Susini, B.; Varner, J.A. Integrins in angiogenesis and lymphangiogenesis. *Nat. Rev. Cancer* **2008**, *8*, 604–617, doi:10.1038/nrc2353.

34. Khalili, A.A.; Ahmad, M.R. A Review of Cell Adhesion Studies for Biomedical and Biological Applications. *Int. J. Mol. Sci.* **2015**, *16*, 18149–18184, doi:10.3390/ijms160818149.
35. Schaller, M.D. Paxillin: A focal adhesion-associated adaptor protein. *Oncogene* **2001**, *20*, 6459–6472, doi:10.1038/sj.onc.1204786.
36. Dejana, E.; Orsenigo, F. Endothelial adherens junctions at a glance. *J. Cell Sci.* **2013**, *126*, 2545–2549, doi:10.1242/jcs.124529.
37. Komarova, Y.A.; Kruse, K.; Mehta, D.; Malik, A.B. Protein Interactions at Endothelial Junctions and Signaling Mechanisms Regulating Endothelial Permeability. *Circ. Res.* **2017**, *120*, 179–206, doi:10.1161/CIRCRESAHA.116.306534.
38. Pulous, F.E.; Petrich, B.G. Integrin-dependent regulation of the endothelial barrier. *Tissue Barriers* **2019**, *7*, 1685844, doi:10.1080/21688370.2019.1685844.
39. Puhlmann, M.; Weinreich, D.M.; Farma, J.M.; Carroll, N.M.; Turner, E.M.; Alexander, H.R., Jr. Interleukin-1beta induced vascular permeability is dependent on induction of endothelial tissue factor (TF) activity. *J. Transl. Med.* **2005**, *3*, 37, doi:10.1186/1479-5876-3-37.
40. Dejana, E.; Orsenigo, F.; Molendini, C.; Baluk, P.; McDonald, D.M. Organization and signaling of endothelial cell-to-cell junctions in various regions of the blood and lymphatic vascular trees. *Cell Tissue Res.* **2009**, *335*, 17–25, doi:10.1007/s00441-008-0694-5.
41. Tornavaca, O.; Chia, M.; Dufton, N.; Almagro, L.O.; Conway, D.E.; Randi, A.M.; Schwartz, M.A.; Matter, K.; Balda, M.S. ZO-1 controls endothelial adherens junctions, cell-cell tension, angiogenesis, and barrier formation. *J. Cell Biol.* **2015**, *208*, 821–838, doi:10.1083/jcb.201404140.
42. Ristori, E.; Donnini, S.; Ziche, M. New Insights Into Blood-Brain Barrier Maintenance: The Homeostatic Role of β-Amyloid Precursor Protein in Cerebral Vasculature. *Front. Physiol.* **2020**, *11*, 1056, doi:doi.org/10.3389/fphys.2020.01056.
43. Izawa, Y.; Gu, Y.H.; Osada, T.; Kanazawa, M.; Hawkins, B.T.; Koziol, J.A.; Papayannopoulou, T.; Spatz, M.; Del Zoppo, G.J. beta1-integrin-matrix interactions modulate cerebral microvessel endothelial cell tight junction expression and permeability. *J. Cereb. Blood Flow Metab.* **2018**, *38*, 641–658, doi:10.1177/0271678X17722108.
44. Somanath, P.R.; Malinin, N.L.; Byzova, T.V. Cooperation between integrin alphavbeta3 and VEGFR2 in angiogenesis. *Angiogenesis* **2009**, *12*, 177–185, doi:10.1007/s10456-009-9141-9.
45. Rognoni, E.; Ruppert, R.; Fassler, R. The kindlin family: Functions, signaling properties and implications for human disease. *J. Cell Sci.* **2016**, *129*, 17–27, doi:10.1242/jcs.161190.
46. Sun, Z.; Costell, M.; Fassler, R. Integrin activation by talin, kindlin and mechanical forces. *Nat. Cell Biol.* **2019**, *21*, 25–31, doi:10.1038/s41556-018-0234-9.
47. Chapuis, J.; Flaig, A.; Grenier-Boley, B.; Eysert, F.; Pottiez, V.; Deloison, G.; Vandeputte, A.; Ayral, A.M.; Mendes, T.; Desai, S.; et al. Genome-wide, high-content siRNA screening identifies the Alzheimer's genetic risk factor FERMT2 as a major modulator of APP metabolism. *Acta Neuropathol* **2017**, *133*, 955–966, doi:10.1007/s00401-016-1652-z.
48. Harburger, D.S.; Calderwood, D.A. Integrin signalling at a glance. *J. Cell Sci.* **2009**, *122*, 159–163, doi:10.1242/jcs.018093.
49. Yamazaki, T.; Koo, E.H.; Selkoe, D.J. Cell surface amyloid beta-protein precursor colocalizes with beta 1 integrins at substrate contact sites in neural cells. *J. Neurosci.* **1997**, *17*, 1004–1010.
50. Liang, M.; Wang, Y.; Liang, A.; Dong, J.F.; Du, J.; Cheng, J. Impaired integrin beta3 delays endothelial cell regeneration and contributes to arteriovenous graft failure in mice. *Arter. Thromb. Vasc. Biol.* **2015**, *35*, 607–615, doi:10.1161/ATVBAHA.114.305089.
51. Ren, J.; Avery, J.; Zhao, H.; Schneider, J.G.; Ross, F.P.; Muslin, A.J. Beta3 integrin deficiency promotes cardiac hypertrophy and inflammation. *J. Mol. Cell Cardiol.* **2007**, *42*, 367–377, doi:10.1016/j.yjmcc.2006.11.002.
52. Byzova, T.V.; Goldman, C.K.; Pampori, N.; Thomas, K.A.; Bett, A.; Shattil, S.J.; Plow, E.F. A mechanism for modulation of cellular responses to VEGF: Activation of the integrins. *Mol. Cell* **2000**, *6*, 851–860.
53. Corti, F.; Wang, Y.; Rhodes, J.M.; Atri, D.; Archer-Hartmann, S.; Zhang, J.; Zhuang, Z.W.; Chen, D.; Wang, T.; Wang, Z.; et al. N-terminal syndecan-2 domain selectively enhances 6-O heparan sulfate chains sulfation and promotes VEGFA165-dependent neovascularization. *Nat. Commun.* **2019**, *10*, 1562, doi:10.1038/s41467-019-09605-z.

54. Wang, X.; Freire Valls, A.; Schermann, G.; Shen, Y.; Moya, I.M.; Castro, L.; Urban, S.; Solecki, G.M.; Winkler, F.; Riedemann, L.; et al. YAP/TAZ Orchestrate VEGF Signaling during Developmental Angiogenesis. *Dev. Cell* **2017**, *42*, 462–478 e467, doi:10.1016/j.devcel.2017.08.002.
55. Kirouac, L.; Rajic, A.J.; Cribbs, D.H.; Padmanabhan, J. Activation of Ras-ERK Signaling and GSK-3 by Amyloid Precursor Protein and Amyloid Beta Facilitates Neurodegeneration in Alzheimer's Disease. *eNeuro* **2017**, *4*, doi:10.1523/ENEURO.0149-16.2017.
56. Nizzari, M.; Thellung, S.; Corsaro, A.; Villa, V.; Pagano, A.; Porcile, C.; Russo, C.; Florio, T. Neurodegeneration in Alzheimer disease: Role of amyloid precursor protein and presenilin 1 intracellular signaling. *J. Toxicol.* **2012**, *2012*, 187297, doi:10.1155/2012/187297.
57. Nizzari, M.; Venezia, V.; Repetto, E.; Caorsi, V.; Magrassi, R.; Gagliani, M.C.; Carlo, P.; Florio, T.; Schettini, G.; Tacchetti, C.; et al. Amyloid precursor protein and Presenilin1 interact with the adaptor GRB2 and modulate ERK 1,2 signaling. *J. Biol. Chem.* **2007**, *282*, 13833–13844, doi:10.1074/jbc.M610146200.
58. Venezia, V.; Nizzari, M.; Repetto, E.; Violani, E.; Corsaro, A.; Thellung, S.; Villa, V.; Carlo, P.; Schettini, G.; Florio, T.; et al. Amyloid precursor protein modulates ERK-1 and -2 signaling. *Ann. N. Y. Acad. Sci.* **2006**, *1090*, 455–465, doi:10.1196/annals.1378.048.
59. Kern, A.; Roempp, B.; Prager, K.; Walter, J.; Behl, C. Down-regulation of endogenous amyloid precursor protein processing due to cellular aging. *J. Biol. Chem.* **2006**, *281*, 2405–2413, doi:10.1074/jbc.M505625200.
60. Sun, R.; He, T.; Pan, Y.; Katusic, Z.S. Effects of senescence and angiotensin II on expression and processing of amyloid precursor protein in human cerebral microvascular endothelial cells. *Aging* **2018**, *10*, 100–114, doi:10.18632/aging.101362.
61. Dawson, G.R.; Seabrook, G.R.; Zheng, H.; Smith, D.W.; Graham, S.; O'Dowd, G.; Bowery, B.J.; Boyce, S.; Trumbauer, M.E.; Chen, H.Y.; et al. Age-related cognitive deficits, impaired long-term potentiation and reduction in synaptic marker density in mice lacking the beta-amyloid precursor protein. *Neuroscience* **1999**, *90*, 1–13, doi:10.1016/s0306-4522(98)00410-2.
62. Senechal, Y.; Kelly, P.H.; Dev, K.K. Amyloid precursor protein knockout mice show age-dependent deficits in passive avoidance learning. *Behav. Brain Res.* **2008**, *186*, 126–132, doi:10.1016/j.bbr.2007.08.003.
63. Chiocco, M.J.; Lamb, B.T. Spatial and temporal control of age-related APP processing in genomic-based beta-secretase transgenic mice. *Neurobiol. Aging* **2007**, *28*, 75–84, doi:10.1016/j.neurobiolaging.2005.11.011.

Amyloid-β Precursor Protein APP down-regulation alters actin cytoskeleton-interacting proteins in endothelial cells.

Emma Ristori, Vittoria Cicaloni, Laura Salvini, Laura Tinti, Cristina Tinti, Michael Simons, Federico Corti, Sandra Donnini* and Marina Ziche*.

Supplementary Materials:

- Figure S1: Selection of APP targeting siRNAs.
- Figure S2: Label free proteomic analysis of HUVEC following APP knockdown.
- Figure S3: APP doesn't physically interact with VEGFR2 and APP knockdown doesn’t reduce mRNA levels of VEGFR2-VEGF downstream signaling.
- Figure S4: Western blot analysis with alternative antibodies.
- Table S1: List of up-regulated and down-regulated proteins.

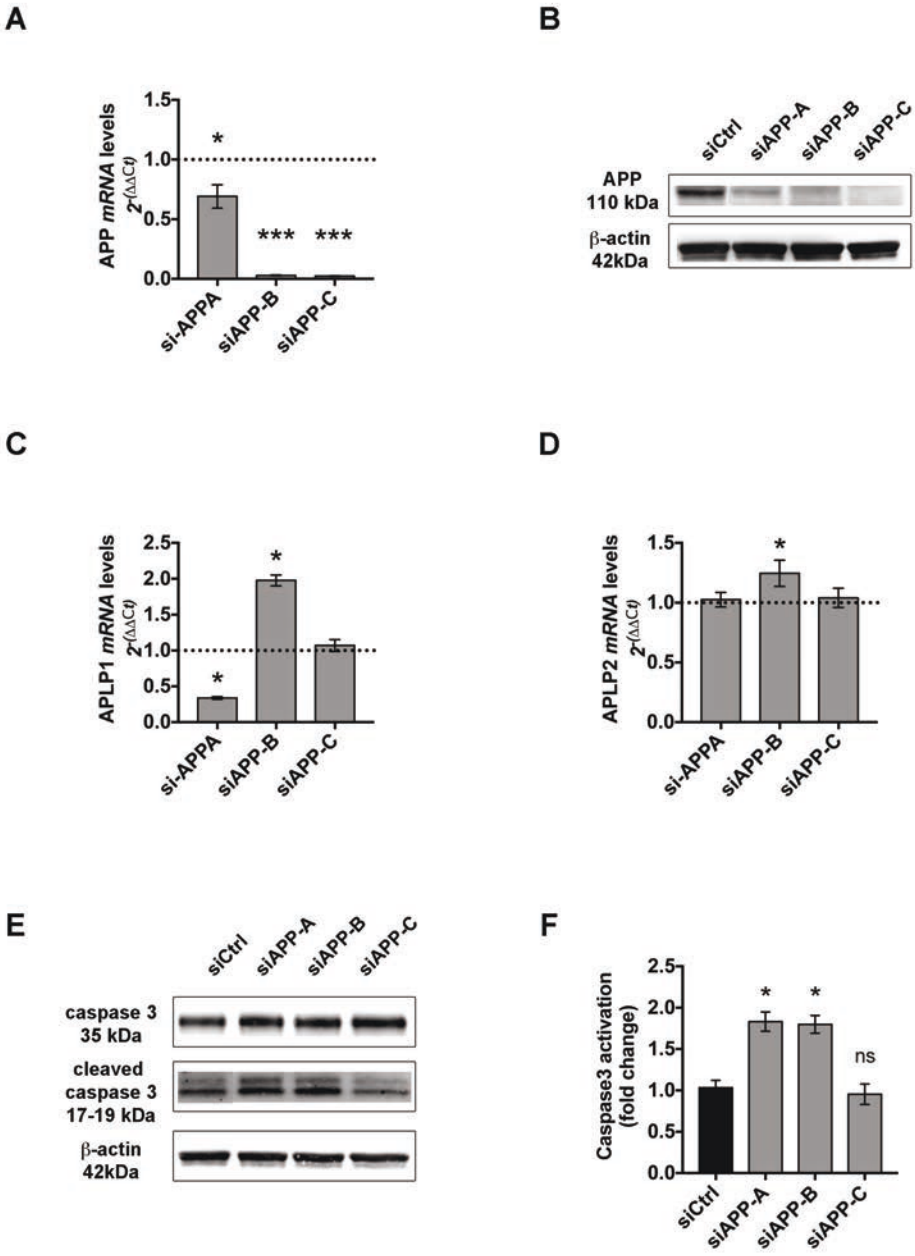

Figure S1. Selection of APP targeting siRNAs: **(a)** RTqPCR showing APP mRNA expression levels upon silencing for 48 hours with siAPP-A, -B or -C respectively; **(b)** Western blot showing reduced protein expression levels of APP upon silencing for 48 hours with siAPP-A, -B or -C respectively; **(c-d)** RTqPCR showing mRNA expression levels of APLP1 (c) and APLP2 (d). siAPP-C doesn't affect APLP1 and APLP2 expression. On the contrary, siAPP-A and siAPP-B show an aspecific off-target effect on APLP1 and APLP2; **(e)** Western-blot showing activation of apoptotic Caspase-3 in silenced cells (siAPP) and control (siCtrl). Activation of Caspase-3 was measured as cleaved Caspase-3/total Caspase3 ratio expression; **(f)** Quantification of western blot analysis (n 3) in (e) shows that siAPP-C doesn't promote apoptosis in silenced cells, whereas Caspase-3 is significantly activated by siAPP-A and siAPP-B. All data are presented as mean ± SEM, n 3 replicates, *P<0.05, ***P<0.001.

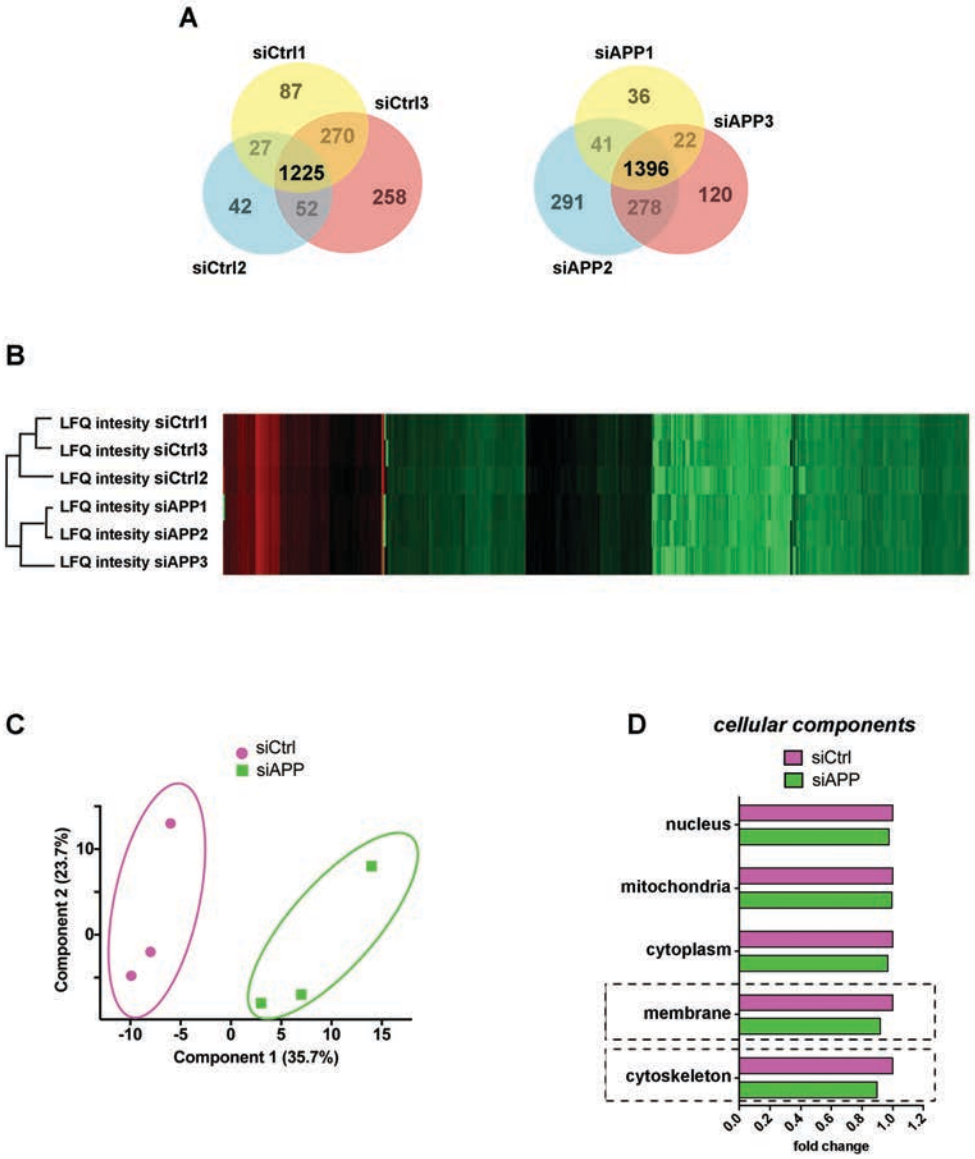

Figure S2. Label free proteomic analysis of HUVEC following APP knockdown: **(a)** Venn diagrams representing the number of reproducibly quantified proteins from three biological replicates of the HUVEC control and HUVEC silenced for APP for 48 hours. The common protein ensembles amount to 1225 and 1396 for siCrl and siAPP respectively; **(b)** Hierarchical clustering. Heatmap shows LFQ intensity values for triplicates of every sample. Within each group, proteins are sorted according to their LFQ intensity values: red (max value), green (min value). Clustering tree resulting from unsupervised clustering of samples is shown on the left and confirms a differentiation between siCtrl and siAPP samples; **(c)** PCA-biplot showing a principal component analysis of all siCtrl and siAPP samples analyzed by mass spectrometry. All the triplicates of siCtrl and siAPP samples appeared to cluster in two distinct groups confirming a clear proteomic differentiation between the two datasets. The percentage of the variance contributed by each principal component is indicated in the axis: 35,7% for the first component and 23.7% for the second component; **(d)** Functional comparison between siCtrl common dataset and siAPP common dataset was performed to analyze differences (p-value < 0.001) in cellular components.

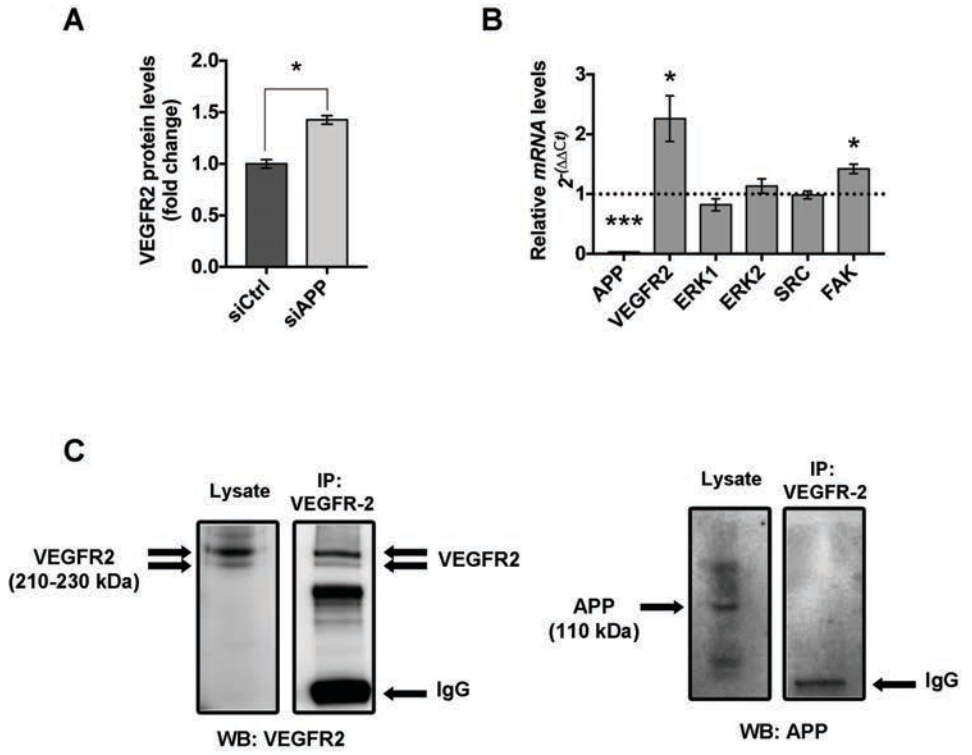

Figure S3. APP doesn't physically interact with VEGFR2 and APP knockdown doesn't reduce mRNA levels of VEGFR2-VEGF downstream signaling **(a)** Western blot analysis of total VEGFR2 protein expression in siAPP HUVEC **(b)** RTqPCR analysis of VEGFR2 and downstream signaling mRNA levels **(c)** Immunoprecipitation (IP) was performed using anti-VEGFR2 antibody (IP: anti-VEGFR2), followed by western blot analysis to check the presence of APP in the pulled-down complex (WB). The presence of VEGFR2 in the immunoprecipitate was used as positive control. Whole cell lysates (Lysate) were also analyzed for total VEGFR2 and APP protein level. The pulled down of anti-VEGFR2 antibody showed that it was able to bind the VEGFR2 protein but not APP, suggesting that the two proteins don't physically interact.

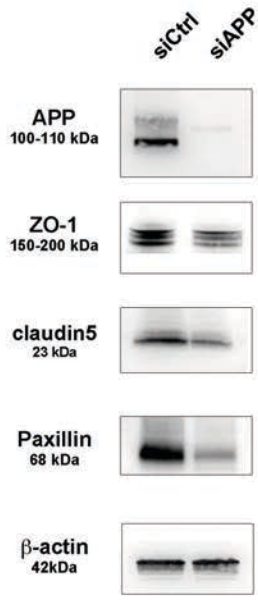

Figure S4: Western Blot analysis with alternative antibodies. ZO-1, Claudin5 and paxillin protein expression was assessed with different antibodies. Detection of ZO-1 with Life Technologies antibody (#61-7300), gives comparable results to Thermo Fisher Scientific antibody reported on the main text (# 33-9100). Similarly, protein expression levels resulted reduced in siAPP HUVEC using anti-claudin5 antibody from Thermo Fisher Scientific (#35-250) and anti-paxillin antibody from Abcam (#ab32084), and this result is comparable to the blots reported in the main text and obtained using respectively anti-claudin5 from Abcam (#ab53765), and anti-paxillin from Millipore (#3794).

Table S1: List of up-regulated and down-regulated proteins.

significance	-LOG(p-value)	Uniprot Accession	Uniprot ID	Name	Gene	Up/down regulation
+	1.696933953	A0AVT1	UBA6_HUMAN	Ubiquitin-like modifier-activating enzyme 6	UBA6	up-regulated
+	2.522674384	A5A6H4	ROA1_HUMAN	Heterogeneous nuclear ribonucleo protein A1	HNRNPA1	down-regulated
+	1.706431017	O00151	PDLI1_HUMAN	PDZ and LIM domain protein 1	PDL1	down-regulated
+	2.090178398	O00159	MYO1C_HUMAN	Unconventional myosin-Ic	MYO1C	down-regulated
+	3.17838226	O00469	PLOD2_HUMAN	Procollagen-lysine, 2-oxoglutarate 5-dioxygenase 2	PLOD2	down-regulated
+	2.743386048	O00571	DDX3X_HUMAN	ATP-dependent RNA helicase DDX3X	DDX3X	down-regulated
+	2.750845176	O00625	PIR_HUMAN	Pirin	PIR	down-regulated
+	1.514993551	O00767	ACOD_HUMAN	Acyl-CoA desaturase	SCD	down-regulated
+	1.160610103	O14561	ACPM_HUMAN	Acyl carrier protein, mitochondrial	NDUFAB1	down-regulated
+	3.687649448	O14879	IFIT3_HUMAN	Interferon-induced protein with tetratrico peptide repeats 3	IFIT3	up-regulated
+	2.015502669	O14933	UB2L6_HUMAN	Ubiquitin/ISG15-conjugating enzyme E2L6	UBE2L6	up-regulated
+	2.440057636	O15173	PGRC2_HUMAN	Membrane-associated progesterone receptor component 2	PGRMC2	up-regulated
+	1.054930824	O15460	P4HA2_HUMAN	Prolyl4-hydroxylase subunit alpha-2	P4HA2	up-regulated
+	1.757811053	O15533	TPSN_HUMAN	Tapasin	TAPBP	up-regulated
+	1.387369479	O75352	MPU1_HUMAN	Mannose-P-dolicholutilization defect 1 protein	MPDU1	up-regulated
+	2.236427975	O75964	ATP5L_HUMAN	ATPsynthase subunitg, mitochondrial	ATP5MG	down-regulated
+	1.899778643	O94760	DDAH1_HUMAN	N(G),N(G)-dimethyl arginine dimethyl aminohydrolase 1	DDAH1	up-regulated
+	1.765031675	O95340	PAPS2_HUMAN	Bifunctional 3'-phosphoadenosine 5'-phosphosulfate synthase 2	PAPSS2	up-regulated
+	1.53277814	O95394	AGM1_HUMAN	Phospho acetyl glucosamine mutase	PGM3	up-regulated
+	2.534386104	O95786	DDX58_HUMAN	Probable ATP-dependent RNA helicase DDX58	DDX58	up-regulated
+	1.114553442	O95864	FADS2_HUMAN	Acyl-CoA6-desaturase	FADS2	down-regulated
+	2.052784401	P00352	AL1A1_HUMAN	Retinaldehydrogenase 1	ALDH1A1	down-regulated
+	2.160872861	P02751	FINC_HUMAN	Fibronectin	FN1	up-regulated
+	1.440434415	P00973	OAS1_HUMAN	2'-5'-oligoadenylatesynthase 1	OAS1	up-regulated
+	2.251688608	P04406	G3P_HUMAN	Glyceraldehyde-3-phosphatedehydrogenase	GAPDH	down-regulated
+	2.717914577	P05121	PAI1_HUMAN	Plasminogen activator inhibitor 1	SERPINE1	up-regulated
+	1.603052806	P05556	ITB1_HUMAN	Integrin beta-1	ITGB1	down-regulated
+	1.526031727	P07737	PROF1_HUMAN	Profilin-1	PFN1	down-regulated
+	2.518157148	P05161	ISG15_HUMAN	Ubiquitin-like protein ISG15	ISG15	up-regulated
+	3.119174198	P05362	ICAM1_HUMAN	Intercellular adhesion molecule 1	ICAM1	up-regulated
+	2.209848209	P07996	THBS1_HUMAN	Thrombospondin-1	THBS1	down-regulated
+	1.242351574	P06703	S10A6_HUMAN	Protein S100-A6	S100A6	down-regulated
+	2.25465283	P06744	G6PI_HUMAN	Glucose-6-phosphateisomerase	GPI	down-regulated

significance	-LOG(p-value)	Uniprot Accession	Uniprot ID	Name	Gene	Up/down regulation
+	1.855508392	P09211	GSTP1_HUMAN	Glutathione S-transferaseP	GSTP1	up-regulated
+	1.740222305	P09382	LEG1_HUMAN	Galectin-1	LGALS1	down-regulated
+	2.368520131	P08195	4F2_HUMAN	4F2 cell-surface antigen heavy chain	SLC3A2	down-regulated
+	1.891527327	P09493	TPM1_HUMAN	Tropomyosin alpha-1 chain	TPM1	up-regulated
+	1.443180756	P09874	PARP1_HUMAN	Poly [ADP-ribose] polymerase1	PARP1	down-regulated
+	3.032771209	P12814	ACTN1_HUMAN	Alpha-actinin-1	ACTN1	down-regulated
+	2.692592448	P09525	ANXA4_HUMAN	AnnexinA4	ANXA4	down-regulated
+	1.897264404	P09601	HMOX1_HUMAN	Hemeoxygenase 1	HMOX1	down-regulated
+	2.727149711	P14550	AK1A1_HUMAN	Aldo-ketoreductase family 1 member A1	AKR1A1	down-regulated
+	2.790370236	P09914	IFIT1_HUMAN	Interferon-induced protein with tetratricopeptide repeats 1	IFIT1	up-regulated
+	1.609073654	Q6PI52	CALM_HUMAN	Calmodulin	CALM3	down-regulated
+	3.095542821	P10644	KAP0_HUMAN	cAMP-dependent protein kinase type I-alpha regulatory subunit	PRKAR1A	down-regulated
+	3.620163005	P11413	G6PD_HUMAN	Glucose-6-phosphate1-dehydrogenase	G6PD	down-regulated
+	2.40258352	P11586	C1TC_HUMAN	C-1-tetrahydrofolate synthase, cytoplasmic	MTHFD1	down-regulated
+	4.625454001	P12268	IMDH2_HUMAN	Inosine-5'-monophosphatedehydrogenase 2	IMPDH2	down-regulated
+	1.894706253	P15121	ALDR_HUMAN	Aldo-ketoreductasefamily 1 member B1	AKR1B1	down-regulated
+	2.581743903	P13164	IFM1_HUMAN	Interferon-induced transmembrane protein 1	IFITM1	up-regulated
+	2.327212877	P13473	LAMP2_HUMAN	Lysosome-associated membrane glycoprotein 2	LAMP2	down-regulated
+	3.263787615	P13598	ICAM2_HUMAN	Intercellular adhesion molecule 2	ICAM2	down-regulated
+	1.564748621	P14174	MIF_HUMAN	Macrophage migration inhibitory factor	MIF	down-regulated
+	2.989539155	P14317	HCLS1_HUMAN	Hematopoietic lineage cell-specific protein	HCLS1	up-regulated
+	2.910071374	P35241	RADI_HUMAN	Radixin	RDX	down-regulated
+	3.191404542	P48681	NEST_HUMAN	Nestin	NES	down-regulated
+	3.559212247	P15144	AMPN_HUMAN	Aminopeptidase N	ANPEP	down-regulated
+	1.415200052	P15559	NQO1_HUMAN	NAD(P)Hdehydrogenase[quinone]1	NQO1	down-regulated
+	3.442546508	P16949	STMN1_HUMAN	Stathmin	STMN1	down-regulated
+	1.901770836	P17301	ITA2_HUMAN	Integrin alpha-2	ITGA2	down-regulated
+	1.640455436	P17612	KAPCA_HUMAN	cAMP-dependent protein kinase catalytic subunit alpha	PRKACA	down-regulated
+	2.284685181	P17655	CAN2_HUMAN	Calpain-2 catalytic subunit	CAPN2	down-regulated
+	3.048530771	P19971	TYPH_HUMAN	Thymidinephosphorylase	TYMP	up-regulated
+	3.336400095	P20591	MX1_HUMAN	Interferon-induced GTP-binding protein Mx1	MX1	up-regulated
+	2.287577839	P20700	LMNB1_HUMAN	Lamin-B1	LMNB1	down-regulated
+	1.857054822	P21589	5NTD_HUMAN	5'-nucleotidase	NT5E	down-regulated
+	1.982435862	P21964	COMT_HUMAN	CatecholO-methyltransferase	COMT	up-regulated
+	1.757846938	P22626	ROA2_HUMAN	Heterogeneous nuclear ribonucleo proteins A2/B1	HNRNPA2B1	up-regulated
+	1.722048997	P23497	SP100_HUMAN	Nuclear autoantigen Sp-100	SP100	up-regulated

significance	-LOG(p-value)	Uniprot Accession	Uniprot ID	Name	Gene	Up/down regulation
+	2.81892956	P25205	MCM3_HUMAN	DNA replication licensing factor MCM3	MCM3	down-regulated
+	1.347814439	P26640	SYVC_HUMAN	Valine--tRNAligase	VARS	down-regulated
+	1.171753598	P49419	AL7A1_HUMAN	Alpha-amino adipicsemialdehyde dehydrogenase	ALDH7A1	down-regulated
+	1.346818553	P29466	CASP1_HUMAN	Caspase-1	CASP1	up-regulated
+	1.638845632	P29590	PML_HUMAN	Protein PML	PML	up-regulated
+	1.43416805	P30043	BLVRB_HUMAN	Flavin reductase(NADPH)	BLVRB	up-regulated
+	2.540767736	P30837	AL1B1_HUMAN	Aldehyde dehydrogenase X, mitochondrial	ALDH1B1	down-regulated
+	2.795995598	P32455	GBP1_HUMAN	Guanylate-binding protein 1	GBP1	up-regulated
+	2.464128618	P33316	DUT_HUMAN	Deoxyuridine 5'-triphosphate nucleotido hydrolase, mitochondrial	DUT	down-regulated
+	2.558422427	P33991	MCM4_HUMAN	DNA replication licensing factor MCM4	MCM4	down-regulated
+	2.884703964	P33992	MCM5_HUMAN	DNA replication licensing factor MCM5	MCM5	down-regulated
+	2.754910472	P33993	MCM7_HUMAN	DNA replication licensing factor MCM7	MCM7	down-regulated
+	1.604719285	P52943	CRIP2_HUMAN	Cysteine-richprotein 2	CRIP2	down-regulated
+	1.333266232	P37268	FDFT_HUMAN	Squalene synthase	FDFT1	down-regulated
+	1.212427275	P41226	UBA7_HUMAN	Ubiquitin-like modifier-activating enzyme 7	UBA7	up-regulated
+	1.821453521	P42224	STAT1_HUMAN	Signal transducer and activator of transcription 1-alpha/beta	STAT1	up-regulated
+	2.449511919	P42892	ECE1_HUMAN	Endothelin-converting enzyme 1	ECE1	down-regulated
+	2.298576947	P43121	MUC18_HUMAN	Cell surface glycoprotein MUC18	MCAM	down-regulated
+	1.679473775	P43246	MSH2_HUMAN	DNA mismatch repair protein Msh2	MSH2	down-regulated
+	1.861651687	P56556	NDUA6_HUMAN	NADH dehydrogenase [ubiquinone] 1 alpha subcomplex subunit 6	NDUFA6	down-regulated
+	2.200140577	P48735	IDHP_HUMAN	Isocitrate dehydrogenase [NADP], mitochondrial	IDH2	down-regulated
+	1.593918793	P68366	TBA4A_HUMAN	Tubulin alpha-4A chain	TUBA4A	down-regulated
+	1.597223282	P49593	PPM1F_HUMAN	Protein phosphatase 1F	PPM1F	down-regulated
+	1.49838734	P49736	MCM2_HUMAN	DNA replication licensing factor MCM2	MCM2	down-regulated
+	2.07882652	Q10739	MMP14_HUMAN	Matrix metalloproteinase-14	MMP14	down-regulated
+	2.609896121	P50453	SPB9_HUMAN	Serpin B9	SERPINB9	up-regulated
+	2.514183214	P98160	PGBM_HUMAN	Basement membrane-specific heparan sulfate proteoglycan core protein	HSPG2	down-regulated
+	2.274894235	P51991	ROA3_HUMAN	Heterogeneous nuclear ribonucleo protein A3	HNRNPA3	up-regulated
+	1.611304258	P52306	GDS1_HUMAN	Rap1GTPase-GDP dissociation stimulator 1	RAP1GDS1	down-regulated
+	2.321143717	P52597	HNRPF_HUMAN	Heterogeneous nuclear ribonucleo protein F	HNRNPF	down-regulated
+	1.329352619	Q03252	LMNB2_HUMAN	Lamin-B2	LMNB2	down-regulated
+	1.751193241	P53999	TCP4_HUMAN	Activated RNA polymerase II transcriptional coactivator p15	SUB1	up-regulated
+	2.646805136	Q09666	AHNK_HUMAN	Neuroblast differentiation-associated protein AHNAK	AHNAK	down-regulated
+	1.729091791	P60903	S10AA_HUMAN	Protein S100-A10	S100A10	down-regulated

significance	-LOG(p-value)	Uniprot Accession	Uniprot ID	Name	Gene	Up/down regulation
+	1.942369382	P62805	H4_HUMAN	Histone H4	HIST1H4A	down-regulated
+	2.10781878	P62873	GBB1_HUMAN	Guaninenucleotide-binding protein G(I)/G(S)/G(T) subunit beta-1	GNB1	down-regulated
+	2.121541309	Q13045	FLII_HUMAN	Proteinflightless-1homolog	FLII	down-regulated
+	1.752420731	Q71DI3	H32_HUMAN	HistoneH3.2	HIST2H3A	down-regulated
+	1.247860179	P80217	IN35_HUMAN	Interferon-induced 35kDa protein	IFI35	up-regulated
+	2.580596148	Q14315	FLNC_HUMAN	Filamin-C	FLNC	down-regulated
+	1.878338705	Q01813	PFKAP_HUMAN	ATP-dependent 6-phospho fructokinase, platelettype	PFKP	down-regulated
+	2.280218766	Q01995	TAGL_HUMAN	Transgelin	TAGLN	down-regulated
+	2.452618714	Q02790	FKBP4_HUMAN	Peptidyl-prolylcis-transisomerase FKBP4	FKBP4	up-regulated
+	2.102109949	Q15019	SEPT2_HUMAN	Septin-2	SEPT2	down-regulated
+	2.315430492	Q03518	TAP1_HUMAN	Antigen peptide transporter 1	TAP1	up-regulated
+	1.363322983	Q05519	SRS11_HUMAN	Serine/arginine-rich splicing factor 11	SRSF11	down-regulated
+	2.233465532	Q06210	GFPT1_HUMAN	Glutamine--fructose-6-phosphate aminotransferase [isomerizing]1	GFPT1	up-regulated
+	2.236564905	Q15149	PLEC_HUMAN	Plectin	PLEC	down-regulated
+	1.549274675	Q10471	GALT2_HUMAN	PolypeptideN-acetyl galactosaminyl transferase2	GALNT2	down-regulated
+	1.320606115	Q10472	GALT1_HUMAN	Polypeptide N-acetyl galactosaminyl transferase 1	GALNT1	up-regulated
+	2.260549256	Q12874	SF3A3_HUMAN	Splicing factor 3A subunit 3	SF3A3	down-regulated
+	1.201522635	Q13011	ECH1_HUMAN	Delta (3,5)-Delta (2,4)-dienoyl-CoA isomerase, mitochondrial	ECH1	down-regulated
+	1.628826877	Q16181	SEPT7_HUMAN	Septin-7	SEPT7	down-regulated
+	1.354861439	Q13451	FKBP5_HUMAN	Peptidyl-prolylcis-transisomerase FKBP5	FKBP5	down-regulated
+	2.102855785	Q13619	CUL4A_HUMAN	Cullin-4A	CUL4A	down-regulated
+	1.878398865	Q14108	SCRB2_HUMAN	Lysosome membrane protein 2	SCARB2	up-regulated
+	1.549515149	Q16555	DPYL2_HUMAN	Dihydropyrimidinase-related protein 2	DPYSL2	down-regulated
+	3.398949891	Q14554	PDIA5_HUMAN	Protein disulfide-isomerase A5	PDIA5	down-regulated
+	2.4553328	Q14764	MVP_HUMAN	Majorvaultprotein	MVP	down-regulated
+	2.324005502	Q14914	PTGR1_HUMAN	Prostaglandinreductase1	PTGR1	down-regulated
+	3.406335429	Q16658	FSCN1_HUMAN	Fascin	FSCN1	down-regulated
+	2.302852662	Q99439	CNN2_HUMAN	Calponin-2	CNN2	up-regulated
+	3.283138273	Q15646	OASL_HUMAN	2'-5'-oligoadenylate synthase-like protein	OASL	up-regulated
+	2.217394578	Q9BUF5	TBB6_HUMAN	Tubulin beta-6 chain	TUBB6	down-regulated
+	2.561061429	Q9NZN4	EHD2_HUMAN	EH domain-containingprotein2	EHD2	down-regulated
+	1.577606286	Q9ULV4	COR1C_HUMAN	Coronin-1C	CORO1C	down-regulated
+	1.999767899	Q16836	HCDH_HUMAN	Hydroxyacyl-coenzymeA dehydrogenase, mitochondrial	HADH	down-regulated
+	1.826012273	Q53EP0	FND3B_HUMAN	Fibronectin typeIII domain-containing protein 3B	FNDC3B	up-regulated

significance	-LOG(p-value)	Uniprot Accession	Uniprot ID	Name	Gene	Up/down regulation
+	1.552276205	Q58FF8	H90B2_HUMAN	Putative heat shock protein HSP90-beta2	HSP90AB2P	up-regulated
+	1.270364733	Q5EBM0	CMPK2_HUMAN	UMP-CMP kinase2, mitochondrial	CMPK2	up-regulated
+	1.463361821	Q5U651	RAIN_HUMAN	Ras-interacting protein 1	RASIP1	down-regulated
+	1.787507794	Q9C0H2	TTYH3_HUMAN	Protein tweety homolog 3	TTYH3	down-regulated
+	1.650812059	Q6P5R6	RL22L_HUMAN	60S ribosomal protein L22-like 1	RPL22L1	down-regulated
+	2.039280783	Q7Z2W4	ZCCHV_HUMAN	Zinc finger CCCH-type antiviral protein 1	ZC3HAV1	up-regulated
+	1.878171649	Q86UX7	URP2_HUMAN	Fermitin family homolog 3	FERMT3	down-regulated
+	1.583697895	Q8NC42	RN149_HUMAN	E3ubiquitin-proteinligaseRNF149	RNF149	down-regulated
+	1.497383781	Q8WWM7	ATX2L_HUMAN	Ataxin-2-likeprotein	ATXN2L	up-regulated
+	1.694896568	Q92890	UFD1_HUMAN	Ubiquitin recognition factorin ER-associated degradation protein 1	UFD1	up-regulated
+	1.969505466	Q969H8	MYDGF_HUMAN	Myeloid-derived growth factor	MYDGF	up-regulated
+	1.382502901	Q96C19	EFHD2_HUMAN	EF-hand domain-containing protein D2	EFHD2	down-regulated
+	1.542673009	Q96CV9	OPTN_HUMAN	Optineurin	OPTN	up-regulated
+	1.613865805	Q96HY6	DDRGK_HUMAN	DDRGK domain-containing protein 1	DDRGK1	up-regulated
+	2.875678045	Q96IZ0	PAWR_HUMAN	PRKC apoptosis WT1 regulator protein	PAWR	up-regulated
+	1.211081218	Q96JJ7	TMX3_HUMAN	Proteindisulfide-isomeraseTMX3	TMX3	up-regulated
+	1.801323121	Q96S97	MYADM_HUMAN	Myeloid-associated differentiation marker	MYADM	up-regulated
+	4.192993681	P00441	SODC_HUMAN	Superoxidedismutase [Cu-Zn]	SOD1	up-regulated
+	1.392978492	Q99584	S10AD_HUMAN	Protein S100-A13	S100A13	up-regulated
+	1.63392292	Q9BRX8	PXL2A_HUMAN	Peroxiredoxin-like2A	PRXL2A	down-regulated
+	1.948658409	Q9BS26	ERP44_HUMAN	Endoplasmic reticulum resident protein 44	ERP44	up-regulated
+	1.617333177	P04275	VWF_HUMAN	von Willebrand factor	VWF	down-regulated
+	1.766838223	Q9H173	SIL1_HUMAN	Nucleotide exchange factor SIL1	SIL1	up-regulated
+	1.943140258	Q9NTK5	OLA1_HUMAN	Obg-likeATPase1	OLA1	down-regulated
+	1.830215639	Q9NUL5	RYDEN_HUMAN	Repressor of yield of DENV protein	RYDEN	up-regulated
+	0.842053064	Q9NY15	STAB1_HUMAN	Stabilin-1	STAB1	up-regulated
+	2.598572211	Q9NYL4	FKB11_HUMAN	Peptidyl-prolylcis-transisomerase FKBP11	FKBP11	up-regulated
+	1.329038421	Q9NZ45	CISD1_HUMAN	CDGSH iron-sulfur domain-containing protein 1	CISD1	up-regulated
+	2.438077482	Q9NZM1	MYOF_HUMAN	Myoferlin	MYOF	down-regulated
+	1.548401269	P29279	CCN2_HUMAN	CCN family member 2	CCN2	up-regulated
+	1.789612702	Q9UBS4	DJB11_HUMAN	DnaJhomolog subfamily B member 11	DNAJB11	up-regulated
+	1.932532493	Q9UKK3	PARP4_HUMAN	Protein mono-ADP-ribosyltransferase PARP4	PARP4	down-regulated
+	2.121041419	P50570	DYN2_HUMAN	Dynamin-2	DNM2	up-regulated
+	1.663875263	Q9UHB6	SREBP3_HUMAN	LIM domain and actin-binding protein 1	LIMA1	up-regulated
+	2.614951661	Q9Y3Z3	SAMH1_HUMAN	Deoxy nucleoside triphosphatetri phosphohydrolase SAMHD1	SAMHD1	down-regulated
+	2.108161482	Q9Y570	PPME1_HUMAN	Protein phosphatase methyl esterase 1	PPME1	up-regulated

4. VEGF SIGNALING AND VASCULAR DEVELOPMENT: ROLE OF AKT IN ARTERY-VEIN SPECIFICATION

(PAPER II)

4.1 ZEBRAFISH AS A MODEL TO STUDY VASCULAR DEVELOPMENT

Zebrafish (*Danio rerio*) is a small tropical freshwater fish often used as a vertebrate organism model to study angiogenesis and vascular development *in vivo*.

Zebrafish presents a series key advantages over other vertebrate models. First, they are faster and cheaper compared to mice. A single breeding pair produces hundreds of eggs weekly, facilitating genetic and statistical analysis. Eggs are fertilized externally and embryonic development can be easily observed. Most importantly, zebrafish embryos are optically transparent allowing the *in vivo* study of organs development in a non-invasive manner. Transgenic technology has enhanced *in vivo* imaging capabilities that zebrafish larvae may offer to the investigator. Many vascular-specific fluorescent transgenic lines allowing the direct visualization of *in vivo* vessel formation have greatly advanced our understanding of vascular biology (Lawson & Weinstein, 2002; Schuermann et al., 2014) (**Figure 7**). Last but not the least, the high level of evolutionary conservation between zebrafish and humans highlights the utility of zebrafish as a model of human disease. In the recent years, the use of zebrafish-oriented targeted knockout technologies to study genes implicated in human diseases, substantially accelerated the study of vascular biology (Lieschke & Currie, 2007).

All these characteristics make zebrafish a powerful and highly versatile model to study cardiovascular embryonic development.

Zebrafish embryonic development is very rapid. All major organs form within the first 24 hours post fertilization (hpf), and within 3 days embryos hatch and larvae start looking for food. After 3-4 months zebrafish are sexually mature and ready to generate new offspring.

The cardiovascular system is one of the first to develop (Gore et al., 2012). It originates from the lateral plate mesoderm, where hemangioblasts, cells co-expressing both hematopoietic and endothelial genes and able to form both blood and endothelium. In zebrafish hemangioblasts are present until the 10-somite stage.

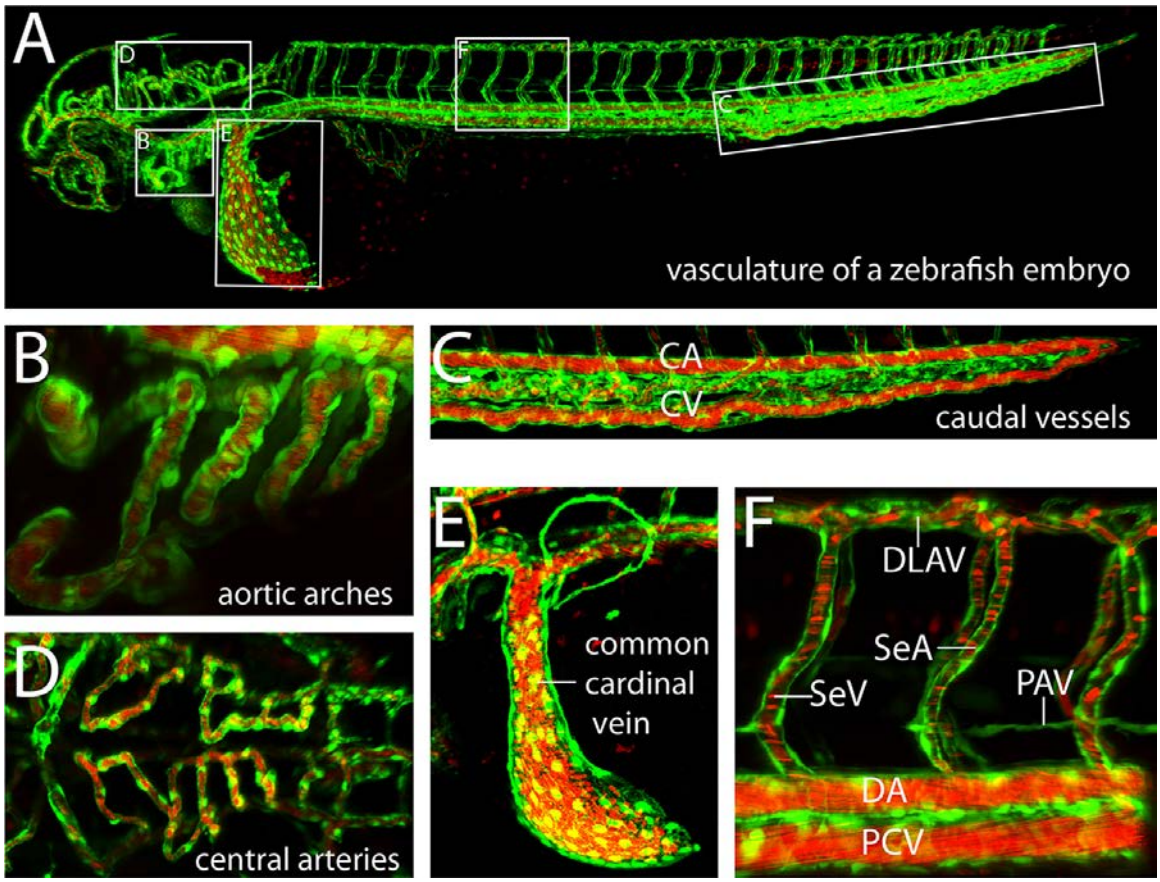

Figure 7: **The vasculature of a double transgenic zebrafish embryo at 2.5 days post fertilization.** In green, the embryonic vasculature is visualized by transgenic GFP expression using the vascular specific transgenic line *Tg(kdrl:EGFP)*^{s843}. In reed, blood red cells are visualized by transgenic dsRed expression using the transgenic line *(gata1:dsRed)*^{sd2}. (A) Lateral view of the whole embryo; (B) lateral view of the aortic arches (high magnification); (C) lateral view of the caudal vessels showing the caudal aorta (CA), the caudal vein (CV), and the caudal vein plexus (high magnification); (D) dorsal view of the cranial central arteries (high magnification); (E) high magnification of the common cardinal vein (CCV); (F) the intersegmental vessels (Se/ISV), consisting of arteries (SeA) and veins (SeV), contacting the dorsal longitudinal anastomotic vessel (DLAV), parachordal vessel (PAV), and dorsal aorta (DA) and posterior cardinal vein (PCV). (From Schuermann et al., 2014)

Angioblasts start to migrate toward the midline in two separate waves in an anterior-posterior direction to form the two major embryonic vessels, the dorsal aorta (DA) and the posterior cardinal vein (PCV) via a process known as vasculogenesis.

The first wave of angioblasts reaches the midline around 14-15 somites stage, and will give rise to embryonic arteries and DA. The second wave contains primitive erythroid progenitors and angioblasts destined to form the PCV.

Following their arrival at the midline, angioblasts coalesce to form a single vascular cord by 19.5 hpf (21-somite stage) and remodelling of this vascular cord leads to vascular lumenization by approximately 22 hpf.

Differentially expressed endothelial markers can be observed at this stage as ECs undergo arterial–venous specification, with arteries expressing ephrin-B2 ligand and veins expressing ephB4 receptor tyrosine kinase. The interaction of ligand and receptor requires cell–cell contact and defines and maintains the complex boundaries between arterial and venous territories (Swift & Weinstein, 2009).

Within the common vessel primordium, venous angioblasts expressing ephb4 migrate ventrally, away from ephrinb2a-expressing angioblasts and toward the territory of the PCV, via a process limited by VEGF and Notch signalling (Herbert et al., 2009)

The sequential activation of hedgehog (Hh), VEGF and Notch signalling promotes arterial determination (Lawson et al., 2002). In mice, the Notch1, Notch3, and Notch4 receptors, and the Dll4, Jagged1, and Jagged2 ligands, exhibit arterially restricted expression (Villa et al., 2001), and murine and zebrafish knockout studies showed that these molecules play an important functional role in the vasculature (Lawson et al., 2001; Lin et al., 2007; Swift & Weinstein, 2009)

Most postnatal blood vessel formation occurs via the remodelling of pre-existing vessels in a process known as angiogenesis.

The intersegmental vessels (Se/ISVs) of the trunk are among the first angiogenic vessels to form in all vertebrates. Time-lapse imaging of transgenic zebrafish lines allows the visualization of this angiogenic process *in vivo* (**Figure 8**).

ISVs sprout bilaterally from the dorsal wall of the DA, anterior to each somite boundary from approximately 22 hpf. Venous ISVs (SeV) sprout later than arterial ISVs (SeA), from approximately 36 hpf onward. While the initial stages of aISV sprouting occur independently of blood flow, the onset of circulation, that occurs around 24 hpf, provides a further level of regulation governing the development of the vasculature. Trunk vascularization is concluded by 32hpf with the formation of the DLAV plexus, which requires both circulatory flow and VEGF signalling. In this process, the aISVs, which sprout from the DA, continue their dorsal migration until they reach dorsal-lateral surface of the neural tube, at which point they bifurcate along the anteroposterior axis and then interconnect to form the dorsal anastomotic vessels (DLAV) plexus (Gore et al., 2012).

VEGF and Notch signalling are the major regulators of trunk angiogenesis (Siekmann & Lawson, 2007; Torres-Vázquez et al., 2004).

Regulation of the number of tip cells is essential for the proper patterning of the vasculature and is dictated by VEGF and Notch signalling through lateral inhibition of an angiogenic state in stalk cells (**Figure 8**). As previously mentioned, VEGFR2 activation in the tip cells leads to an up-regulation of the Dll4 and a subsequent up-regulation of Notch activity (internalization of Notch) in the neighbouring stalk cells. Increased Notch activity promotes stalk cell behaviour at the expense of tip cell behaviour. Notch activation in the stalk cells suppresses VEGFR3/FLT4 signalling and a pro-angiogenic fate (Siekmann & Lawson, 2007). This mechanism is highly conserved through evolution.

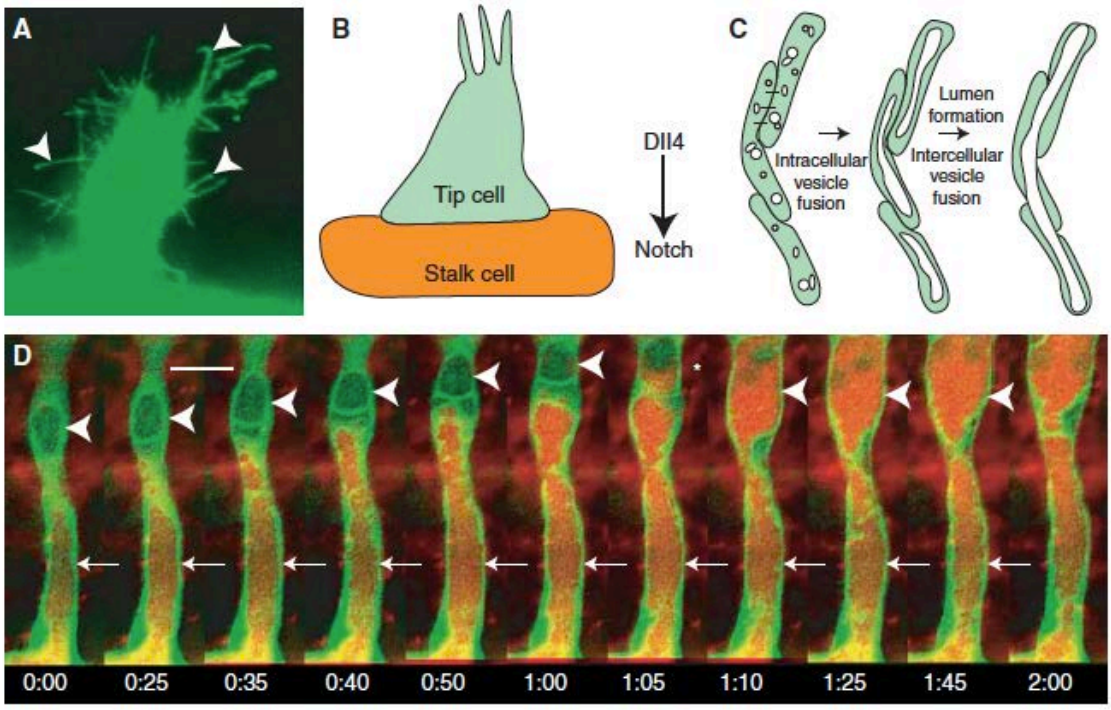

Figure 8: **Development of intersegmental vessels (ISV).** (A) Growing intersegmental vessel sprout with multiple cellular processes (arrowheads). (B) Diagram of tip cells, expressing Dll4 ligand and and stalk cells expressing Notch receptor; Dll4 in tip cells activates Notch in adjacent ECs to promote stalk cell identity. (C) Schematic diagram of vascular lumen formation in intersegmental vessels (D) Live time-lapse imaging of lumen formation of trunk intersegmental vessel (in green) in a vascular specific transgenic embryo *Tg(fli1:EGFP-cdc42wt)*^{y48} injected intravascular with quantum dots (in red, 605 nm). Scale bar 1⁄4 20 mm. (from Gore et al., 2012.)

4.2 AKT SIGNALLING IN THE VASCULAR ENDOTHELIUM

VEGF pro-angiogenic effects are mediated in part by the P13K/Akt pathway. Akt is a serine/threonine protein kinase, also known as protein kinase B (PKB) that is activated by a number of growth factors and cytokines in a phosphatidylinositol-3 kinase (PI3K)–dependent manner.

Akt has anti-apoptotic activity by regulating PI3K-mediated cell survival (Yao & Cooper, 1995; Franke et al., 1995). Furthermore, Akt regulates glucose metabolism (Wang et al., 1999) and protein synthesis (Downward, 1998) in many cell types.

Mammalian genomes contain three Akt genes, Akt1/PKBα, Akt2/PKBβ, and Akt3/PKBγ, whereas *Drosophila melanogaster* and *Caenorhabditis elegans* contain one and two Akt genes, respectively (Datta et al., 1999; Scheid et al., 2001). In zebrafish, several distinct Akt proteins have been identified: zebrafish Akt1, Akt2, Akt2-like, Akt3a, and Akt3b (ZFIN: The Zebrafish Model Organism Database). All 3 mammalian Akt genes are widely expressed in various tissues but Akt1 is predominantly expressed in heart, lung and brain whereas Akt2 is most abundant in embryonic brown fat and in skeletal muscle, and Akt3 is predominantly expressed in embryonic heart, brain, and kidney (Shiojima & Walsh, 2002).

Different isoforms have preferential substrates and distinctive functions. Loss of Akt1 gene in mice results in growth retardation due to defects during placental development, as well as impaired extra-embryonic vascular pattern. Mice lacking Akt2 exhibit impaired insulin signalling and a type 2 diabetes-like syndrome. Akt3 knockout mice show predominantly a neurological phenotype and reduced brain sizes (Somanath et al., 2006).

The isoform Akt1 plays a major role in angiogenesis (Lee et al., 2014) and in sustain vessel integrity during adulthood (Kerr et al., 2016). However, constitutive Akt1 knockouts are viable suggesting an overlapping function between Akt isoforms during vascular embryonic development (Chen et al., 2001).

Akt proteins contain a lipid-binding pleckstrin homology (PH) domain in the amino terminus, a central kinase domain, and a carboxy terminal regulatory domain. In unstimulated cells, Akt protein exists in cytoplasm and the two regulatory phosphorylation sites at threonine at 308 (T308) and serine at 473 (S473) are in an unphosphorylated state. On growth factor stimulation, the PH domain binds to the lipid products of PI3K, and Akt is recruited to plasma membrane. Akt is then sequentially phosphorylated at T308 and

S473 by upstream kinases PDK1 and PDK2, to yield a fully activated kinase (Hemmings, 1997; Downward, 1998). Fully activated Akt becomes available to phosphorylate its downstream substrates and a portion of these molecules detaches from the plasma membrane and translocate to various subcellular locations including the nucleus. Akt is then dephosphorylated and inactivated by protein phosphatases such as protein phosphatase 2A (PP2A) (Shiojima & Walsh, 2002).

In ECs, Akt has critical roles in the regulation of vascular homeostasis and VEGF-mediated angiogenesis (Somanath et al., 2006; Shiojima & Walsh, 2002). In particular, VEGF effects on EC survival have been shown to be mediated by VEGFR2/PI3K/Akt pathway (Gerber et al., 1998). Furthermore, VEGF activation of Akt in ECs is dependent on matrix attachment, and constitutively active Akt blocks cell detachment–induced apoptosis (Fujio et al., 1999).

Akt also directly phosphorylates and activates eNOS, which produces NO in endothelial cells to control vascular tone (Lee et al., 2014).

Finally Akt regulates endothelial cells migration in response to growth factors via actin reorganization and through phosphorylation of a cytoskeletal protein called Girdin. Silencing of the Akt substrate Girdin abolished VEGF-induced EC tube formation (Kitamura et al., 2007).

Akt phosphorylation promotes the activation of multifunctional signalling nodes such as GSK3, FOXO and mTOR (mammalian target of rapamycin) (Manning & Toker, 2017). In particular, FOXO transcription factor is a key effector of angiogenesis. Mice global knockout for FOXO1 show to aberrant vascular growth and embryonic lethality indicating a central role of FOXO1 isoform in vascular development (Furuyama et al., 2004; Hosaka et al., 2004; Dharaneeswaran et al., 2014).

Due to the highly branched signalling network downstream of Akt, and different and sometimes opposite effects of short-term versus long-term Akt activation, its role in pathophysiological processes and embryonic development remains elusive.

3.3 AIM PAPER 2

The serine/threonine protein kinase Akt is involved in a variety of cellular processes including cell proliferation, survival, metabolism and gene expression. It is essential in vascular endothelial growth factor (VEGF)-mediated angiogenesis (Somanath et al., 2006; Shiojima & Walsh, 2002); however, it is not known how Akt regulates cardiovascular development during early embryogenesis.

In this study we used zebrafish as an animal model to investigate the role of Akt during early vascular development.

We showed that the genetic loss of Akt in zebrafish impairs arterial EC specification. Live cell imaging coupled with single cell RNA sequencing of akt mutants revealed that Akt sustains arterial cell progenitor specification and segregation.

We found that the loss of Akt alters the size of distinct ECs subpopulations, in particular we observed a reduction in arterial markers and an increase of EC subpopulation co-expressing arterial and venous markers, suggesting a defect in arteriovenous segregation.

Interestingly, loss of Akt did not impact the migration of endothelial progenitors towards the midline. Moreover, loss of Akt didn't affect VEGFA availability or ERK activation, but regulated the expression arterial fate markers dependent on FOXO and Notch. Indeed, inhibition of active FOXO in Akt mutants could rescue impaired arterial development, but not the expression of arterial markers, whereas Notch activation rescued arterial marker expression.

These data place Akt at a critical signalling node during early artery-vein fate decisions in zebrafish and suggest that Akt activity is critical for early artery development, in part via FOXO and Notch-mediated regulation.

Further studies will be necessary to investigate the Akt-mediated regulation of genes expressed in unsegregated arteriovenous cells, and to establish if the defect we observed is the result of Akt-FOXO-Notch or/and Akt-Notch regulation.

This study provides novel insights into the important role of Akt signalling pathway during early vascular development.

Akt is required for artery formation during embryonic vascular development

Wenping Zhou[1,2], Emma Ristori[4,8] , Liqun He[6], Joey Ghersi[4,5], Sameet Mehta[5], Rong Zhang[2,3], Christer Betsholtz[6,7], Stefania Nicoli[2,3,4,5*] William C. Sessa[2,3*]

[1]Department of Cell Biology, Yale University School of Medicine, New Haven, CT 06511, USA

[2]Vascular Biology & Therapeutics Program, Yale University School of Medicine, New Haven, CT 06520, USA

[3]Department of Pharmacology, Yale University School of Medicine, New Haven, CT 06510, USA

[4]Yale Cardiovascular Research Center, Department of Internal Medicine, Section of Cardiology, Yale University School of Medicine, New Haven, CT 06511, USA

[5]Department of Genetics, Yale University School of Medicine, New Haven, CT 06510, USA

[6]Department of Immunology, Genetics and Pathology, Rudbeck Laboratory, Uppsala University, Dag Hammarskjölds väg 20, SE-751 85 Uppsala, Sweden.

[7]ICMC (Integrated Cardio Metabolic Centre), Karolinska Institutet, Novum, Blickagången 6, SE-141 57 Huddinge, Sweden

[8]Department of Life Sciences, University of Siena, 53100 Siena, Italy.

Correspondence: stefania.nicoli@yale.edu or willam.sessa@yale.edu

SUMMARY

One of the first events in the development of the cardiovascular system is morphogenesis of the main embryonic artery, the dorsal aorta (DA). The DA forms via a conserved genetic process mediated by the migration, specification, and organization of endothelial progenitor cells into a distinct arterial lineage and vessel type. Several angiogenic factors activate different signaling pathways to control DA formation, however the physiological relevance of distinct kinases in this complex process remains unclear. Here, we identify the role of Akt during early vascular development by generating mutant zebrafish lines that lack expression of akt isoforms. Live cell imaging coupled with single cell RNA sequencing of akt mutants reveal that Akt is required for proper development of the DA by sustaining arterial cell progenitor specification and segregation. Mechanistically, inhibition of active FOXO in akt mutants rescues impaired arterial development but not the expression of arterial markers, whereas Notch activation rescues arterial marker

expression. Our work suggests that Akt activity is critical for early artery development, in part via FOXO and Notch-mediated regulation.

Keywords: zebrafish embryo, vascular development, endothelial cells, artery identity, akt signaling, FOXO1, Notch.

INTRODUCTION

The cardiovascular system is essential to supply oxygen and nutrients to vital organs and tissues and is the first organ to function during vertebrate development. The dorsal aorta (DA) primordium is the main embryonic blood vessel that forms via endothelial progenitor cells (or angioblast) migration from the lateral posterior mesoderm, acquire arterial and venous gene expression programs, and then segregate to form the posterior cardinal vein (PCV) (Herbert et al., 2009a; Lawson and Weinstein, 2002a). With the formation of the vascular lumen and the initiation of the blood circulation, the DA and PCV acquire functional differences in vascular diameter, extracellular matrix and smooth muscle cell coverage (dela Paz and D'Amore, 2009; Lawson and Weinstein, 2002a) that are maintained into adulthood. Importantly, the molecular cues that dictate morphogenesis of the DA and PCV are conserved amongst vertebrates (Gore et al., 2012; Isogai et al., 2001).

The Ser and Thr kinase Akt, is a key element of the phosphotidylinositol 3-kinase (PI3K) /Akt signaling pathway and regulates the hallmarks of tissue formation such as growth and survival. Akt activation involves the phosphorylation of multiple substrates signaling network which enable Akt to exert diverse downstream effects from the activation of an individual upstream growth factor signaling. For example, during the formation of the DA, PI3K-Akt signaling is implicated in transducing multiple Vascular Endothelia Growth Factor a (Vegfa)-dependent cell behaviors, such as migration, differentiation and proliferation of endothelial cells. (Ackah et al., 2005; Liu et al., 2008; Phung et al., 2006; Zhu et al., 2013). Importantly, how Akt-substrate activation is involved in this multi phased process remain not fully understood.

Vertebrates encode three Akt isoforms: Akt1, Akt2, and Akt3 and these unique gene products are highly homologous between species. The Akt-signaling module is implicated in arteriogenesis by exerting an inhibitory influence on Raf-Erk-signaling (Ren et al., 2010) or in venogenesis via phosphorylation of the COUP TFII, a key driver of venous fate (Chu et al., 2016). However mice globally lacking Akt-1, the main isoform

expressed in endothelial cells, are viable, smaller in size, with reduced angiogenesis in the placenta, retina and limbs (Ackah et al., 2005; Ha et al., 2019; Schleicher et al., 2009; Yang et al., 2003) whereas the conditional loss of Akt-1 in the endothelium demonstrates reduced post-natal arteriogenesis and sprouting of retinal (Lee et al., 2014) and coronary vessels (Kerr et al., 2016). Thus, the genetic loss of Akt1 or other Akt isoforms in vertebrate has not established clear roles for Akt during the early DA and/or PCV development.

To assess the role of Akt in the early embryonic vascular development, we generated a novel loss of function model in zebrafish. The external development and optical transparency of zebrafish embryos facilitate the temporal dissection of vascular defects that are difficult to assess in other vertebrates such as mice. Using CRISPR/Cas9, we mutated all four akt genes encoding all three Akt isoforms and crossed them to a reporter line to image arterial and venous structures during development. Live cell imaging coupled with single cell RNA sequencing analysis of endothelial cells reveal that Akt is required for arterial specification, and arteriovenous (A-V) segregation but not for progenitor migration, during the initial formation/remodeling of the DA.

Mechanistically, our data suggest that the loss of Akt activates FOXO and reduces Notch dependent gene expression in arterial endothelium. Inhibition of FOXO1 in Akt deficient embryos increases DA development, whereas activation of Notch in these embryos enhances arterial specification. Thus, Akt controls two key transcription factors to coordinately govern DA morphology and arterial specification.

RESULTS

Embryonic loss of Akt results in artery-vein malformations.

To investigate the role of Akt signaling in early embryonic vascular development, we generated a complete akt loss-of-function model in zebrafish. In zebrafish, Akt1 is encoded by akt-1, Akt2 is encoded by akt-2, and Akt3 is encoded by akt-3a and -3b. Of these four genes, akt1 showed the highest expression in endothelial cells isolated from zebrafish (Figure S1A), consistent with observations in mice (Lee et al., 2014).

To establish a complete akt loss-of-function model, and avoid genetic compensation, we used CRISPR/Cas9 (Moreno-Mateos et al., 2015) to mutate all four akt genes (Figure 1A). We selected loss-of-function founders and established a quadruple homozygous mutant (aktΔ/Δ). Compared to wild-type (WT), aktΔ/Δ embryos had an ~80% reduction in the mRNA levels of each akt isoform (Figure 1B). aktΔ/Δ embryos were not

viable to adulthood, thus we established an akt1Δ/Δ, 3aΔ/Δ, 3bΔ/Δ, 2 Δ/+ which we named "mixed aktΔ/Δ". The levels of total and phosphorylated Akt were significantly reduced in mixed aktΔ/Δ relative to WT embryos (Figure 1B).

We assessed the overall morphology of aktΔ/Δ embryos at early stages of development. Compared to WT, aktΔ/Δ embryos exhibited a reduction in pigmented cells at 48 hours post fertilization (hpf) (Figure S1B) consistent with the chemical inhibition of Akt signaling (Ciarlo et al., 2017). Moreover, aktΔ/Δ had normal body and head size (Figure S1B) and were viable until 6 days post fertilization (dpf), enabling the analysis of specific vascular patterns in during early development.

We crossed mixed aktΔ/Δ line to a transgenic reporter line flt4:YFP; kdrl:hRasmCherryhu4881; s896 to enable the analysis of arteries (mCherry+) and veins (YFP+/mCherry+) during embryonic development (Figure 1C). We performed live imaging of the vasculature at 24 hpf and found that aktΔ/Δ embryos had decreased diameters of the endothelium of dorsal aorta (DA) and posterior cardinal vein (PCV) compared to WT embryos (Figure 1C images on left and quantified on right). The lengths of the Intersegmental vessels (ISV) that sprout from the DA appeared similar in both strains at this developmental time point. However, aktΔ/Δ embryos showed ectopic connections between the DA and PCV (Figure 1C, arrowheads in magnified image and quantified on right) suggesting a lack of proper artery-vein segregation.

These data suggest that Akt signaling input is necessary for proper patterning of the main embryonic blood vessels but dispensable for vascular cell migration of ISVs at 24 hpf.

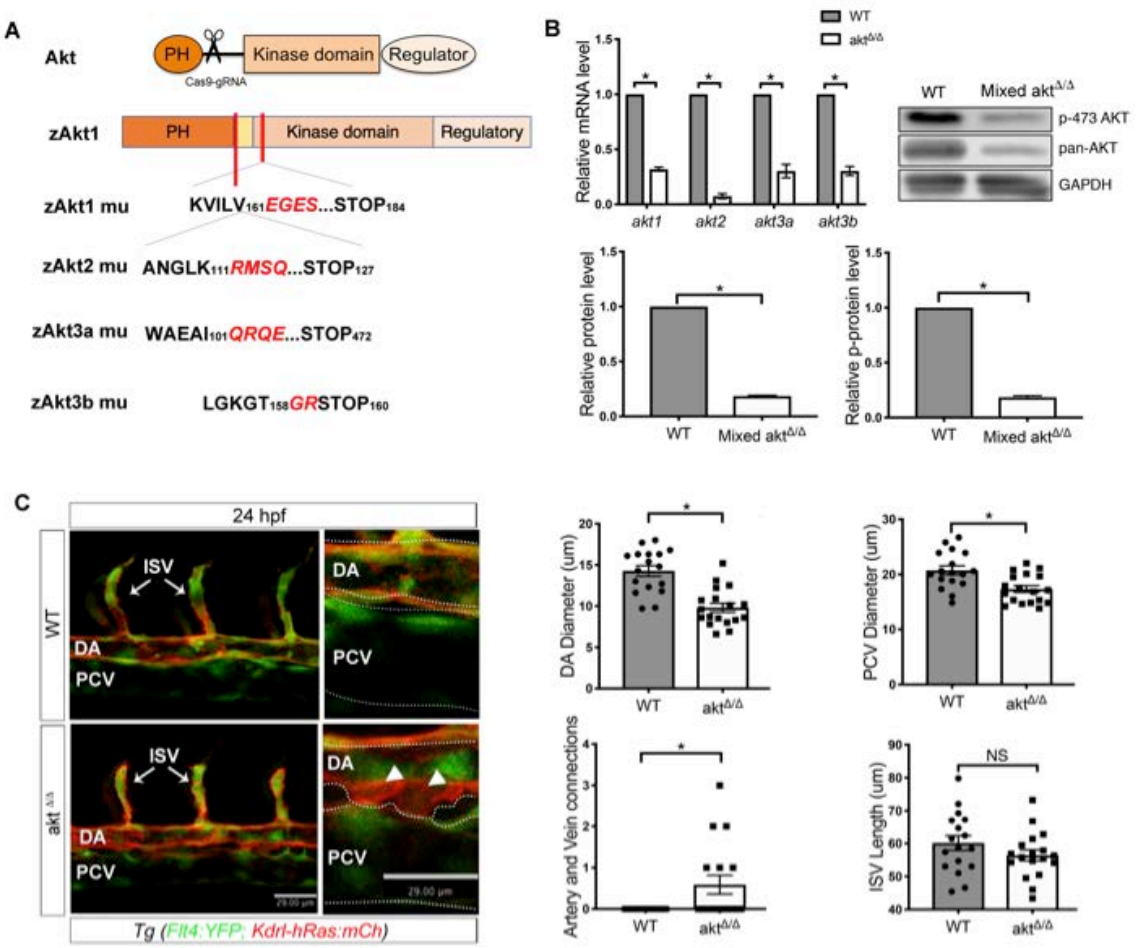

Figure 1. akt Δ/Δ embryos exhibit decreased DA diameter and abnormal arterial and venous connections. (A) Schematic of the domain structure of Akt isoforms and sequence alignment of wildtype (zAKt1) and mutant (mu) zebrafish lines. (B) qRT-PCR showing WT and mutant mRNA levels in WT and quadruple mutant aktΔ/Δ embryos on a Tg (flt4:YFP; kdrl:hRasmCherry) hu4881;s896 at 4 days post fertilization (dpf). Expression levels were normalized to the WT from three biological replicates. Western blot analysis of WT and mixed aktΔ/Δ embryos in Tg (flt4:YFP; kdrl:hRas-mCherry)hu4881;s896 from three biological replicates. *p< 0.05. (C) Confocal lateral view live images of WT and aktΔ/Δ embryos at 24 hpf trunk in Tg (flt4:YFP; kdrl:hRas-mCherry)hu4881;s896. White arrowheads indicate the abnormal artery and vein connection in the representative images. Bar plots on right show in WT, and aktΔ/Δ quantification. The embryos were placed in the lateral view with dorsal side up and anterior to left. Data are mean + SEM for DA and PCV diameters and artery and vein connections; *p< 0.05. DA=Dorsal Aorta, PCV=Posterior Cardinal Vein, ISV=intersegmental vessels.

Loss of Akt impairs arterial specification.

To investigate the molecular mechanisms that underline the vascular defects in embryos lacking Akt, we used single cell RNA sequencing analysis (scRNA-seq) of FAC-sorted endothelial cells (kdrl+ mCherry) from WT and mixed aktΔ/Δ reporter embryos at 24 hpf. Mixed aktΔ/Δ embryos showed substantially loss of Akt activity and recapitulated the same vascular defects of aktΔ/Δ full mutants (Figure 1B and S1C).

Artery and vein formation during development generates cellular diversity in endothelial cells, reflected by different subpopulations with distinct gene expression. To preserve the developmental progression of these subsets of endothelial cells, we used PHATE (Potential of Heat-diffusion for Affinity-based Trajectory Embedding) to analyze our scRNA-seq data (Moon et al., 2017). PHATE analysis demonstrated that kdrl+ mCherry cells formed a main vascular tree composed of 17 different branches corresponding to embryonic specification trajectories that were identified based on the expression of specific markers (Figure 2A). Based on the higher enrichment of artery and vein defining markers, we identified branches 1 and 2, as the main venous and arterial cell populations, respectively (Figure 2B). Branch 6 displayed co-expression of arterial and venous markers with cardiac genes, suggesting that this population mainly contributes to the heart vasculature. Branch 7 was enriched for markers of lymphatic endothelium, while the remaining cell pools expressed hemogenic, hematopoietic stem cells or blood progenitor markers (Figure 2B). Interestingly, kdrl+ mCherry cells isolated from mixed aktΔ/Δ embryos showed an identical number of branches as those isolated from WT, further supporting that the loss of Akt did not grossly affect the patterning of the embryonic cardiovascular system (Figure 2C and D).

Next, we examined the differential expression of known vascular genes in the kdrl+ mCherry cell subsets from WT and mutant embryos. Strikingly, we observed diminished expression in mixed aktΔ/Δ kdrl+ mCherry cells of genes that are mainly associated with artery differentiation and Notch regulated genes (efnb2a, cxcr4, dlc, dll4, notch3), but not venous fate (Figure 2E). Moreover, the fraction of cells within the branch 1 (vein) and 2 (artery) was reduced in the mutant endothelial cell population compared to WT, whereas the fraction of cells within the branch 11, which express both arterial and venous markers, was increased in the population of mutant endothelial cells as the expression of the arterial markers, cxcr4 and dlc (Figure 2E and 2F).

These data suggest that, at the molecular level, an excessive number of endothelial cells lacking akt fail to fully segregate into the arterial or/and the venous cell pool.

To verify the scRNA-seq results and add spatial resolution, we performed whole mount in situ hybridization of 24 hpf embryos to test the expression of artery markers efnb2a, dlc and notch3 genes in the DA. Relative to WT embryos, aktΔ/Δ embryos showed a decreased expression of all these arterial genes at 24 hpf (Figure 2G). In contrast, the expression of the venous marker, ftl4, or other markers for the maturation of spinal cord neurons (ngn1, elav13) or somites (myoD), showed no obvious changes in aktΔ/Δ embryos versus WT (Figure S2). Thus, gene expression defects associated with altered arterial specification were specific and not the result of global developmental anomalies. Collectively, these data suggest that Akt signaling is required to sustain arterial endothelial cells specification.

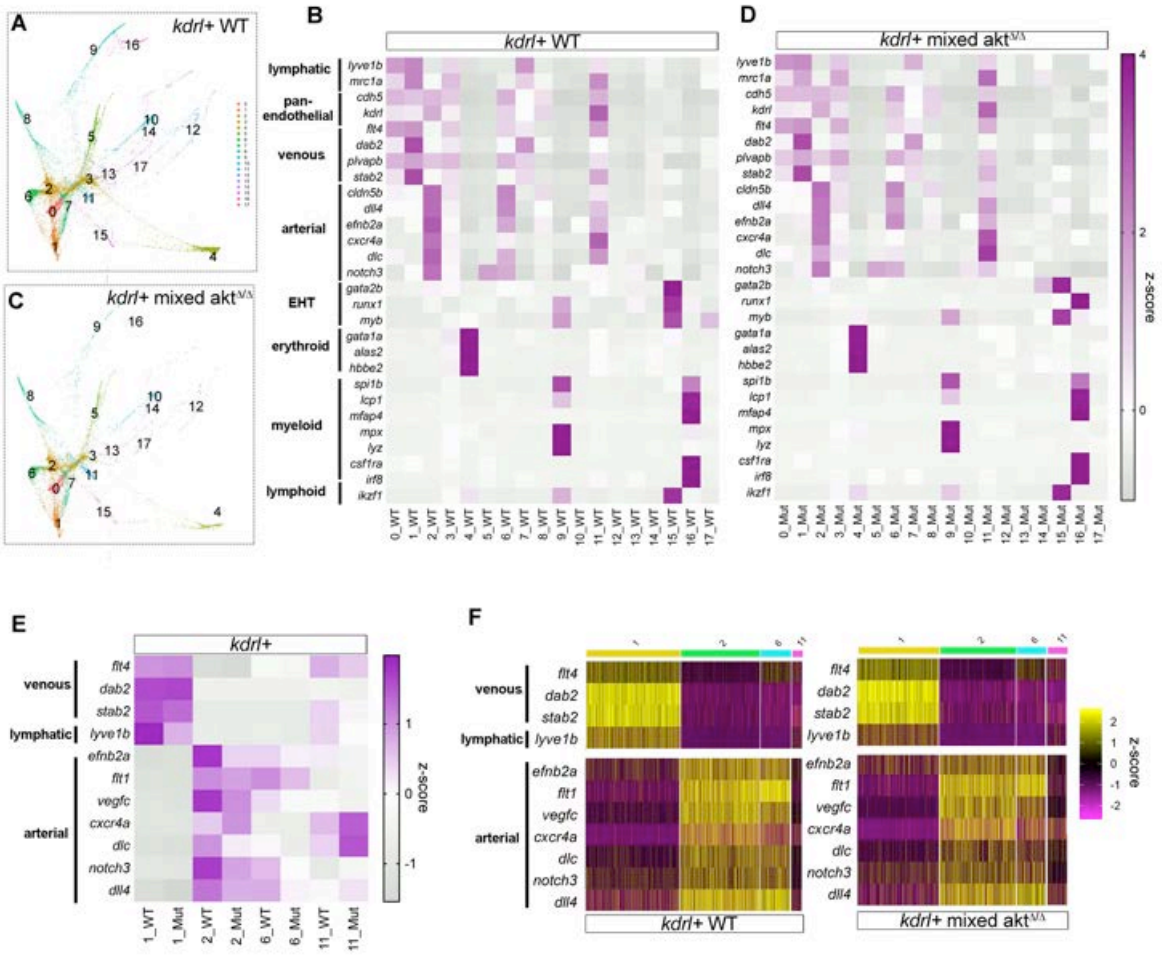

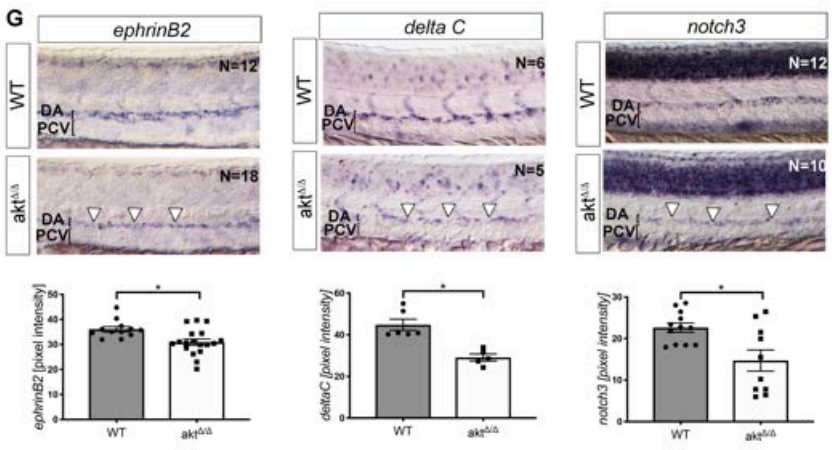

Figure 2. Single cell sequencing and in situ confirmation of diminished arterial markers expression in aktΔ/Δ zebrafish. PHATE plots (A,C) and heat maps (B,D) of scRNASeq data from WT and mixed aktΔ/Δ embryonic kdrl+ endothelial cells, respectively. All heatmaps depict z-score of vascular gene expression levels in kdrl+ endothelial cells expressing transcripts in scRNA-seq PHATE branches. (E) Heatmap highlighting the expression of venous, lymphatic and arterial markers from branches 1, 2, 6 and 11. (F) Heatmap showing increased fraction of cells in branch #11 in mixed aktΔ/Δ embryos with the length of the line on the top delineating the fraction of cells within the endothelial cell population. (G) Whole mount n situ hybridization bright field images of arterial markers ephrinB2, delta C (dlc) and notch3 in trunk vasculature of WT and aktΔ/Δ embryos at 24 hpf. The embryos were placed in the lateral view with dorsal side up and anterior to left. Bar plots quantify pixel intensity of each marker. Data are mean + SEM; *p< 0.05. DA=Dorsal Aorta, PCV=Posterior Cardinal Vein.

Akt drives artery specification independently of progenitor cell migration and ERK activity.

To further investigate the mechanism(s) behind the vascular morphogenesis defects in aktΔ/Δ embryos, we performed time lapse imaging from 20 to 22hpf in WT and mutant embryos. In WT embryos, endothelial progenitor cells sprouted from the DA primordium into the PCV at 20 hpf and fully segregated by 22-24 hpf (Figure 3A, left panel), as previously reported (Herbert et al., 2009b). Interestingly, in aktΔ/Δ embryos, DA progenitors sprouted in greater numbers toward the PCV yet failed to completely separate within 22 hpf (Figure 3A, right panel). These data in aktΔ/Δ embryos are reminiscent of loss of function notch mutants which manifest reduced Notch dependent gene expression (ephrinB2, dl4, dlc) in the DA (Lawson et al., 2002b; Quillien et al., 2014)(Figure 2F) or efnb2 morphants which result in the loss of artery specification and abnormal arteriovenous structures (Herbert et al., 2009a; Lawson et al., 2002b).

The migration of endothelial progenitor cells from the lateral posterior mesoderm (LPM) toward the embryonic midline ensures vasculogenesis and artery specification via VEGFa-mediated regulation of ephrinB2 and Notch-signaling (Lawson et al., 2002a; Zhong et al., 2001). Given that Akt can be downstream of VEGFa, we investigated whether endothelial progenitor cells (fli1a+) in aktΔ/Δ embryos have impaired migration from the LPM (Lawson and Weinstein, 2002b). Fli1a+ cells were visualized at different somite stages (ss) and no distinguishable differences were found between WT and mixed aktΔ/Δ embryos from 10 to 18 ss (Figure 3B). Interestingly, the levels of somitic Vegfa expression at 18 ss were enhanced (Figure S3A) in aktΔ/Δ versus WT embryos. Thus, the artery specification or altered arteriovenous separation defects in aktΔ/Δ embryos were not a consequence of impaired Fli1a+ cell migration or reduced Vegfa expression.

We also examined whether anomalies in cell survival could explain aktΔ/Δ vascular phenotypes, but we did not observe significant differences in the number of apoptotic cells between WT and akt mutants (Figure S3B).

Previous studies suggested that ERK activation is required downstream of VEGFa for arterial identity and proliferation and that input from the PI3 kinase/Akt pathway may negatively regulate the extent of ERK activation (Hong et al., 2006; Ren et al., 2010). Notably, p-ERK was localized in endothelial progenitor cells of the DA primordium (Shin et al., 2016) however, the number of p-ERK+ cells was comparable in WT and aktΔ/Δ 20 ss embryos (Figure 3C). Thus, our data suggest that Akt is distinctly required for specification of the main embryonic artery, independent of ERK-signaling.

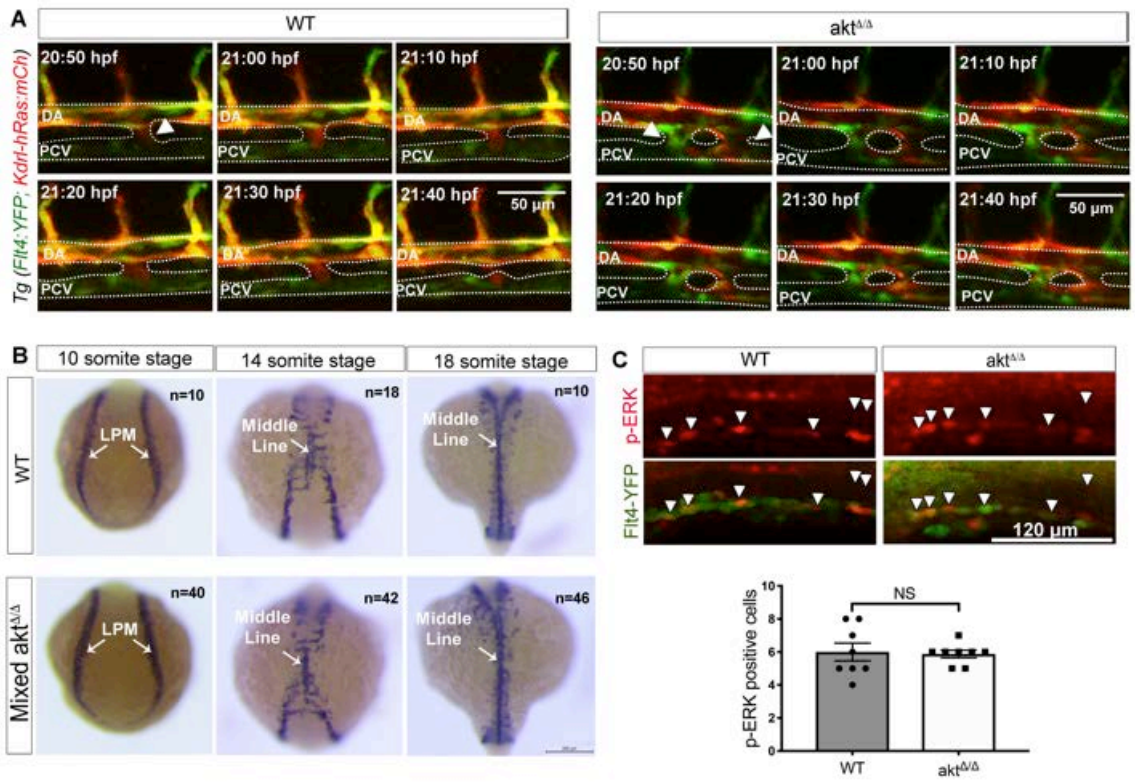

Figure. 3. Loss of akt impedes arteriovenous separation, but not angioblast homing or ERK signaling. (A) Images from time lapse movies of WT and aktΔ/Δ in Tg (flt4:YFP; kdrl:hRasmCherry) hu4881;s896 embryos (20-22 hpf). The embryos were placed in the lateral view with dorsal side up and anterior to left. Timestamps are in upper left of each panel. White arrows indicate connection between the artery and vein. B) In situ hybridization of marker fli1a labels the position of angioblasts at 10 ss, 14 ss and 18ss in WT and aktΔ/Δ embryos. White arrows point to the lateral posterior mesoderm (LPM) at 10 ss and indicates the middle line formation at 14 ss and 18 ss. (C) Lateral view of immunofluorescence images showing phosphorylated ERK in DA of WT and aktΔ/Δ in Tg (flt4:YFP;)hu4881 embryos at 14 ss. Data are mean+SEM. NS=non-significant.

Akt controls DA formation upstream FOXO and Notch signaling pathways.

We found that the DA specification is severely affected in the Akt loss of function embryos, while the PCV specified normally. Interestingly, both vessels showed a reduction in vascular diameter likely due to the excessive number of cells failing to segregate either in the DA or PCV.

To interrogate the signaling pathways upstream and downstream of Akt we therefore use DA morphology and arteriovenous (A-V) connections at 24hpf as the main phenotypic read-out of Akt loss of function. We first employed pharmacological agents that selectively interfere with components of the VEGF-PI3K pathway, which lie upstream in the Akt signaling cascade. Treatment of embryos with SU5416, a selective inhibitor the VEGF receptor 2 kinase (kdrl) (Kasper et al., 2017), decreased DA diameter in both WT

and mixed aktΔ/Δ embryos (Figure 4A, top for images and 4B for quantification). Interestingly, SU5416 enhanced A-V connections in WT but not further in mutant embryos indicating that VEGF signaling contributes to DA assembly and A-V separation but the effect on A-V connections is impeded in mixed aktΔ/Δ mutants. Treatment with the PI3K inhibitor LY-294,002 (Chen et al., 2017) reduced DA diameter in WT embryos but did not further impact DA in aktΔ/Δ embryos (Figure 4C, top for images and 4B for quantification). Similarly to SU5416 treated embryos, blockade PI3K increased A-V connections in WT but not further in mutant zebrafish (Figure 4B, top for images and below for quantification). These results indicate that VEGF-kdrl-PI3K signaling is critical for DA development and A-V separation, in part, via Akt.

To investigate pathways downstream of Akt that may contribute to the vascular defects in mutant embryos, we investigated the transcription factor FOXO1, an established Akt substrate known to be critical for several aspects of angiogenesis (Dharaneeswaran et al., 2014). Akt phosphorylation of FOXO1 leads to its nuclear exclusion and alterations FOXO1 dependent gene expression. Notably, treatment with AS1842856, which binds and inhibits the non-phosphorylated, active form of the transcription factor FOXO1 in the nucleus (Gays et al., 2017) reduced the DA diameter in the WT embryos but increased DA diameter in mixed aktΔ/Δ mutants (Figure 4E, top for images and 4F below for quantification), thus implying FOXO hyperactivation contributes to reduced DA in aktΔ/Δ embryos (Wilhelm et al., 2016). However, FOXO did not contribute to A-V separation in WT or A-V in mutant embryos since inhibition of FOXO did not impact the number of A-V connections in any genotype, suggesting that FOXO contribute differently to DA formation and specification.

Since the loss of Akt reduces the levels of several Notch-dependent genes, dll4, dlc, and notch3 in DA (Figure 2E), we assessed if FOXO can regulate the expression of the well characterized Notch dependent arterial specification marker dlc. Strikingly, inhibition of FOXO reduced the expression of dlc in the DA of WT embryos but did not further reduce the levels detected in aktΔ/Δ embryos (Figure 4G, compare top and middle panels and 4H for quantification). These data suggest Akt phosphorylation of FOXO regulates dlc levels, arterial specification and DA morphology. However, in the Akt depleted state, FOXO blockage induces uncoupling of arterial specification (Figure 4H) from DA morphology (Figure 4F where FOXO inhibition rescues DA phenotype in mixed aktΔ/Δ embryos).

Previous work has shown that Notch is downstream of Akt signaling (Bedogni et al., 2008; Kerr et al., 2016; Konantz et al., 2016; Zhang et al., 2011a). To verify if Notch is

downstream of Akt during the DA specification, we expressed the Notch 1 intracellular domain (NICD) under the endothelial fli1a promoter to ectopically activate Notch signaling in WT and mixed aktΔ/Δ embryos. Notably, NICD did not impact dlc expression in WT embryos, however NICD increased dlc levels in mixed aktΔ/Δ embryos (Figure 4G, bottom panels and 4H for quantification in right graph). Thus, expression of NICD normalizes dlc expression in mixed aktΔ/Δ embryos.

These data suggest that Akt signaling to FOXO and Notch is critical for early arterial development and arterial specification.

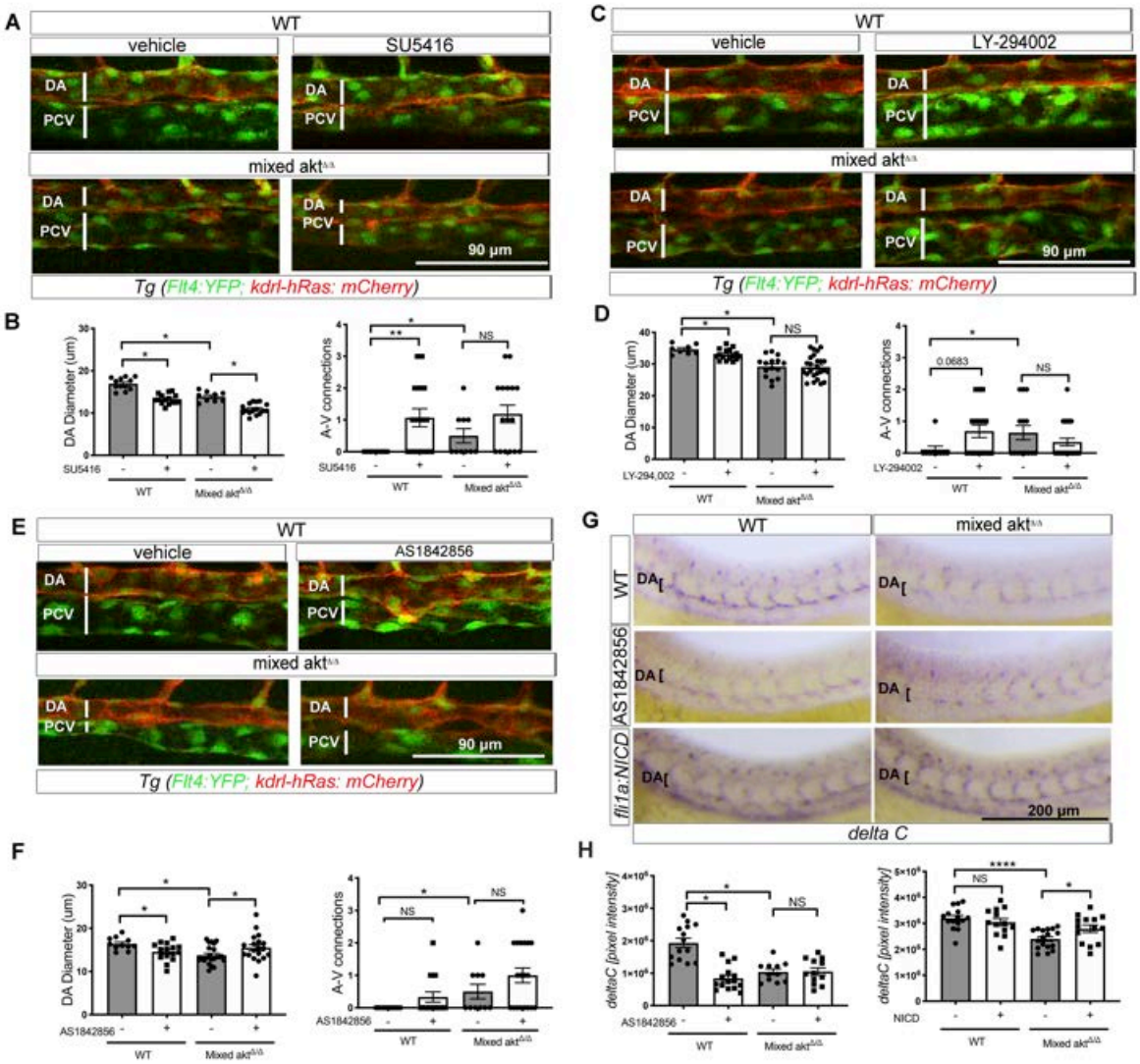

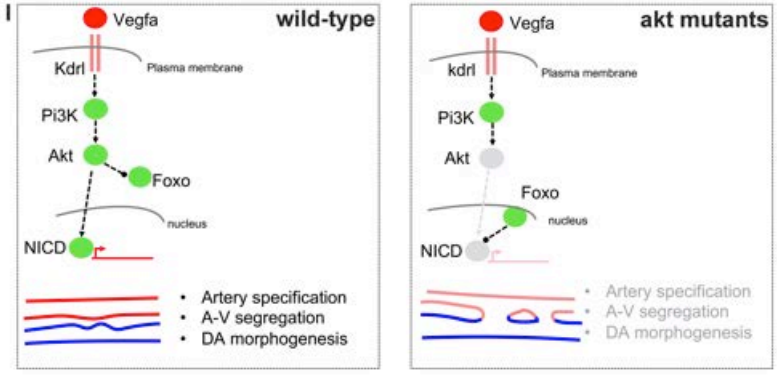

Figure. 4. Loss of akt reduces DA diameter and arterial specification via FOXO and Notch. (A) Lateral view images and (B) quantification of DA diameters and A-V connections in the trunk vasculature after treatment of WT and mixed aktΔ/Δ embryos at 24 hpf with a selective inhibitor of the VEGF receptor 2 (SU-5416, 1 μM). (C) Lateral view images and (D) quantification of DA diameters and A-V connections of the trunk vasculature after treatment of WT and mixed aktΔ/Δ embryos at 24 hpf with a PI-3K inhibitor (LY-294,002, 80 μM) (E) Lateral view images and (F) quantification of DA diameters and A-V connections of the trunk vasculature after treatment of WT and mixed aktΔ/Δ embryos at24 hpf with a FOXO inhibitor (AS1842856, 0.1 μM). (G) In situ hybridization and (H) quantification of arterial marker dlc in WT and mixed aktΔ/Δ embryos with and without treatment with FOXO1 inhibitor (AS1842856, 0.025 μM) and injection of an endothelia specific plasmid, Fli1a:Notch-NICD. Data are mean+SEM, * $p<0.05$, ** $p<0.01$, **** $p<0.0001$. NS=non-significant. (I) Model for Akt signaling in WT and akt mutant zebrafish.

DISCUSSION

Akt is considered as an important signaling node co-opted by several angiogenic factors (VEGF, angiopoietin, ephrin B2, fibroblast growth factor) that integrates signal transduction mechanisms during angiogenesis and vascular homeostasis (Manning and Cantley, 2007). Despite this central role, the importance of Akt signaling during early vascular development has not been thoroughly addressed. Here, we show that the loss of akt in zebrafish impairs the formation of the first major vessel, the DA, by reducing arterial specification and arterio-venous segregation. Our single cell sequencing analysis of akt mutant endothelial cells support this phenotype. We found that the loss of Akt alters the size of distinct endothelial cell subpopulations, particularly those expressing arterial markers, and reduces the expression of several Notch-dependent genes as confirmed by in situ analysis. Similarly, Akt loss of function cells have an increased cell pool with arterial and venous co-expressed markers, thus fail to segregate within the DA and PCV vessels.

Mechanistic analysis suggests that the loss of Akt did not impact the migration of endothelial progenitors towards the midline, the Vegfa availability or ERK activation but regulated the expression arterial fate markers dependent on FOXO and Notch (Figure 4I).

Thus, these data place Akt at a critical signaling node during early artery-vein fate decisions in zebrafish. Moreover, in Akt mutant embryos inhibition of FOXO increases the DA diameter to WT levels, while in presence of Akt, inhibition of FOXO has the opposite effect on the DA morphogenesis. This would suggest that FOXO function to control both DA diameter and specification is dependent on a threshold; namely that too high or too low FOXO activity results in similar DA defects. Another hypothesis is that FOXO controls DA morphogenesis and/or specification via parallel but independent mechanisms that might be antagonistic when the Akt-signaling pathway is lost (Figure 4I). Further studies will be required to characterize how FOXO function in Akt dependent and independent fashion.

Additionally, we show that Akt is required for expression of arterial endothelial cell specification genes independent of ERK, but dependent on Notch activity. Indeed, several Notch-dependent arterial markers were reduced in aktΔ/Δ zebrafish, and overexpression NICD restored the expression of dlc, suggesting that Akt impacts Notch dependent arterial specification. Akt can regulate Notch activity via a direct or indirect function. For example, Akt functions upstream of Notch in aortic endothelial cells (Konantz et al., 2016) can directly phosphorylate Notch4-ICD (Lee et al., 2014) and regulate Notch4 nuclear localization (Ramakrishnan et al., 2015). Alternatively, angiopoietin-1 can activate Akt and promotes Notch signaling indirectly by phosphorylating glycogen synthase kinase 3b (GSK3b), thereby enhancing b-catenin activity and upregulating Dll4-Notch in endothelial cells (Lawson and Weinstein, 2002a; Zhang et al., 2011b). Furthermore, FOXO and Notch can directly interact to coordinate cell specification and function in the context of other tissues (Kitamura et al., 2007; Pajvani et al., 2011). Thus, it is possible that arterial cell specification is mediated by direct regulation of the Akt-FOXO-Notch pathway (Figure 4I).

Interestingly, single cell RNA sequencing of endothelial cells from embryos lacking Akt reveals an increase fraction of cells that co-express arteriovenous genes that do not segregate within classic artery and vein trajectories. The expression of genes controlling cellular responses to stress (e.g.: the myeloperoxidase mpx and a regulator of ERmitochondrial contacts, Nogo-B) were decreased in this cell pool from aktD/D embryos compared to WT(Astern et al., 2007) (Acevedo et al., 2004; Sutendra et al., 2011; Yu et al., 2009). Further studies will be necessary to investigate if and how genes within the

arteriovenous unsegregated cells are directly regulated by Akt or if this defect is the result of Akt-Notch and/or Akt-FOXO-Notch regulation.

In summary, the genetic loss of Akt in zebrafish impairs arterial endothelial cell specification providing novel insights into the important role of Akt signaling pathway during early vascular development.

Acknowledgements

This work was supported by Grants R01HL130246 (to SN), R35 HL139945, the Leducq Foundation (MIRVAD network), P01 HL1070205, AHA MERIT Award (to WCS), AHA Predoctoral fellowship (to WZ) and by the Swedish Cancer Foundation, Science Council and Knut and Alice Wallenberg Foundation (to CB).

Author Contributions

WZ, SN, WCS designed experiments. WZ, ER, RZ and JJG performed experiments and/or analyzed the data. LH, SM and CB assisted with single cell sequencing analysis. WZ, SN and WCS wrote the manuscript. All authors contributed to the review of the manuscript.

Declaration of Interests

The authors declare no competing interests.

Reference

Acevedo, L., Yu, J., Erdjument-Bromage, H., Miao, R.Q., Kim, J.E., Fulton, D., Tempst, P., Strittmatter, S.M., and Sessa, W.C. (2004). A new role for Nogo as a regulator of vascular remodeling. Nat Med 10, 382-388.

Ackah, E., Yu, J., Zoellner, S., Iwakiri, Y., Skurk, C., Shibata, R., Ouchi, N., Easton, R.M., Galasso, G., and Birnbaum, M.J. (2005). Akt1/protein kinase Bα is critical for ischemic and VEGF-mediated angiogenesis. The Journal of clinical investigation 115, 2119-2127.

Astern, J.M., Pendergraft III, W.F., Falk, R.J., Jennette, J.C., Schmaier, A.H., Mahdi, F., and Preston, G.A. (2007). Myeloperoxidase interacts with endothelial cell-surface cytokeratin 1 and modulates bradykinin production by the plasma Kallikrein-Kinin system. The American journal of pathology 171, 349-360.

Bedogni, B., Warneke, J.A., Nickoloff, B.J., Giaccia, A.J., and Powell, M.B. (2008). Notch1 is an effector of Akt and hypoxia in melanoma development. J Clin Invest 118, 3660-3670.

Chen, S., Liu, Y., Rong, X., Li, Y., Zhou, J., and Lu, L. (2017). neuroprotective role of the Pi3 Kinase/akt signaling Pathway in Zebrafish. Frontiers in endocrinology 8, 21.

Chu, M., Li, T., Shen, B., Cao, X., Zhong, H., Zhang, L., Zhou, F., Ma, W., Jiang, H., Xie, P., et al. (2016). Angiopoietin receptor Tie2 is required for vein specification and maintenance via regulating COUP-TFII. Elife 5.

Ciarlo, C., Kaufman, C.K., Kinikoglu, B., Michael, J., Yang, S., Christopher, D., Blokzijl-Franke, S., den Hertog, J., Schlaeger, T.M., and Zhou, Y. (2017). A chemical screen in zebrafish embryonic cells establishes that Akt activation is required for neural crest development. Elife 6, e29145.

dela Paz, N.G., and D'Amore, P.A. (2009). Arterial versus venous endothelial cells. Cell and tissue research 335, 5-16.

Dharaneeswaran, H., Abid, M.R., Yuan, L., Dupuis, D., Beeler, D., Spokes, K.C., Janes, L., Sciuto, T., Kang, P.M., and Jaminet, S.-C.S. (2014). FOXO1-mediated activation of Akt plays a critical role in vascular homeostasis. Circulation research 115, 238-251.

Gore, A.V., Monzo, K., Cha, Y.R., Pan, W., and Weinstein, B.M. (2012). Vascular development in the zebrafish. Cold Spring Harbor perspectives in medicine 2, a006684.

Ha, J.M., Jin, S.Y., Lee, H.S., Vafaeinik, F., Jung, Y.J., Keum, H.J., Song, S.H., Lee, D.H., Kim, C.D., and Bae, S.S. (2019). Vascular leakage caused by loss of Akt1 is associated with impaired mural cell coverage. FEBS Open Bio 9, 801-813.

Herbert, S.P., Huisken, J., Kim, T.N., Feldman, M.E., Houseman, B.T., Wang, R.A., Shokat, K.M., and Stainier, D.Y. (2009a). Arterial-venous segregation by selective cell sprouting: an alternative mode of blood vessel formation. Science 326, 294-298.

Herbert, S.P., Huisken, J., Kim, T.N., Feldman, M.E., Houseman, B.T., Wang, R.A., Shokat, K.M., and Stainier, D.Y. (2009b). Arterial-venous segregation by selective cell sprouting: an alternative mode of blood vessel formation. Science 326, 294-298.

Hong, C.C., Peterson, Q.P., Hong, J.-Y., and Peterson, R.T. (2006). Artery/vein specification is governed by opposing phosphatidylinositol-3 kinase and MAP kinase/ERK signaling. Current biology 16, 1366-1372.

Isogai, S., Horiguchi, M., and Weinstein, B.M. (2001). The vascular anatomy of the developing zebrafish: an atlas of embryonic and early larval development. Developmental biology 230, 278-301.

Kasper, D.M., Moro, A., Ristori, E., Narayanan, A., Hill-Teran, G., Fleming, E., Moreno-Mateos, M., Vejnar, C.E., Zhang, J., and Lee, D. (2017). MicroRNAs establish uniform traits during the architecture of vertebrate embryos. Developmental cell 40, 552-565. e555.

Kerr, B.A., West, X.Z., Kim, Y.W., Zhao, Y., Tischenko, M., Cull, R.M., Phares, T.W., Peng, X.D., Bernier-Latmani, J., Petrova, T.V., et al. (2016). Stability and function of adult vasculature is sustained by Akt/Jagged1 signalling axis in endothelium. Nat Commun 7, 10960.

Kitamura, T., Kitamura, Y.I., Funahashi, Y., Shawber, C.J., Castrillon, D.H., Kollipara, R., DePinho, R.A., Kitajewski, J., and Accili, D. (2007). A Foxo/Notch pathway controls myogenic differentiation and fiber type specification. J Clin Invest 117, 2477-2485.

Konantz, M., Alghisi, E., Muller, J.S., Lenard, A., Esain, V., Carroll, K.J., Kanz, L., North, T.E., and Lengerke, C. (2016). Evi1 regulates Notch activation to induce zebrafish hematopoietic stem cell emergence. EMBO J 35, 2315-2331.

Lawson, N.D., Vogel, A.M., and Weinstein, B.M. (2002a). sonic hedgehog and vascular endothelial growth factor act upstream of the Notch pathway during arterial endothelial differentiation. Developmental cell 3, 127-136.

Lawson, N.D., Vogel, A.M., and Weinstein, B.M. (2002b). sonic hedgehog and vascular endothelial growth factor act upstream of the Notch pathway during arterial endothelial differentiation. Dev Cell 3, 127-136.

Lawson, N.D., and Weinstein, B.M. (2002a). Arteries and veins: making a difference with zebrafish. Nature Reviews Genetics 3, 674.
Lawson, N.D., and Weinstein, B.M. (2002b). In vivo imaging of embryonic vascular development using transgenic zebrafish. Developmental biology 248, 307-318.
Lee, M.Y., Luciano, A.K., Ackah, E., Rodriguez-Vita, J., Bancroft, T.A., Eichmann, A., Simons, M., Kyriakides, T.R., Morales-Ruiz, M., and Sessa, W.C. (2014). Endothelial Akt1 mediates angiogenesis by phosphorylating multiple angiogenic substrates. Proceedings of the National Academy of Sciences 111, 12865-12870.
Liu, L., Zhu, S., Gong, Z., and Low, B.C. (2008). K-ras/PI3K-Akt signaling is essential for zebrafish hematopoiesis and angiogenesis. PLoS One 3, e2850.
Manning, B.D., and Cantley, L.C. (2007). AKT/PKB signaling: navigating downstream. Cell 129, 1261-1274.
Moon, K.R., van Dijk, D., Wang, Z., Chen, W., Hirn, M.J., Coifman, R.R., Ivanova, N.B., Wolf, G., and Krishnaswamy, S. (2017). PHATE: a dimensionality reduction method for visualizing trajectory structures in high-dimensional biological data. bioRxiv, 120378.
Moreno-Mateos, M.A., Vejnar, C.E., Beaudoin, J.-D., Fernandez, J.P., Mis, E.K., Khokha, M.K., and Giraldez, A.J. (2015). CRISPRscan: designing highly efficient sgRNAs for CRISPR-Cas9 targeting in vivo. Nature methods 12, 982.
Pajvani, U.B., Shawber, C.J., Samuel, V.T., Birkenfeld, A.L., Shulman, G.I., Kitajewski, J., and Accili, D. (2011). Inhibition of Notch signaling ameliorates insulin resistance in a FoxO1-dependent manner. Nat Med 17, 961-967.
Phung, T.L., Ziv, K., Dabydeen, D., Eyiah-Mensah, G., Riveros, M., Perruzzi, C., Sun, J., Monahan-Earley, R.A., Shiojima, I., and Nagy, J.A. (2006). Pathological angiogenesis is induced by sustained Akt signaling and inhibited by rapamycin. Cancer cell 10, 159-170.
Quillien, A., Moore, J.C., Shin, M., Siekmann, A.F., Smith, T., Pan, L., Moens, C.B., Parsons, M.J., and Lawson, N.D. (2014). Distinct Notch signaling outputs pattern the developing arterial system. Development 141, 1544-1552.
Ramakrishnan, G., Davaakhuu, G., Chung, W.C., Zhu, H., Rana, A., Filipovic, A., Green, A.R., Atfi, A., Pannuti, A., and Miele, L. (2015). AKT and 14-3-3 regulate Notch4 nuclear localization. Scientific reports 5, 8782.
Ren, B., Deng, Y., Mukhopadhyay, A., Lanahan, A.A., Zhuang, Z.W., Moodie, K.L., Mulligan-Kehoe, M.J., Byzova, T.V., Peterson, R.T., and Simons, M. (2010). ERK1/2-Akt1 crosstalk regulates arteriogenesis in mice and zebrafish. J Clin Invest 120, 1217-1228.
Schleicher, M., Yu, J., Murata, T., Derakhshan, B., Atochin, D., Qian, L., Kashiwagi, S., Di Lorenzo, A., Harrison, K.D., and Huang, P.L. (2009). The Akt1-eNOS axis illustrates the specificity of kinase-substrate relationships in vivo. Sci Signal 2, ra41-ra41.
Shin, M., Beane, T.J., Quillien, A., Male, I., Zhu, L.J., and Lawson, N.D. (2016). Vegfa signals through ERK to promote angiogenesis, but not artery differentiation. Development 143, 3796-3805.
Sutendra, G., Dromparis, P., Wright, P., Bonnet, S., Haromy, A., Hao, Z., McMurtry, M.S., Michalak, M., Vance, J.E., Sessa, W.C., et al. (2011). The role of Nogo and the mitochondria-endoplasmic reticulum unit in pulmonary hypertension. Sci Transl Med 3, 88ra55.

Wilhelm, K., Happel, K., Eelen, G., Schoors, S., Oellerich, M.F., Lim, R., Zimmermann, B., Aspalter, I.M., Franco, C.A., and Boettger, T. (2016). FOXO1 couples metabolic activity and growth state in the vascular endothelium. Nature 529, 216.
Yang, Z.Z., Tschopp, O., Hemmings-Mieszczak, M., Feng, J., Brodbeck, D., Perentes, E., and Hemmings, B.A. (2003). Protein kinase B alpha/Akt1 regulates placental development and fetal growth. J Biol Chem 278, 32124-32131.
Yu, J., Fernandez-Hernando, C., Suarez, Y., Schleicher, M., Hao, Z., Wright, P.L., DiLorenzo, A., Kyriakides, T.R., and Sessa, W.C. (2009). Reticulon 4B (Nogo-B) is necessary for macrophage infiltration and tissue repair. Proc Natl Acad Sci U S A 106, 17511-17516.
Zhang, J., Fukuhara, S., Sako, K., Takenouchi, T., Kitani, H., Kume, T., Koh, G.Y., and Mochizuki, N. (2011a). Angiopoietin-1/Tie2 signal augments basal Notch signal controlling vascular quiescence by inducing delta-like 4 expression through AKTmediated activation of beta-catenin. J Biol Chem 286, 8055-8066.
Zhang, J., Fukuhara, S., Sako, K., Takenouchi, T., Kitani, H., Kume, T., Koh, G.Y., and Mochizuki, N. (2011b). Angiopoietin-1/Tie2 signal augments basal Notch signal controlling vascular quiescence by inducing delta-like 4 expression through AKTmediated activation of β-catenin. Journal of Biological Chemistry 286, 8055-8066.
Zhong, T.P., Childs, S., Leu, J.P., and Fishman, M.C. (2001). Gridlock signalling pathway fashions the first embryonic artery. Nature 414, 216.
Zhu, Y.-M., Wang, C.-C., Chen, L., Qian, L.-B., Ma, L.-L., Yu, J., Zhu, M.-H., Wen, C.-Y., Yu, L.-N., and Yan, M. (2013). Both PI3K/Akt and ERK1/2 pathways participate in the protection by dexmedetomidine against transient focal cerebral ischemia/reperfusion injury in rats. Brain research 1494, 1-8.

EXPERIMENTAL MODEL AND SUBJECT DETAILS

Generation of Akt loss-of-function zebrafish and zebrafish husbandry

Zebrafish were raised and maintained at 28.5˚C using standard methods (unless otherwise indicated), and according to protocols approved by Yale University Institutional Animal Care and Use Committee (# 2017-11473).

gRNA generation & injection: CRISPRScan (Moreno-Mateos et al., 2015; Vejnar et al., 2016) was used to design gRNAs to mutate the Akt 1, 2, 3a 3b loci with CRISPR/Cas9 genome editing (sequence Table S1). The gRNA template for in vitro transcription was PCR amplified and purified with Qiaquick PCR purification Kit (Qiagen). In vitro transcription followed and was performed as described (Narayanan et al., 2016). F0 *Tg(flt:YFP; kdrl: mCherry)*^{hu4881s916}embryos injected with 100 pg of gRNA and 200 pg of Cas9 mRNA at the one-cell stage were used to confirm mutagenesis via T7 endonuclease I (T7E1) assay and sequencing as described (Narayanan et al., 2016) or were analyzed in phenotypic assays. Genomic DNA was isolated from a clutch of injected embryos with 100

mM sodium hydroxide and 1M pH 7.5 Tris-HCl and then amplified regions including the mutation site using PCR. After 3 months, the F0 founder fish was genotyped using fragment analysis (DNA analysis Facility Yale University) and out-crossed with WT (sequence Table S1). F1 allele were identified, genome PCR product were cloned into TOPO vector with the TOPO TA cloning kit (Invitrogen) for sequencing. The sequencing results showed that the mutant alleles carried the following out loss of function mutation: Akt1 ^{ya348} (-1 based pair deletion), Akt2 ^{ya349} (+10 based pair insertion), Akt3a ^{ya350} (-21 based pair deletion) and Akt3b ^{ya351} (-4 based pair deletion), which are labeled as homozygous *akt1*$^{\Delta/\Delta}$, *akt2*$^{\Delta/\Delta}$, *akt3a*$^{\Delta/\Delta}$ and *akt3b*$^{\Delta/\Delta}$ in the paper. The mixed *akt*$^{\Delta/\Delta}$ in this study were generated from the in-cross of akt1, akt3a, akt3b homozygous and akt2 heterozygous mutant.

For DNA injection, embryos were injected in the one-cell with 25 pg of the expression construct Tol2-Fli1a-NICD-v2a-cherry and Tol2 transposase mRNA, and later selected for mCherry expression.

METHOD DETAILS

Single cell RNA sequencing

WT and Akt loss-of function zebrafish embryos were collected at 24 hpf, dechorionated and placed in 2 ml tubes with egg water. Embryos were disassociated into single cell suspensions and subjected to Fluorescence Activated Cell Sorting (FACS) as described for transgenic zebrafish previously (Ristori and Nicoli, 2015),

Tg(flt:YFP; kdrl: mCherry)^{hu4881s916}endothelial cells were FAC-sorted into 0.04% BSA in PBS and the captured endothelial cell fraction was loaded onto the 10X Genomics Chromium instrument for a targeted recovery of 10,000 cells per sample. The reaction was then reverse transcribed and barcoded using the 10X Genomics Chromium Next GEM Single Cell 3' Library Construction Kit v2.1 according to manufacturer instructions.

The barcoded libraries were sequenced on Illumina HiSeq 4000 instrument. The reads were de-multiplexed using 10X Genomics provided version of program bcl2fastq. These fastq files were further processed with cellranger and indexed custom genome for *D. rerio* with sequences for mCherry. The output of cellranger program was processed using the package Seurat (Satija et al., 2015; Stuart et al., 2019) in R (Team, 2019). Briefly, the data was filtered such that all the cells that had less than unique transcripts detected or had more than 10% of the transcripts coming from mitochondrial genes were eliminated, as were the genes that were seen in less than 3 cells. Filtered data was then normalized and scaled

using sctransform (Hafemeister and Satija, 2019). The data was further clustered in Seurat, and then rendered as a PHATE plot (Moon et al., 2019).

Quantitative RT-PCR

Embryos were processed whole or disassociated into single cell suspensions and subjected to FACS as described above for zebrafish scRNA-seq. 300 ng RNA was mixed with iScript Reaction mix and reverse Transcriptase (Bio-Rad) to generate cDNA with a 20 ul reaction (Kasper et al., 2017). qRT-PCR primers are listed in Table S1.

The $2^{-\Delta CT}$ or $2^{-\Delta\Delta CT}$ method was used to determine relative gene expression for quantitative RT-PCR analyses as indicated. mRNA levels were normalized to the beta actin housekeeping gene, *actb1* and was relative to the indicated control. Statistical comparisons between replicate pair DCT values for indicated groups were determined by a paired, two-tailed Student's t-test.

Western Blot

Protein extraction was performed as following: 10-20 WT and Akt loss-of function zebrafish embryos (4 days post fertilization) were placed in 1.5 ml tubes and 1x PBS. Embryos were pipetted with 20 ul tip to break the zebrafish tissues and centrifuged at 1300 rpm for 10 minutes. After removing the supernatant, pellets were re-suspended in the lysis buffer with 2 ul per embryo. The lysates were left on ice for 15 minutes, mixed for 15 seconds and span at 12000 rpm for 10 minutes at 4 C. The supernatant was transferred to new cold tubes, sonicated for 6 seconds and protein concentration measured using DC Protein Assay (Bio-rad). Samples were mixed with 6x protein buffer and boiled for 5 minutes. About 20 ug protein samples were added into 10% SDS–polyacrylamide gel electrophoresis (SDS-PAGE) well and run at 80 V for 20 minutes and 100 V for about 1 hour. Then the SDS-PAGE was transferred to 0.45-μm nitrocellulose membranes (Bio-Rad) at 100 V for 2 hours. The nitrocellulose membranes were by 5% Bovine serum albumin (BSA) blocking buffer for 1 hour, incubated with primary antibody at $4^{o}C$ overnight, washed with TBST (Tris-buffered saline, 0.1% Tween 20) for 5 minutes 3 times, incubated with and washed with TBST for 5 minutes 3 times. Blots were visualized by Li-COR Odyssey and analyzed by the Image Studio software (Li-COR).

Lysis buffer included 50 mM Tris-HCl, 1% NP-40 (v/v), 0.1% SDS, 0.1% Deoxycholic acid, 0.1 mM EDTA, 0.1 mM EGTA and 8 mg NaF, 4 mg sodium pyrophosphate, 20 mg Complete Protease Inhibitors (Roche), 3 mg Pefabloc SC AEBSF (Roche), 0.25 mM Sodium orthovanadate and 50 mM β- glycerolphosphate in 10 ml lysis buffer. Protein

buffer contains 70 ml Tris-HCl, 36 ml glycerol, 10 g SDS, 6 ml 2-Methylbutane, 40 mg bromphenol-blue and water to 120 ml. Primary antibodies (1:1000) were monoclonal rabbit phospho-Akt T308 (cell signaling #2965), monoclonal mouse pan-Akt (cell signaling #2920) and monoclonal mouse anti-actin (Sigma-Aldrich). Secondary antibodies (1:10,000) were goat anti-rabbit Alexa Fluor 680 (Invitrogen), goat anti-mouse Alexa Fluor 680 (Invitrogen) and goat anti-mouse 800 (Rockland).

Whole mount in situ hybridization.

Whole mount in situ hybridization (WISH) was performed using hybridization probes previously described (Kasper et al., 2017). Images of at least 6-12 stained embryos per replicate were blinded and quantified as follows. Briefly, images were converted to 8-bit and processed with FFT bandpass filter, filtering large structures to 200 pixels. Region(s) of interest were identified via thresholding and staining area or cluster number was measured using Analyze Particles. Area measurements or cluster counts from biological replicates per genotype were combined and an unpaired, two-tailed Mann-Whitney U test was applied to detect statistical differences between conditions.

Immunofluorescence

WT and Akt loss-of-function embryos (24 hpf) were fixed and washed with the same condition as performed in WISH. After permeabilization with 0.125% Trypsin in PBS on ice for 20 minutes, samples were washed with PBST for 5 minutes 3 times and blocked at 4^{o}C for 3-4 hours. Primary antibodies were monoclonal rabbit phospho-Erk (cell signaling #4695) (1:100), chicken polyclonal anti-GFP (1:300) (Abcam) and rabbit polyclonal RFP antibody (antibodies online) (1:300) were mixed with samples overnight. Samples were washed 6 times 45 minutes each and incubated with secondary antibodies (invitrogen) (1:300) goat anti-rat Alexa Fluor 594, goat anti-chicken Alexa Fluor 488 and goat anti-rabbit Alexa Fluor 633 overnight and washed with PBSTw 6 times each 45 minutes. Embryos were imaged with Lecia SP8 microscope.

TUNEL assay

30-40 WT and Akt loss-of-function zebrafish were placed in 1.5 ml tubes and fixed with 4% PFA at 4 ^{o}C overnight. Samples were washed with PBS for 3 times, placed in MeOH at -20 C overnight and washed with 75% MeOH/PBST, 50% MeOH/PBST, 25% MeOH/PBST and PBST for 5 minutes respectively. After treatment with 10 ug/ml proteinase K at room temperature for 1.5 minutes, samples were washed with PBST twice

and re-fixed in 4% PFA at room temperature for 20 minutes. Samples were washed with PBST for 5 minutes 5 times and incubated with pre-chilled Ethanol:Acetic Acid (2:1) at -20 ^{o}C for 10 minutes. Followed with 3 times wash of PBST for 5 minutes each, samples were incubated at room temperature in 75 ul equilibration buffer for 1 hour (ApopTag Red *in situ* Apoptosis Detection kit (Millipore)). A small volume of working strength TdT (70% reaction buffer and 30% TdT with 0.3% Triton 100) was added into the reaction and incubated at 37 ^{o}C overnight. The positive control was incubated with DNAseI overnight. The negative control was without TdT. The reaction was stopped with working strength stop/wash buffer (1 ml concentrated buffer with 34 ml dH_2O) for 3-4 hours at 37 ^{o}C. After wash with PBST 3 times for 5 minutes, samples were blocked with 2 mg/ml BSA, 5% sheep serum in PBST for 1 hour at room temperature and incubated in dark for 45-60 minutes at room temperature with working strength rhodamine antibody solution. After 30 minutes wash with PBST for 4 times, samples were incubated for 15 minutes with DAPI (1:200) in PBST and washed 3 times with PBST.

Chemical treatments

10 hpf zebrafish embryos were treated with 0.025 mM and 0.1 mM FOXO1 inhibitor (AS1842856, Millipore Sigma), 1 mM Sugen 5416 (SU5416, Sigma-Aldrich), 80 mM PI3K inhibitor (LY-294,002, Sigma-Aldrich) . At 24 hpf treated embryos were fixed an processed for immunofluorescence or whole mount in situ hybridization.

Image Acquisition

Zebrafish embryos imaged by confocal or bright-field microscopy were raised in 0.003% 1-phenyl-2-thiourea (PTU) starting after the gastrulation stage to prevent pigmentation. Embryos imaged live by confocal microscopy were anesthetized in 0.1% tricaine and mounted in 1% low melt agarose. The majority of fluorescent images and timelapse movies were captured with an upright Leica Microsystems SP8 confocal microscope. Confocal timelapse movies were performed at room temperature starting at ~20 hpf with z-stacks acquired at an interval of 11 minutes for a total of 15 hours. Bright field images of whole mount in situ staining were acquired with a Leica Microsystems M165FC stereomicroscope equipped with Leica DFC295 camera.

QUANTIFICATION AND STATISTICAL ANALYSIS

Live fish imaging quantification

Using the software Imaris, DA, PCV and ISV were tracked manually and information of DA and PCV diameters and ISV length quantified and used for statistical analysis.

Statistical analysis

The quantification of *in situ* hybridization is followed the method of the Monteiro group (Dobrzycki et al., 2018). The difference is that I used the nonparametric t-test (Mann-Whitney test) instead of 2-tailed ANOVA test. The other quantification is also nonparametric t-test (Mann-Whitney test).

DATA AND CODE AVAILABILITY

The sc-RNA sequencing results were submitted to Gene Expression Omnibus.

References:

Dobrzycki, T., Krecsmarik, M., Bonkhofer, F., Patient, R., and Monteiro, R. (2018). An optimised pipeline for parallel image-based quantification of gene expression and genotyping after in situ hybridisation. Biology open *7*, bio031096.

Hafemeister, C., and Satija, R. (2019). Normalization and variance stabilizationof single-cell RNA-seq data using regularized negative binomial regression. BioRxiv.

Kasper, D.M., Moro, A., Ristori, E., Narayanan, A., Hill-Teran, G., Fleming, E., Moreno-Mateos, M., Vejnar, C.E., Zhang, J., Lee, D.*, et al.* (2017). MicroRNAs Establish Uniform Traits during the Architecture of Vertebrate Embryos. Dev Cell *40*, 552-565 e555.

Moon, K.R., van Dijk, D., Wang, Z., Gigante, S., Burkhardt, D.B., Chen, W.S., Yim, K., Elzen, A.V.D., Hirn, M.J., Coifman, R.R.*, et al.* (2019). Visualizing structure and transitions in high-dimensional biological data. Nat Biotechnol *37*, 1482-1492.

Moreno-Mateos, M.A., Vejnar, C.E., Beaudoin, J.D., Fernandez, J.P., Mis, E.K., Khokha, M.K., and Giraldez, A.J. (2015). CRISPRscan: designing highly efficient sgRNAs for CRISPR-Cas9 targeting in vivo. Nat Methods *12*, 982-988.

Narayanan, A., Hill-Teran, G., Moro, A., Ristori, E., Kasper, D.M., C, A.R., Lu, J., and Nicoli, S. (2016). In vivo mutagenesis of miRNA gene families using a scalable multiplexed CRISPR/Cas9 nuclease system. Sci Rep *6*, 32386.

Ristori, E., and Nicoli, S. (2015). miRNAs expression profile in zebrafish developing vessels. Methods Mol Biol *1214*, 129-150.

Satija, R., Farrell, J.A., Gennert, D., Schier, A.F., and Regev, A. (2015). Spatial reconstruction of single-cell gene expression data. Nat Biotechnol *33*, 495-502.

Stuart, T., Butler, A., Hoffman, P., Hafemeister, C., Papalexi, E., Mauck, W.M., 3rd, Hao, Y., Stoeckius, M., Smibert, P., and Satija, R. (2019). Comprehensive Integration of Single-Cell Data. Cell *177*, 1888-1902 e1821.

Team, R.C. (2019). R: A Language and Environment for Statistical Computing.

Vejnar, C.E., Moreno-Mateos, M.A., Cifuentes, D., Bazzini, A.A., and Giraldez, A.J. (2016). Optimized CRISPR-Cas9 System for Genome Editing in Zebrafish. Cold Spring Harb Protoc *2016*.

SUPPLEMENTAL INFORMATION FOR

Akt is required for artery formation during embryonic vascular development

Wenping Zhou, Emma Ristori, Liqun He, Joey Ghersi, Sameet Mehta, Rong Zhang, Christer Betsholtz, Stefania Nicoli, William C. Sessa

Correspondence: stefania.nicoli@yale.edu or willam.sessa@yale.edu

Supplemental figures:

Supplemental table:

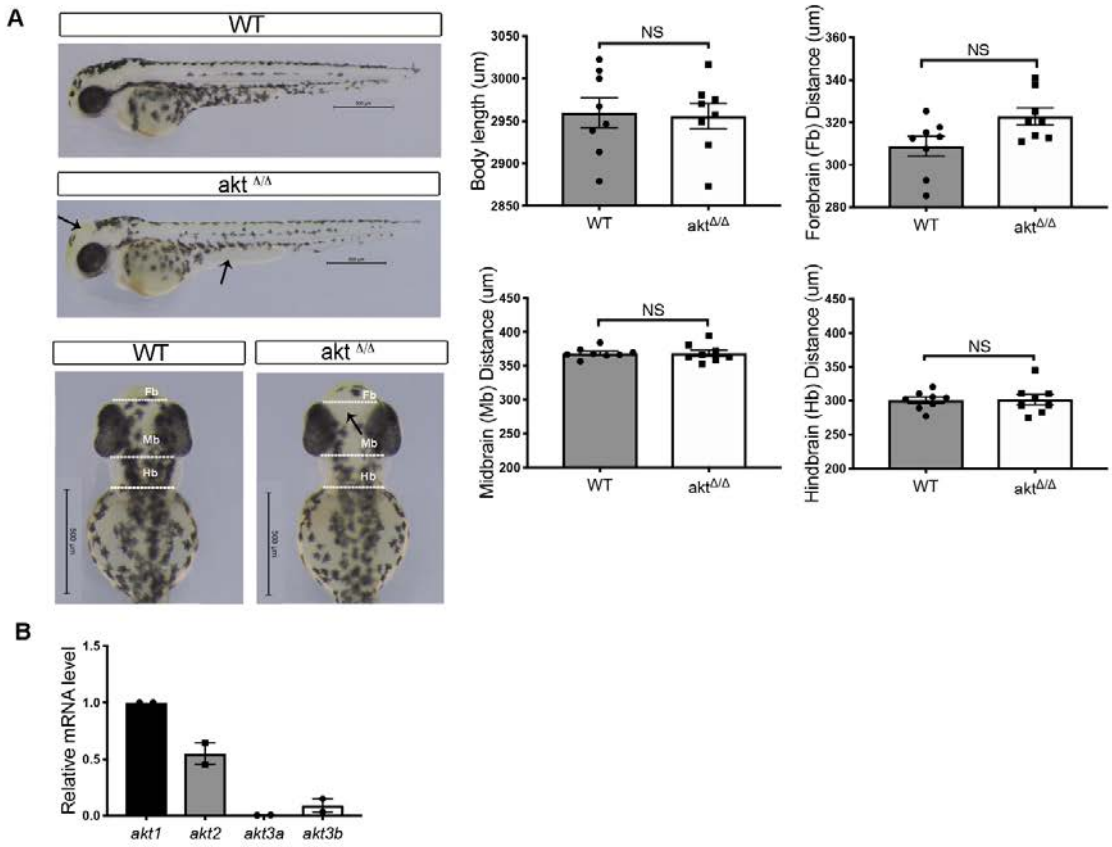

Figure. S1. ***Akt*** $^{\Delta/\Delta}$ ***embryos exhibit normal morphology.*** (A) Bright field images of the body and head morphology of WT and *akt*$^{\Delta/\Delta}$ embryos at 48 hpf and quantification on right side. Black arrows demonstrate the less pigment in the embryos. (B) *akt1, 2, 3a* and *3b* mRNA levels in endothelial cells at 24 hpf. Endothelial cells are isolated from *Tg (kdrl:mcherry)* using FACS. N= 8 embryos for A and 2 for B. Data are mean±SEM, * $p<0.05$. NS=non-significant.

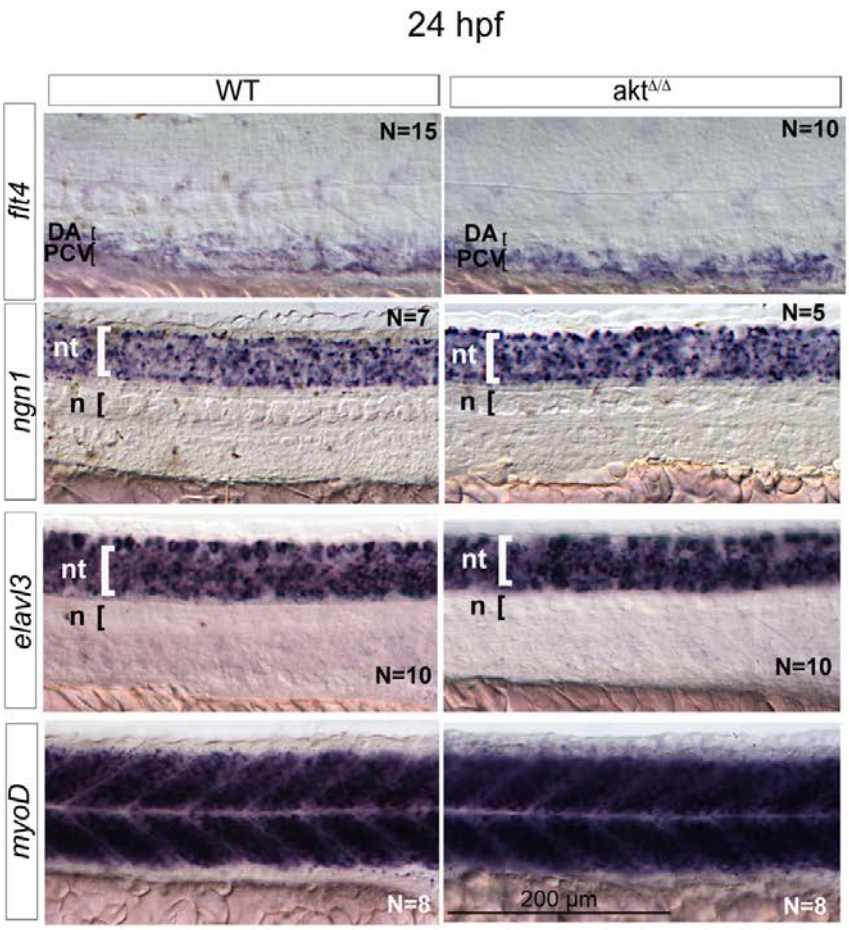

Figure. S2. *akt*$^{\Delta/\Delta}$ embryos express normal venous and non-vascular specification markers. *Whole mount situ* hybridization images show flt4 venous marker, mature neuron markers *ngn1* and *elavl3* and somite marker *myoD* in WT and *akt*$^{\Delta/\Delta}$ embryos at 24 hpf trunk. All images represent the lateral view of zebrafish embryos, head to the left. nt: neural tube, n: notochord, DA=dorsal aorta, PCV=posterior cardinal vein.

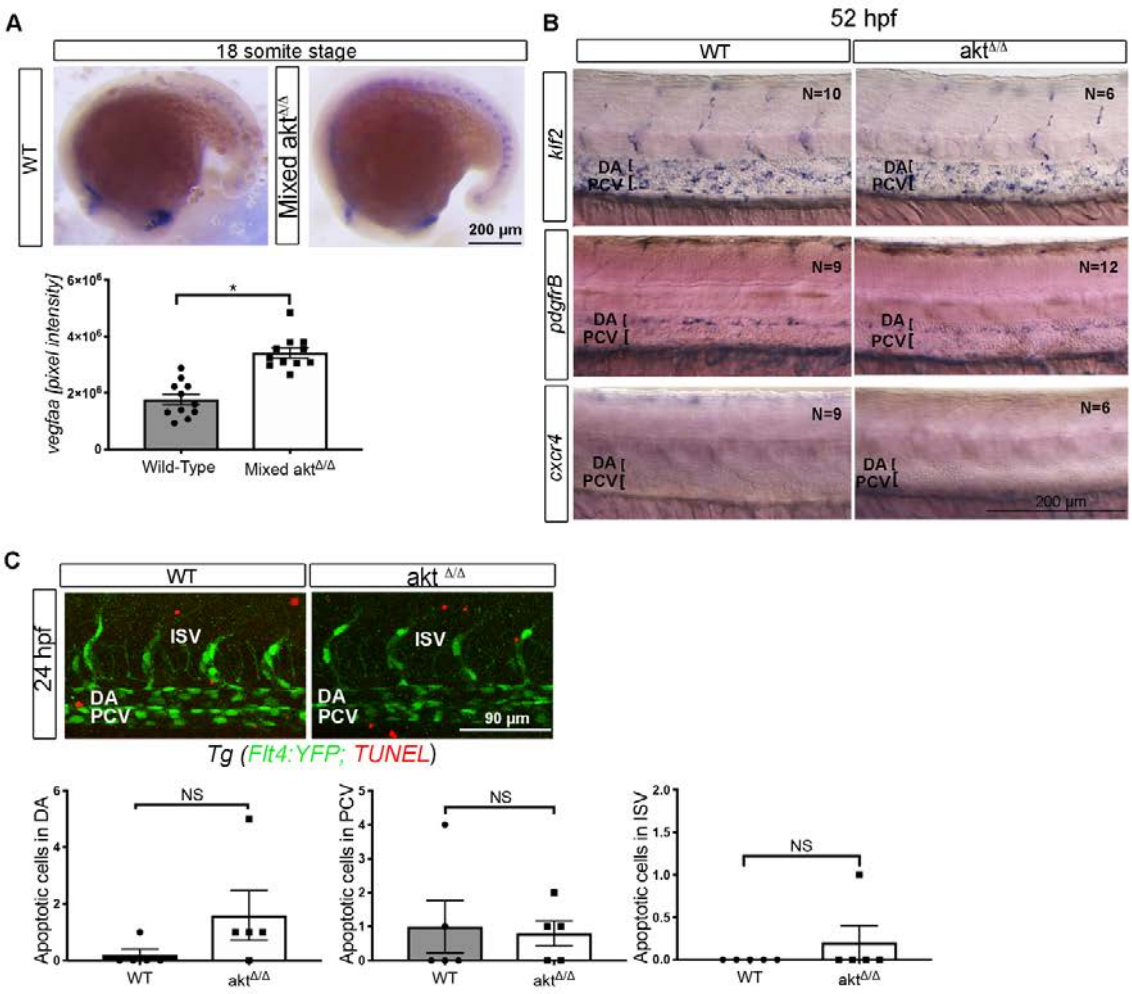

Figure. S3. Akt drives DA specification without inhibiting vegfa, flow or promoting cell death. (A) bright field images of whole mount *in situ* hybridization (WISH) showing *vefgaa* expression at 18ss and quantification. (B) WISH of flow-regulated markers (*klf2, pdgfB, cxcr4*) in WT and $akt^{\Delta/\Delta}$ embryos at 52 hpf trunk. (C) Confocal image of WT or $akt^{\Delta/\Delta}$ embryos at 24 hpf trunk with TUNEL assay labeling the apoptotic cells and quantification. All images represent the lateral view of zebrafish embryos, head to the left. Data from 5 embryos and are expressed as mean±SEM, *p<0.05 and NS=non-significant. DA=dorsal aorta, PCV=posterior cardinal vein, ISV=intersegmental vessels.

Table S1. gRNA, qPCR and genotyping primers used in the paper.

Primer name	F/R	Primer sequence (5'-3')	Assay
Akt1	F	TGCAGCGGTTAGGTGGAGGT	qPCR
	R	CTTGTCCAGGTGGTGTGATG	qPCR
Akt2	F	GATCCGCTTCCCTAGAAACC	qPCR
	R	GGTGGAACGAGCTTCTTTTG	qPCR
Akt3a	F	CAAGAGACTTGGTGGAGGTC	qPCR
	R	AGGAGAACTGGGGGAAGTGT	qPCR
Akt3b	F	CCAATAAGAGGCTCGGAGGA	qPCR
	R	CTGGCTTTCTCTCGCACCAG	qPCR
actin	F	TTCCTCCGCTTTCTCTGCAG	qPCR
	R	CCGAGCATCTCAGGGAATCC	qPCR
F-Akt1	F	AGGGCCTAAAGCTGATCCAT	genotyping
	R	CTGTGAGGCCACATTGCTAA	genotyping
F-Akt2	F	AGGAAGGGGTAGGGGTACAA	genotyping
	R	TGAGTCAAGGCACTCACCAC	genotyping
F-Akt3a	F	GGCCTGACGACTTAAGCAAA	genotyping
	R	CACTGGATTCGCTCCTCTTC	genotyping
F-Akt3b	F	GGGTCAAAAACAGGCCATAA	genotyping
	R	TGGGAGCGGTGATTAAATTG	genotyping
Akt1	F	GGGAAGGTGATTCTGGTGA	gRNA
Akt2	F	GGCATCCAGGCTGTGGCCAA	gRNA
Akt3a	F	GGCAGAGGCGATCCAGATGG	gRNA
Akt3b	F	GGCAGACAAGCTGGCCAAAC	gRNA

5. CONCLUSION

Understanding the molecular mechanisms underlying VEGF-mediated behaviours in ECs has been the central goal of this thesis.

VEGF-VEGFR signalling has a key role in development and adult physiology, and alterations of this regulatory signalling have been linked to several pathologies, including neurodegenerative and neurovascular diseases.

In adult vasculature, repression of VEGF signalling affects ECs survival, proliferation and angiogenic activity. On the contrary overexpression of VEGF signalling results in pathogenic outcomes primarily due to its effects on vascular permeability and neo-angiogenesis (neovascularization) (Plate et al., 1993; Millauer et al., 1994; Ferrara & Adamis, 2016).

In AD, studies showed that VEGF can interact with Aβ peptides, however the role of VEGF signalling is still unclear. Furthermore, the lack of efficacy of treatments targeting Aβ metabolism indicates that more effort is needed to understand the interaction of these key proteins in physiological conditions before investigating the pathological state.

In this thesis I investigated the role of the Aβ precursor APP in ECs homeostasis and its interaction with VEGF-VEGFR signalling. I found that APP is an important regulator of ECs homeostasis by indirectly modulating VEGF-VEGFR signalling. APP controls actin cytoskeleton-interacting proteins such as integrins and takes part to ECs response to extracellular stimuli, including VEGF. Future studies should investigate APP physiological regulation of VEGF signalling in *in vivo* models.

During embryonic development, VEGF is one of the key players involved in vasculogenesis and early angiogenesis (Simons et al., 2016), and loss of VEGF signalling is incompatible with life (Carmeliet et al, 1996; Ferrara et al., 2006). In this thesis I contributed to show that loss of VEGF downstream signalling PI3K/Akt causes a defective artery-vein specification in vertebrate embryos via FOXO and Notch-mediated regulation. Importantly, the genetic loss of Akt inhibits arteriovenous segregation independently from VEGFA availability. This study provides novel insights into the important role of Akt signalling in embryonic vasculogenesis.

Altogether, my thesis work contributed to shed light on the complex modulation of the VEGF signalling in embryonic development and vascular maintenance.

6. REFERENCES

Adams, R. H., & Alitalo, K. (2007). Molecular regulation of angiogenesis and lymphangiogenesis. *Nature reviews. Molecular cell biology*, *8*(6), 464–478. https://doi.org/10.1038/nrm2183

Adams, R. H., Diella, F., Hennig, S., Helmbacher, F., Deutsch, U., & Klein, R. (2001). The cytoplasmic domain of the ligand ephrinB2 is required for vascular morphogenesis but not cranial neural crest migration. *Cell*, *104*(1), 57–69. https://doi.org/10.1016/s0092-8674(01)00191-x

Aird W. C. (2007a). Phenotypic heterogeneity of the endothelium: I. Structure, function, and mechanisms. *Circulation research*, *100*(2), 158–173. https://doi.org/10.1161/01.RES.0000255691.76142.4a

Aird W. C. (2007b). Phenotypic heterogeneity of the endothelium: II. Representative vascular beds. *Circulation research*, *100*(2), 174–190. https://doi.org/10.1161/01.RES.0000255690.03436.ae

Albuquerque, R. J., Hayashi, T., Cho, W. G., Kleinman, M. E., Dridi, S., Takeda, A., Baffi, J. Z., Yamada, K., Kaneko, H., Green, M. G., Chappell, J., Wilting, J., Weich, H. A., Yamagami, S., Amano, S., Mizuki, N., Alexander, J. S., Peterson, M. L., Brekken, R. A., Hirashima, M., … Ambati, J. (2009). Alternatively spliced vascular endothelial growth factor receptor-2 is an essential endogenous inhibitor of lymphatic vessel growth. Nature medicine, 15(9), 1023–1030. https://doi.org/10.1038/nm.2018

Alitalo K. (2011). The lymphatic vasculature in disease. Nature medicine, 17(11), 1371–1380. https://doi.org/10.1038/nm.2545

Ambati, B. K., Nozaki, M., Singh, N., Takeda, A., Jani, P. D., Suthar, T., Albuquerque, R. J., Richter, E., Sakurai, E., Newcomb, M. T., Kleinman, M. E., Caldwell, R. B., Lin, Q., Ogura, Y., Orecchia, A., Samuelson, D. A., Agnew, D. W., St Leger, J., Green, W. R., Mahasreshti, P. J., … Ambati, J. (2006). Corneal avascularity is due to soluble VEGF receptor-1. *Nature*, *443*(7114), 993–997. https://doi.org/10.1038/nature05249

Ando, J., & Yamamoto, K. (2009). Vascular mechanobiology: endothelial cell responses to fluid shear stress. Circulation journal : official journal of the Japanese Circulation Society, 73(11), 1983–1992. https://doi.org/10.1253/circj.cj-09-0583

Benedito, R., Rocha, S. F., Woeste, M., Zamykal, M., Radtke, F., Casanovas, O., Duarte, A., Pytowski, B., & Adams, R. H. (2012). Notch-dependent VEGFR3 upregulation allows angiogenesis without VEGF-VEGFR2 signalling. Nature, 484(7392), 110–114. https://doi.org/10.1038/nature10908

Bhadada, S. V., Goyal, B. R., & Patel, M. M. (2011). Angiogenic targets for potential disorders. *Fundamental & clinical pharmacology*, *25*(1), 29–47. https://doi.org/10.1111/j.1472-8206.2010.00814.x

Biron, K. E., Dickstein, D. L., Gopaul, R., & Jefferies, W. A. (2011). Amyloid triggers extensive cerebral angiogenesis causing blood brain barrier permeability and hypervascularity in Alzheimer's disease. *PloS one*, *6*(8), e23789. https://doi.org/10.1371/journal.pone.0023789

Brown W. R. (2010). A review of string vessels or collapsed, empty basement membrane tubes. *Journal of Alzheimer's disease : JAD*, *21*(3), 725–739. https://doi.org/10.3233/JAD-2010-100219

Bürger, S., Noack, M., Kirazov, L. P., Kirazov, E. P., Naydenov, C. L., Kouznetsova, E., Yafai, Y., & Schliebs, R. (2009). Vascular endothelial growth factor (VEGF) affects processing of amyloid precursor protein and beta-amyloidogenesis in brain slice cultures derived from transgenic Tg2576 mouse brain. *International journal of developmental neuroscience : the official journal of the International Society for Developmental Neuroscience*, *27*(6), 517–523. https://doi.org/10.1016/j.ijdevneu.2009.06.011

Byzova, T. V., Goldman, C. K., Pampori, N., Thomas, K. A., Bett, A., Shattil, S. J., & Plow, E. F. (2000). A mechanism for modulation of cellular responses to VEGF: activation of the integrins. *Molecular cell*, *6*(4), 851–860.

Cackowski, F. C., Xu, L., Hu, B., & Cheng, S. Y. (2004). Identification of two novel alternatively spliced Neuropilin-1 isoforms. *Genomics*, *84*(1), 82–94. https://doi.org/10.1016/j.ygeno.2004.02.001

Cameron, D. J., Galvin, C., Alkam, T., Sidhu, H., Ellison, J., Luna, S., & Ethell, D. W. (2012). Alzheimer's-related peptide amyloid-β plays a conserved role in angiogenesis. *PloS one*, *7*(7), e39598. https://doi.org/10.1371/journal.pone.0039598

Canobbio, I., Abubaker, A. A., Visconte, C., Torti, M., & Pula, G. (2015). Role of amyloid peptides in vascular dysfunction and platelet dysregulation in Alzheimer's disease. *Frontiers in cellular neuroscience*, *9*, 65. https://doi.org/10.3389/fncel.2015.00065

Cantara, S., Donnini, S., Morbidelli, L., Giachetti, A., Schulz, R., Memo, M., & Ziche, M. (2004). Physiological levels of amyloid peptides stimulate the angiogenic response through FGF-2. *FASEB journal : official publication of the Federation of American Societies for Experimental Biology*, *18*(15), 1943–1945. https://doi.org/10.1096/fj.04-2114fje

Cao, X., & Südhof, T. C. (2001). A transcriptionally [correction of transcriptively] active complex of APP with Fe65 and histone acetyltransferase Tip60. *Science (New York, N.Y.)*, *293*(5527), 115–120. https://doi.org/10.1126/science.1058783

Carmeliet, P., Ferreira, V., Breier, G., Pollefeyt, S., Kieckens, L., Gertsenstein, M., Fahrig, M., Vandenhoeck, A., Harpal, K., Eberhardt, C., Declercq, C., Pawling, J., Moons, L., Collen, D., Risau, W., & Nagy, A. (1996). Abnormal blood vessel development and lethality in embryos lacking a single VEGF allele. *Nature*, *380*(6573), 435–439. https://doi.org/10.1038/380435a0

Chen, R. R., Silva, E. A., Yuen, W. W., & Mooney, D. J. (2007). Spatio-temporal VEGF and PDGF delivery patterns blood vessel formation and maturation. *Pharmaceutical research*, *24*(2), 258–264. https://doi.org/10.1007/s11095-006-9173-4

Chen, W. S., Xu, P. Z., Gottlob, K., Chen, M. L., Sokol, K., Shiyanova, T., Roninson, I., Weng, W., Suzuki, R., Tobe, K., Kadowaki, T., & Hay, N. (2001). Growth retardation and increased apoptosis in mice with homozygous disruption of the Akt1 gene. *Genes & development*, *15*(17), 2203–2208. https://doi.org/10.1101/gad.913901

Cho, S. J., Park, M. H., Han, C., Yoon, K., & Koh, Y. H. (2017). VEGFR2 alteration in Alzheimer's disease. *Scientific reports*, *7*(1), 17713. https://doi.org/10.1038/s41598-017-18042-1

Cifuentes, D., Poittevin, M., Dere, E., Broquères-You, D., Bonnin, P., Benessiano, J., Pocard, M., Mariani, J., Kubis, N., Merkulova-Rainon, T., & Lévy, B. I. (2015).

Hypertension accelerates the progression of Alzheimer-like pathology in a mouse model of the disease. *Hypertension (Dallas, Tex. : 1979)*, *65*(1), 218–224. https://doi.org/10.1161/HYPERTENSIONAHA.114.04139

Coon, B. G., Baeyens, N., Han, J., Budatha, M., Ross, T. D., Fang, J. S., Yun, S., Thomas, J. L., & Schwartz, M. A. (2015). Intramembrane binding of VE-cadherin to VEGFR2 and VEGFR3 assembles the endothelial mechanosensory complex. *The Journal of cell biology*, *208*(7), 975–986. https://doi.org/10.1083/jcb.201408103

Coronel, R., Bernabeu-Zornoza, A., Palmer, C., Muñiz-Moreno, M., Zambrano, A., Cano, E., & Liste, I. (2018). Role of Amyloid Precursor Protein (APP) and Its Derivatives in the Biology and Cell Fate Specification of Neural Stem Cells. *Molecular neurobiology*, *55*(9), 7107–7117. https://doi.org/10.1007/s12035-018-0914-2

Corti, F., Wang, Y., Rhodes, J. M., Atri, D., Archer-Hartmann, S., Zhang, J., Zhuang, Z. W., Chen, D., Wang, T., Wang, Z., Azadi, P., & Simons, M. (2019). N-terminal syndecan-2 domain selectively enhances 6-O heparan sulfate chains sulfation and promotes $VEGFA_{165}$-dependent neovascularization. *Nature communications*, *10*(1), 1562. https://doi.org/10.1038/s41467-019-09605-z

Cudmore, M. J., Hewett, P. W., Ahmad, S., Wang, K. Q., Cai, M., Al-Ani, B., Fujisawa, T., Ma, B., Sissaoui, S., Ramma, W., Miller, M. R., Newby, D. E., Gu, Y., Barleon, B., Weich, H., & Ahmed, A. (2012). The role of heterodimerization between VEGFR-1 and VEGFR-2 in the regulation of endothelial cell homeostasis. Nature communications, 3, 972. https://doi.org/10.1038/ncomms1977

d'Uscio, L. V., He, T., Santhanam, A. V., & Katusic, Z. S. (2018). Endothelium-specific amyloid precursor protein deficiency causes endothelial dysfunction in cerebral arteries. *Journal of cerebral blood flow and metabolism : official journal of the International Society of Cerebral Blood Flow and Metabolism*, *38*(10), 1715–1726. https://doi.org/10.1177/0271678X17735418

d'Uscio, L. V., He, T., & Katusic, Z. S. (2017). Expression and Processing of Amyloid Precursor Protein in Vascular Endothelium. *Physiology (Bethesda, Md.)*, *32*(1), 20–32. https://doi.org/10.1152/physiol.00021.2016

Datta, S. R., Brunet, A., & Greenberg, M. E. (1999). Cellular survival: a play in three Akts. *Genes & development*, *13*(22), 2905–2927. https://doi.org/10.1101/gad.13.22.2905

de la Torre J. (2018). The Vascular Hypothesis of Alzheimer's Disease: A Key to Preclinical Prediction of Dementia Using Neuroimaging. *Journal of Alzheimer's disease : JAD*, *63*(1), 35–52. https://doi.org/10.3233/JAD-180004

dela Paz, N. G., Melchior, B., & Frangos, J. A. (2013). Early VEGFR2 activation in response to flow is VEGF-dependent and mediated by MMP activity. *Biochemical and biophysical research communications*, *434*(3), 641–646. https://doi.org/10.1016/j.bbrc.2013.03.134

Deng, Y., Zhang, X., & Simons, M. (2015). Molecular controls of lymphatic VEGFR3 signaling. *Arteriosclerosis, thrombosis, and vascular biology*, *35*(2), 421–429. https://doi.org/10.1161/ATVBAHA.114.304881

Deyts, C., Thinakaran, G., & Parent, A. T. (2016). APP Receptor? To Be or Not To Be. *Trends in pharmacological sciences*, *37*(5), 390–411. https://doi.org/10.1016/j.tips.2016.01.005

Dharaneeswaran, H., Abid, M. R., Yuan, L., Dupuis, D., Beeler, D., Spokes, K. C., Janes, L., Sciuto, T., Kang, P. M., Jaminet, S. S., Dvorak, A., Grant, M. A., Regan, E. R., & Aird, W. C. (2014). FOXO1-mediated activation of Akt plays a critical role in vascular homeostasis. *Circulation research*, *115*(2), 238–251. https://doi.org/10.1161/CIRCRESAHA.115.303227

Dimmeler, S., Fleming, I., Fisslthaler, B., Hermann, C., Busse, R., & Zeiher, A. M. (1999). Activation of nitric oxide synthase in endothelial cells by Akt-dependent phosphorylation. *Nature*, *399*(6736), 601–605. https://doi.org/10.1038/21224

Dixelius, J., Makinen, T., Wirzenius, M., Karkkainen, M. J., Wernstedt, C., Alitalo, K., & Claesson-Welsh, L. (2003). Ligand-induced vascular endothelial growth factor receptor-3 (VEGFR-3) heterodimerization with VEGFR-2 in primary lymphatic endothelial cells regulates tyrosine phosphorylation sites. The Journal of biological chemistry, 278(42), 40973–40979. https://doi.org/10.1074/jbc.M304499200

Donnini, S., Solito, R., Cetti, E., Corti, F., Giachetti, A., Carra, S., Beltrame, M., Cotelli, F., & Ziche, M. (2010). Abeta peptides accelerate the senescence of endothelial cells in

vitro and in vivo, impairing angiogenesis. *FASEB journal : official publication of the Federation of American Societies for Experimental Biology*, *24*(7), 2385–2395. https://doi.org/10.1096/fj.09-146456

Downward J. (1998). Mechanisms and consequences of activation of protein kinase B/Akt. *Current opinion in cell biology*, *10*(2), 262–267. https://doi.org/10.1016/s0955-0674(98)80149-x

Dumont, D. J., Jussila, L., Taipale, J., Lymboussaki, A., Mustonen, T., Pajusola, K., Breitman, M., & Alitalo, K. (1998). Cardiovascular failure in mouse embryos deficient in VEGF receptor-3. Science (New York, N.Y.), 282(5390), 946–949. https://doi.org/10.1126/science.282.5390.946

Eriksson, E. E., Karlof, E., Lundmark, K., Rotzius, P., Hedin, U., & Xie, X. (2005). Powerful inflammatory properties of large vein endothelium in vivo. *Arteriosclerosis, thrombosis, and vascular biology*, *25*(4), 723–728. https://doi.org/10.1161/01.ATV.0000157578.51417.6f

Ferrara, N., & Adamis, A. P. (2016). Ten years of anti-vascular endothelial growth factor therapy. *Nature reviews. Drug discovery*, *15*(6), 385–403. https://doi.org/10.1038/nrd.2015.17

Ferrara N. (2010). Binding to the extracellular matrix and proteolytic processing: two key mechanisms regulating vascular endothelial growth factor action. Molecular biology of the cell, 21(5), 687–690. https://doi.org/10.1091/mbc.e09-07-0590

Ferrara, N., Carver-Moore, K., Chen, H., Dowd, M., Lu, L., O'Shea, K. S., Powell-Braxton, L., Hillan, K. J., & Moore, M. W. (1996). Heterozygous embryonic lethality induced by targeted inactivation of the VEGF gene. *Nature*, *380*(6573), 439–442. https://doi.org/10.1038/380439a0

Folkman J. (1995). Angiogenesis in cancer, vascular, rheumatoid and other disease. *Nature medicine*, *1*(1), 27–31. https://doi.org/10.1038/nm0195-27

Fong, G. H., Rossant, J., Gertsenstein, M., & Breitman, M. L. (1995). Role of the Flt-1 receptor tyrosine kinase in regulating the assembly of vascular endothelium. *Nature*, *376*(6535), 66–70. https://doi.org/10.1038/376066a0

Forsberg, K., Zhang, Y., Reiners, J., Ander, M., Niedermayer, A., Fang, L., Neugebauer, H., Kassubek, J., Katona, I., Weis, J., Ludolph, A. C., Del Tredici, K., Braak, H., & Yilmazer-Hanke, D. (2018). Endothelial damage, vascular bagging and remodeling of the microvascular bed in human microangiopathy with deep white matter lesions. *Acta neuropathologica communications*, *6*(1), 128. https://doi.org/10.1186/s40478-018-0632-z

Franke, T. F., Yang, S. I., Chan, T. O., Datta, K., Kazlauskas, A., Morrison, D. K., Kaplan, D. R., & Tsichlis, P. N. (1995). The protein kinase encoded by the Akt proto-oncogene is a target of the PDGF-activated phosphatidylinositol 3-kinase. *Cell*, *81*(5), 727–736. https://doi.org/10.1016/0092-8674(95)90534-0

Fujio, Y., Guo, K., Mano, T., Mitsuuchi, Y., Testa, J. R., & Walsh, K. (1999). Cell cycle withdrawal promotes myogenic induction of Akt, a positive modulator of myocyte survival. *Molecular and cellular biology*, *19*(7), 5073–5082. https://doi.org/10.1128/mcb.19.7.5073

Fukumura, D., Gohongi, T., Kadambi, A., Izumi, Y., Ang, J., Yun, C. O., Buerk, D. G., Huang, P. L., & Jain, R. K. (2001). Predominant role of endothelial nitric oxide synthase in vascular endothelial growth factor-induced angiogenesis and vascular permeability. *Proceedings of the National Academy of Sciences of the United States of America*, *98*(5), 2604–2609. https://doi.org/10.1073/pnas.041359198

Fulton, D., Gratton, J. P., McCabe, T. J., Fontana, J., Fujio, Y., Walsh, K., Franke, T. F., Papapetropoulos, A., & Sessa, W. C. (1999). Regulation of endothelium-derived nitric oxide production by the protein kinase Akt. *Nature*, *399*(6736), 597–601. https://doi.org/10.1038/21218

Furuyama, T., Kitayama, K., Shimoda, Y., Ogawa, M., Sone, K., Yoshida-Araki, K., Hisatsune, H., Nishikawa, S., Nakayama, K., Nakayama, K., Ikeda, K., Motoyama, N., & Mori, N. (2004). Abnormal angiogenesis in Foxo1 (Fkhr)-deficient mice. *The Journal of biological chemistry*, *279*(33), 34741–34749. https://doi.org/10.1074/jbc.M314214200

Garcia, K. O., Ornellas, F. L., Martin, P. K., Patti, C. L., Mello, L. E., Frussa-Filho, R., Han, S. W., & Longo, B. M. (2014). Therapeutic effects of the transplantation of VEGF overexpressing bone marrow mesenchymal stem cells in the hippocampus of murine model of Alzheimer's disease. *Frontiers in aging neuroscience*, *6*, 30. https://doi.org/10.3389/fnagi.2014.00030

Gee, E., Milkiewicz, M., & Haas, T. L. (2010). p38 MAPK activity is stimulated by vascular endothelial growth factor receptor 2 activation and is essential for shear stress-induced angiogenesis. *Journal of cellular physiology*, *222*(1), 120–126. https://doi.org/10.1002/jcp.21924

Gerber, H. P., McMurtrey, A., Kowalski, J., Yan, M., Keyt, B. A., Dixit, V., & Ferrara, N. (1998). Vascular endothelial growth factor regulates endothelial cell survival through the phosphatidylinositol 3'-kinase/Akt signal transduction pathway. Requirement for Flk-1/KDR activation. *The Journal of biological chemistry*, *273*(46), 30336–30343. https://doi.org/10.1074/jbc.273.46.30336

Geudens, I., & Gerhardt, H. (2011). Coordinating cell behaviour during blood vessel formation. *Development (Cambridge, England)*, *138*(21), 4569–4583. https://doi.org/10.1242/dev.062323

Goede, V., Schmidt, T., Kimmina, S., Kozian, D., & Augustin, H. G. (1998). Analysis of blood vessel maturation processes during cyclic ovarian angiogenesis. *Laboratory investigation; a journal of technical methods and pathology*, *78*(11), 1385–1394.

Goldman, J., Rutkowski, J. M., Shields, J. D., Pasquier, M. C., Cui, Y., Schmökel, H. G., Willey, S., Hicklin, D. J., Pytowski, B., & Swartz, M. A. (2007). Cooperative and redundant roles of VEGFR-2 and VEGFR-3 signaling in adult lymphangiogenesis. *FASEB journal : official publication of the Federation of American Societies for Experimental Biology*, *21*(4), 1003–1012. https://doi.org/10.1096/fj.06-6656com

Gordon, E. J., Fukuhara, D., Weström, S., Padhan, N., Sjöström, E. O., van Meeteren, L., He, L., Orsenigo, F., Dejana, E., Bentley, K., Spurkland, A., & Claesson-Welsh, L. (2016). The endothelial adaptor molecule TSAd is required for VEGF-induced angiogenic sprouting through junctional c-Src activation. *Science signaling*, *9*(437), ra72. https://doi.org/10.1126/scisignal.aad9256

Gore, A. V., Monzo, K., Cha, Y. R., Pan, W., & Weinstein, B. M. (2012). Vascular development in the zebrafish. *Cold Spring Harbor perspectives in medicine*, *2*(5), a006684. https://doi.org/10.1101/cshperspect.a006684

Grünewald, F. S., Prota, A. E., Giese, A., & Ballmer-Hofer, K. (2010). Structure-function analysis of VEGF receptor activation and the role of coreceptors in angiogenic

signaling. *Biochimica et biophysica acta*, *1804*(3), 567–580. https://doi.org/10.1016/j.bbapap.2009.09.002

Habib, A., Sawmiller, D., & Tan, J. (2017). Restoring Soluble Amyloid Precursor Protein α Functions as a Potential Treatment for Alzheimer's Disease. *Journal of neuroscience research*, *95*(4), 973–991. https://doi.org/10.1002/jnr.23823

Hamid, R., Kilger, E., Willem, M., Vassallo, N., Kostka, M., Bornhövd, C., Reichert, A. S., Kretzschmar, H. A., Haass, C., & Herms, J. (2007). Amyloid precursor protein intracellular domain modulates cellular calcium homeostasis and ATP content. *Journal of neurochemistry*, *102*(4), 1264–1275. https://doi.org/10.1111/j.1471-4159.2007.04627.x

Han, J., Calvo, C. F., Kang, T. H., Baker, K. L., Park, J. H., Parras, C., Levittas, M., Birba, U., Pibouin-Fragner, L., Fragner, P., Bilguvar, K., Duman, R. S., Nurmi, H., Alitalo, K., Eichmann, A. C., & Thomas, J. L. (2015). Vascular endothelial growth factor receptor 3 controls neural stem cell activation in mice and humans. Cell reports, 10(7), 1158–1172. https://doi.org/10.1016/j.celrep.2015.01.049

Harper, S. J., & Bates, D. O. (2008). VEGF-A splicing: the key to anti-angiogenic therapeutics?. *Nature reviews. Cancer*, *8*(11), 880–887. https://doi.org/10.1038/nrc2505

Hemmings B. A. (1997). Akt signaling: linking membrane events to life and death decisions. *Science (New York, N.Y.)*, *275*(5300), 628–630. https://doi.org/10.1126/science.275.5300.628

Herbert, S. P., Huisken, J., Kim, T. N., Feldman, M. E., Houseman, B. T., Wang, R. A., Shokat, K. M., & Stainier, D. Y. (2009). Arterial-venous segregation by selective cell sprouting: an alternative mode of blood vessel formation. *Science (New York, N.Y.)*, *326*(5950), 294–298. https://doi.org/10.1126/science.1178577

Holmqvist, K., Cross, M., Riley, D., & Welsh, M. (2003). The Shb adaptor protein causes Src-dependent cell spreading and activation of focal adhesion kinase in murine brain endothelial cells. *Cellular signalling*, *15*(2), 171–179. https://doi.org/10.1016/s0898-6568(02)00076-1

Hosaka, T., Biggs, W. H., 3rd, Tieu, D., Boyer, A. D., Varki, N. M., Cavenee, W. K., & Arden, K. C. (2004). Disruption of forkhead transcription factor (FOXO) family members in mice reveals their functional diversification. *Proceedings of the National Academy of*

Sciences of the United States of America, *101*(9), 2975–2980. https://doi.org/10.1073/pnas.0400093101

Jakobsson, L., Kreuger, J., Holmborn, K., Lundin, L., Eriksson, I., Kjellén, L., & Claesson-Welsh, L. (2006). Heparan sulfate in trans potentiates VEGFR-mediated angiogenesis. *Developmental cell*, *10*(5), 625–634. https://doi.org/10.1016/j.devcel.2006.03.009

Jiang, S., Li, Y., Zhang, X., Bu, G., Xu, H., & Zhang, Y. W. (2014). Trafficking regulation of proteins in Alzheimer's disease. *Molecular neurodegeneration*, *9*, 6. https://doi.org/10.1186/1750-1326-9-6

Jin, F., Hagemann, N., Brockmeier, U., Schäfer, S. T., Zechariah, A., & Hermann, D. M. (2013). LDL attenuates VEGF-induced angiogenesis via mechanisms involving VEGFR2 internalization and degradation following endosome-trans-Golgi network trafficking. *Angiogenesis*, *16*(3), 625–637. https://doi.org/10.1007/s10456-013-9340-2

Kappas, N. C., Zeng, G., Chappell, J. C., Kearney, J. B., Hazarika, S., Kallianos, K. G., Patterson, C., Annex, B. H., & Bautch, V. L. (2008). The VEGF receptor Flt-1 spatially modulates Flk-1 signaling and blood vessel branching. *The Journal of cell biology*, *181*(5), 847–858. https://doi.org/10.1083/jcb.200709114

Kappert, K., Peters, K. G., Böhmer, F. D., & Ostman, A. (2005). Tyrosine phosphatases in vessel wall signaling. *Cardiovascular research*, *65*(3), 587–598. https://doi.org/10.1016/j.cardiores.2004.08.016

Kendall, R. L., Rutledge, R. Z., Mao, X., Tebben, A. J., Hungate, R. W., & Thomas, K. A. (1999). Vascular endothelial growth factor receptor KDR tyrosine kinase activity is increased by autophosphorylation of two activation loop tyrosine residues. *The Journal of biological chemistry*, *274*(10), 6453–6460. https://doi.org/10.1074/jbc.274.10.6453

Kerr, B. A., West, X. Z., Kim, Y. W., Zhao, Y., Tischenko, M., Cull, R. M., Phares, T. W., Peng, X. D., Bernier-Latmani, J., Petrova, T. V., Adams, R. H., Hay, N., Naga Prasad, S. V., & Byzova, T. V. (2016). Stability and function of adult vasculature is sustained by Akt/Jagged1 signalling axis in endothelium. *Nature communications*, *7*, 10960. https://doi.org/10.1038/ncomms10960

Kim, K. J., Li, B., Winer, J., Armanini, M., Gillett, N., Phillips, H. S., & Ferrara, N. (1993). Inhibition of vascular endothelial growth factor-induced angiogenesis suppresses tumour growth in vivo. *Nature*, *362*(6423), 841–844. https://doi.org/10.1038/362841a0

Kitamura, T., Asai, N., Enomoto, A., Maeda, K., Kato, T., Ishida, M., Jiang, P., Watanabe, T., Usukura, J., Kondo, T., Costantini, F., Murohara, T., & Takahashi, M. (2008). Regulation of VEGF-mediated angiogenesis by the Akt/PKB substrate Girdin. *Nature cell biology*, *10*(3), 329–337. https://doi.org/10.1038/ncb1695

Kitazume, S., Yoshihisa, A., Yamaki, T., Oikawa, M., Tachida, Y., Ogawa, K., Imamaki, R., Hagiwara, Y., Kinoshita, N., Takeishi, Y., Furukawa, K., Tomita, N., Arai, H., Iwata, N., Saido, T., Yamamoto, N., & Taniguchi, N. (2012). Soluble amyloid precursor protein 770 is released from inflamed endothelial cells and activated platelets: a novel biomarker for acute coronary syndrome. *The Journal of biological chemistry*, *287*(48), 40817–40825. https://doi.org/10.1074/jbc.M112.398578

Koch, S., Tugues, S., Li, X., Gualandi, L., & Claesson-Welsh, L. (2011). Signal transduction by vascular endothelial growth factor receptors. The Biochemical journal, 437(2), 169–183. https://doi.org/10.1042/BJ20110301

Koga, K., Osuga, Y., Yoshino, O., Hirota, Y., Ruimeng, X., Hirata, T., Takeda, S., Yano, T., Tsutsumi, O., & Taketani, Y. (2003). Elevated serum soluble vascular endothelial growth factor receptor 1 (sVEGFR-1) levels in women with preeclampsia. *The Journal of clinical endocrinology and metabolism*, *88*(5), 2348–2351. https://doi.org/10.1210/jc.2002-021942

Kopan, R., & Ilagan, M. X. (2004). Gamma-secretase: proteasome of the membrane?. *Nature reviews. Molecular cell biology*, *5*(6), 499–504. https://doi.org/10.1038/nrm1406

Lamalice, L., Houle, F., & Huot, J. (2006). Phosphorylation of Tyr1214 within VEGFR-2 triggers the recruitment of Nck and activation of Fyn leading to SAPK2/p38 activation and endothelial cell migration in response to VEGF. The Journal of biological chemistry, 281(45), 34009–34020. https://doi.org/10.1074/jbc.M603928200

Lamoke, F., Mazzone, V., Persichini, T., Maraschi, A., Harris, M. B., Venema, R. C., Colasanti, M., Gliozzi, M., Muscoli, C., Bartoli, M., & Mollace, V. (2015). Amyloid β

peptide-induced inhibition of endothelial nitric oxide production involves oxidative stress-mediated constitutive eNOS/HSP90 interaction and disruption of agonist-mediated Akt activation. *Journal of neuroinflammation*, *12*, 84. https://doi.org/10.1186/s12974-015-0304-x

Lanahan, A. A., Hermans, K., Claes, F., Kerley-Hamilton, J. S., Zhuang, Z. W., Giordano, F. J., Carmeliet, P., & Simons, M. (2010). VEGF receptor 2 endocytic trafficking regulates arterial morphogenesis. *Developmental cell*, *18*(5), 713–724. https://doi.org/10.1016/j.devcel.2010.02.016

Lawson, N. D., & Weinstein, B. M. (2002). In vivo imaging of embryonic vascular development using transgenic zebrafish. *Developmental biology*, *248*(2), 307–318. https://doi.org/10.1006/dbio.2002.0711

Lawson, N. D., Vogel, A. M., & Weinstein, B. M. (2002). sonic hedgehog and vascular endothelial growth factor act upstream of the Notch pathway during arterial endothelial differentiation. *Developmental cell*, *3*(1), 127–136. https://doi.org/10.1016/s1534-5807(02)00198-3

Lawson, N. D., Scheer, N., Pham, V. N., Kim, C. H., Chitnis, A. B., Campos-Ortega, J. A., & Weinstein, B. M. (2001). Notch signaling is required for arterial-venous differentiation during embryonic vascular development. *Development (Cambridge, England)*, *128*(19), 3675–3683.

Lee, M. Y., Luciano, A. K., Ackah, E., Rodriguez-Vita, J., Bancroft, T. A., Eichmann, A., Simons, M., Kyriakides, T. R., Morales-Ruiz, M., & Sessa, W. C. (2014). Endothelial Akt1 mediates angiogenesis by phosphorylating multiple angiogenic substrates. *Proceedings of the National Academy of Sciences of the United States of America*, *111*(35), 12865–12870. https://doi.org/10.1073/pnas.1408472111

Lieschke, G. J., & Currie, P. D. (2007). Animal models of human disease: zebrafish swim into view. *Nature reviews. Genetics*, *8*(5), 353–367. https://doi.org/10.1038/nrg2091

Lin, F. J., Tsai, M. J., & Tsai, S. Y. (2007). Artery and vein formation: a tug of war between different forces. *EMBO reports*, *8*(10), 920–924. https://doi.org/10.1038/sj.embor.7401076

Luna, S., Cameron, D. J., & Ethell, D. W. (2013). Amyloid-β and APP deficiencies cause severe cerebrovascular defects: important work for an old villain. *PloS one*, *8*(9), e75052. https://doi.org/10.1371/journal.pone.0075052

Mac Gabhann, F., & Popel, A. S. (2007). Dimerization of VEGF receptors and implications for signal transduction: a computational study. Biophysical chemistry, 128(2-3), 125–139. https://doi.org/10.1016/j.bpc.2007.03.010

Mahoney, E. R., Dumitrescu, L., Moore, A. M., Cambronero, F. E., De Jager, P. L., Koran, M., Petyuk, V. A., Robinson, R., Goyal, S., Schneider, J. A., Bennett, D. A., Jefferson, A. L., & Hohman, T. J. (2019). Brain expression of the vascular endothelial growth factor gene family in cognitive aging and alzheimer's disease. *Molecular psychiatry*, 10.1038/s41380-019-0458-5. Advance online publication. https://doi.org/10.1038/s41380-019-0458-5

Mäkinen, T., Veikkola, T., Mustjoki, S., Karpanen, T., Catimel, B., Nice, E. C., Wise, L., Mercer, A., Kowalski, H., Kerjaschki, D., Stacker, S. A., Achen, M. G., & Alitalo, K. (2001). Isolated lymphatic endothelial cells transduce growth, survival and migratory signals via the VEGF-C/D receptor VEGFR-3. *The EMBO journal*, *20*(17), 4762–4773. https://doi.org/10.1093/emboj/20.17.4762

Manning, B. D., & Toker, A. (2017). AKT/PKB Signaling: Navigating the Network. *Cell*, *169*(3), 381–405. https://doi.org/10.1016/j.cell.2017.04.001

Markowska, A. I., Jefferies, K. C., & Panjwani, N. (2011). Galectin-3 protein modulates cell surface expression and activation of vascular endothelial growth factor receptor 2 in human endothelial cells. *The Journal of biological chemistry*, *286*(34), 29913–29921. https://doi.org/10.1074/jbc.M111.226423

Matsumoto, T., Bohman, S., Dixelius, J., Berge, T., Dimberg, A., Magnusson, P., Wang, L., Wikner, C., Qi, J. H., Wernstedt, C., Wu, J., Bruheim, S., Mugishima, H., Mukhopadhyay, D., Spurkland, A., & Claesson-Welsh, L. (2005). VEGF receptor-2 Y951 signaling and a role for the adapter molecule TSAd in tumor angiogenesis. *The EMBO journal*, *24*(13), 2342–2353. https://doi.org/10.1038/sj.emboj.7600709

Matsumoto T, Claesson-Welsh L. VEGF receptor signal transduction. Sci STKE. 2001 Dec 11;2001(112):re21. doi: 10.1126/stke.2001.112.re21. PMID: 11741095.

McColl, B. K., Baldwin, M. E., Roufail, S., Freeman, C., Moritz, R. L., Simpson, R. J., Alitalo, K., Stacker, S. A., & Achen, M. G. (2003). Plasmin activates the lymphangiogenic growth factors VEGF-C and VEGF-D. The Journal of experimental medicine, 198(6), 863–868. https://doi.org/10.1084/jem.20030361

Millauer, B., Shawver, L. K., Plate, K. H., Risau, W., & Ullrich, A. (1994). Glioblastoma growth inhibited in vivo by a dominant-negative Flk-1 mutant. Nature, 367(6463), 576–579. https://doi.org/10.1038/367576a0

Mitola, S., Ravelli, C., Moroni, E., Salvi, V., Leali, D., Ballmer-Hofer, K., Zammataro, L., & Presta, M. (2010). Gremlin is a novel agonist of the major proangiogenic receptor VEGFR2. *Blood*, *116*(18), 3677–3680. https://doi.org/10.1182/blood-2010-06-291930

Müller, U. C., Deller, T., & Korte, M. (2017). Not just amyloid: physiological functions of the amyloid precursor protein family. *Nature reviews. Neuroscience*, *18*(5), 281–298. https://doi.org/10.1038/nrn.2017.29

Nakayama, M., Nakayama, A., van Lessen, M., Yamamoto, H., Hoffmann, S., Drexler, H. C., Itoh, N., Hirose, T., Breier, G., Vestweber, D., Cooper, J. A., Ohno, S., Kaibuchi, K., & Adams, R. H. (2013). Spatial regulation of VEGF receptor endocytosis in angiogenesis. *Nature cell biology*, *15*(3), 249–260. https://doi.org/10.1038/ncb2679

Nannelli, G., Terzuoli, E., Giorgio, V., Donnini, S., Lupetti, P., Giachetti, A., Bernardi, P., & Ziche, M. (2018). ALDH2 Activity Reduces Mitochondrial Oxygen Reserve Capacity in Endothelial Cells and Induces Senescence Properties. *Oxidative medicine and cellular longevity*, *2018*, 9765027. https://doi.org/10.1155/2018/9765027

Nhan, H. S., Chiang, K., & Koo, E. H. (2015). The multifaceted nature of amyloid precursor protein and its proteolytic fragments: friends and foes. *Acta neuropathologica*, *129*(1), 1–19. https://doi.org/10.1007/s00401-014-1347-2

Nicolas, M., & Hassan, B. A. (2014). Amyloid precursor protein and neural development. *Development (Cambridge, England)*, *141*(13), 2543–2548. https://doi.org/10.1242/dev.108712

Nilsson, I., Bahram, F., Li, X., Gualandi, L., Koch, S., Jarvius, M., Söderberg, O., Anisimov, A., Kholová, I., Pytowski, B., Baldwin, M., Ylä-Herttuala, S., Alitalo, K., Kreuger, J., & Claesson-Welsh, L. (2010). VEGF receptor 2/-3 heterodimers detected in

situ by proximity ligation on angiogenic sprouts. *The EMBO journal*, *29*(8), 1377–1388. https://doi.org/10.1038/emboj.2010.30

O'Brien, R. J., & Wong, P. C. (2011). Amyloid precursor protein processing and Alzheimer's disease. *Annual review of neuroscience*, *34*, 185–204. https://doi.org/10.1146/annurev-neuro-061010-113613

Ogawa, S., Oku, A., Sawano, A., Yamaguchi, S., Yazaki, Y., & Shibuya, M. (1998). A novel type of vascular endothelial growth factor, VEGF-E (NZ-7 VEGF), preferentially utilizes KDR/Flk-1 receptor and carries a potent mitotic activity without heparin-binding domain. *The Journal of biological chemistry*, *273*(47), 31273–31282. https://doi.org/10.1074/jbc.273.47.31273

Orlandini, M., Spreafico, A., Bardelli, M., Rocchigiani, M., Salameh, A., Nucciotti, S., Capperucci, C., Frediani, B., & Oliviero, S. (2006). Vascular endothelial growth factor-D activates VEGFR-3 expressed in osteoblasts inducing their differentiation. The Journal of biological chemistry, 281(26), 17961–17967. https://doi.org/10.1074/jbc.M600413200

Ott, M. O., & Bullock, S. L. (2001). A gene trap insertion reveals that amyloid precursor protein expression is a very early event in murine embryogenesis. *Development genes and evolution*, *211*(7), 355–357. https://doi.org/10.1007/s004270100158

Paris, D., Quadros, A., Patel, N., DelleDonne, A., Humphrey, J., & Mullan, M. (2005). Inhibition of angiogenesis and tumor growth by beta and gamma-secretase inhibitors. *European journal of pharmacology*, *514*(1), 1–15. https://doi.org/10.1016/j.ejphar.2005.02.050

Park, M., & Lee, S. T. (1999). The fourth immunoglobulin-like loop in the extracellular domain of FLT-1, a VEGF receptor, includes a major heparin-binding site. Biochemical and biophysical research communications, 264(3), 730–734. https://doi.org/10.1006/bbrc.1999.1580

Patel, N. S., Mathura, V. S., Bachmeier, C., Beaulieu-Abdelahad, D., Laporte, V., Weeks, O., Mullan, M., & Paris, D. (2010). Alzheimer's beta-amyloid peptide blocks vascular endothelial growth factor mediated signaling via direct interaction with VEGFR-2. *Journal of neurochemistry*, *112*(1), 66–76. https://doi.org/10.1111/j.1471-4159.2009.06426.x

Perez, R. G., Zheng, H., Van der Ploeg, L. H., & Koo, E. H. (1997). The beta-amyloid precursor protein of Alzheimer's disease enhances neuron viability and modulates neuronal polarity. *The Journal of neuroscience : the official journal of the Society for Neuroscience*, *17*(24), 9407–9414. https://doi.org/10.1523/JNEUROSCI.17-24-09407.1997

Plate, K. H., Breier, G., Millauer, B., Ullrich, A., & Risau, W. (1993). Up-regulation of vascular endothelial growth factor and its cognate receptors in a rat glioma model of tumor angiogenesis. Cancer research, 53(23), 5822–5827.

Potente, M., & Mäkinen, T. (2017). Vascular heterogeneity and specialization in development and disease. Nature reviews. Molecular cell biology, 18(8), 477–494. https://doi.org/10.1038/nrm.2017.36

Potente, M., Gerhardt, H., & Carmeliet, P. (2011). Basic and therapeutic aspects of angiogenesis. *Cell*, *146*(6), 873–887. https://doi.org/10.1016/j.cell.2011.08.039

Rapraeger, A. C., Ell, B. J., Roy, M., Li, X., Morrison, O. R., Thomas, G. M., & Beauvais, D. M. (2013). Vascular endothelial-cadherin stimulates syndecan-1-coupled insulin-like growth factor-1 receptor and cross-talk between αVβ3 integrin and vascular endothelial growth factor receptor 2 at the onset of endothelial cell dissemination during angiogenesis. *The FEBS journal*, *280*(10), 2194–2206. https://doi.org/10.1111/febs.12134

Reinhard, C., Borgers, M., David, G., & De Strooper, B. (2013). Soluble amyloid-β precursor protein binds its cell surface receptor in a cooperative fashion with glypican and syndecan proteoglycans. *Journal of cell science*, *126*(Pt 21), 4856–4861. https://doi.org/10.1242/jcs.137919

Ristori, E., Donnini, S., & Ziche, M. (2020). New Insights Into Blood-Brain Barrier Maintenance: The Homeostatic Role of β-Amyloid Precursor Protein in Cerebral Vasculature. *Frontiers in physiology*, *11*, 1056. https://doi.org/10.3389/fphys.2020.01056

Ruan, G. X., & Kazlauskas, A. (2013). Lactate engages receptor tyrosine kinases Axl, Tie2, and vascular endothelial growth factor receptor 2 to activate phosphoinositide 3-kinase/Akt and promote angiogenesis. *The Journal of biological chemistry*, *288*(29), 21161–21172. https://doi.org/10.1074/jbc.M113.474619

Ruhrberg, C., Gerhardt, H., Golding, M., Watson, R., Ioannidou, S., Fujisawa, H., Betsholtz, C., & Shima, D. T. (2002). Spatially restricted patterning cues provided by heparin-binding VEGF-A control blood vessel branching morphogenesis. *Genes & development*, *16*(20), 2684–2698. https://doi.org/10.1101/gad.242002

Sakurai, Y., Ohgimoto, K., Kataoka, Y., Yoshida, N., & Shibuya, M. (2005). Essential role of Flk-1 (VEGF receptor 2) tyrosine residue 1173 in vasculogenesis in mice. *Proceedings of the National Academy of Sciences of the United States of America*, *102*(4), 1076–1081. https://doi.org/10.1073/pnas.0404984102

Sawamiphak, S., Seidel, S., Essmann, C. L., Wilkinson, G. A., Pitulescu, M. E., Acker, T., & Acker-Palmer, A. (2010). Ephrin-B2 regulates VEGFR2 function in developmental and tumour angiogenesis. *Nature*, *465*(7297), 487–491. https://doi.org/10.1038/nature08995

Scheid, M. P., & Woodgett, J. R. (2001). PKB/AKT: functional insights from genetic models. *Nature reviews. Molecular cell biology*, *2*(10), 760–768. https://doi.org/10.1038/35096067

Schmeisser, A., Christoph, M., Augstein, A., Marquetant, R., Kasper, M., Braun-Dullaeus, R. C., & Strasser, R. H. (2006). Apoptosis of human macrophages by Flt-4 signaling: implications for atherosclerotic plaque pathology. Cardiovascular research, 71(4), 774–784. https://doi.org/10.1016/j.cardiores.2006.06.012

Schuermann, A., Helker, C. S., & Herzog, W. (2014). Angiogenesis in zebrafish. *Seminars in cell & developmental biology*, *31*, 106–114. https://doi.org/10.1016/j.semcdb.2014.04.037

Schwartz, M. A., Vestweber, D., & Simons, M. (2018). A unifying concept in vascular health and disease. *Science (New York, N.Y.)*, *360*(6386), 270–271. https://doi.org/10.1126/science.aat3470

Selvaraj, D., Gangadharan, V., Michalski, C. W., Kurejova, M., Stösser, S., Srivastava, K., Schweizerhof, M., Waltenberger, J., Ferrara, N., Heppenstall, P., Shibuya, M., Augustin, H. G., & Kuner, R. (2015). A Functional Role for VEGFR1 Expressed in Peripheral Sensory Neurons in Cancer Pain. Cancer cell, 27(6), 780–796. https://doi.org/10.1016/j.ccell.2015.04.017

Senger, D. R., Galli, S. J., Dvorak, A. M., Perruzzi, C. A., Harvey, V. S., & Dvorak, H. F. (1983). Tumor cells secrete a vascular permeability factor that promotes accumulation of ascites fluid. *Science (New York, N.Y.)*, *219*(4587), 983–985. https://doi.org/10.1126/science.6823562

Shalaby, F., Rossant, J., Yamaguchi, T. P., Gertsenstein, M., Wu, X. F., Breitman, M. L., & Schuh, A. C. (1995). Failure of blood-island formation and vasculogenesis in Flk-1-deficient mice. Nature, 376(6535), 62–66. https://doi.org/10.1038/376062a0

Shariati, S. A., & De Strooper, B. (2013). Redundancy and divergence in the amyloid precursor protein family. *FEBS letters*, *587*(13), 2036–2045. https://doi.org/10.1016/j.febslet.2013.05.026

Shibuya M. (2013). VEGFR and type-V RTK activation and signaling. *Cold Spring Harbor perspectives in biology*, *5*(10), a009092. https://doi.org/10.1101/cshperspect.a009092

Shiojima, I., & Walsh, K. (2002). Role of Akt signaling in vascular homeostasis and angiogenesis. *Circulation research*, *90*(12), 1243–1250. https://doi.org/10.1161/01.res.0000022200.71892.9f

Siekmann, A. F., & Lawson, N. D. (2007). Notch signalling limits angiogenic cell behaviour in developing zebrafish arteries. *Nature*, *445*(7129), 781–784. https://doi.org/10.1038/nature05577

Simons, M., Gordon, E., & Claesson-Welsh, L. (2016). Mechanisms and regulation of endothelial VEGF receptor signalling. Nature reviews. Molecular cell biology, 17(10), 611–625. https://doi.org/10.1038/nrm.2016.87

Simons M. (2012). An inside view: VEGF receptor trafficking and signaling. *Physiology (Bethesda, Md.)*, *27*(4), 213–222. https://doi.org/10.1152/physiol.00016.2012

Soker, S., Takashima, S., Miao, H. Q., Neufeld, G., & Klagsbrun, M. (1998). Neuropilin-1 is expressed by endothelial and tumor cells as an isoform-specific receptor for vascular endothelial growth factor. *Cell*, *92*(6), 735–745. https://doi.org/10.1016/s0092-8674(00)81402-6

Somanath, P. R., Razorenova, O. V., Chen, J., & Byzova, T. V. (2006). Akt1 in endothelial cell and angiogenesis. *Cell cycle (Georgetown, Tex.)*, *5*(5), 512–518. https://doi.org/10.4161/cc.5.5.2538

Sosa, L. J., Cáceres, A., Dupraz, S., Oksdath, M., Quiroga, S., & Lorenzo, A. (2017). The physiological role of the amyloid precursor protein as an adhesion molecule in the developing nervous system. *Journal of neurochemistry*, *143*(1), 11–29. https://doi.org/10.1111/jnc.14122

Stakos, D. A., Stamatelopoulos, K., Bampatsias, D., Sachse, M., Zormpas, E., Vlachogiannis, N. I., Tual-Chalot, S., & Stellos, K. (2020). The Alzheimer's Disease Amyloid-Beta Hypothesis in Cardiovascular Aging and Disease: JACC Focus Seminar. *Journal of the American College of Cardiology*, *75*(8), 952–967. https://doi.org/10.1016/j.jacc.2019.12.033

Stefater, J. A., 3rd, Lewkowich, I., Rao, S., Mariggi, G., Carpenter, A. C., Burr, A. R., Fan, J., Ajima, R., Molkentin, J. D., Williams, B. O., Wills-Karp, M., Pollard, J. W., Yamaguchi, T., Ferrara, N., Gerhardt, H., & Lang, R. A. (2011). Regulation of angiogenesis by a non-canonical Wnt-Flt1 pathway in myeloid cells. Nature, 474(7352), 511–515. https://doi.org/10.1038/nature10085

Swift, M. R., & Weinstein, B. M. (2009). Arterial-venous specification during development. *Circulation research*, *104*(5), 576–588. https://doi.org/10.1161/CIRCRESAHA.108.188805

Takahashi, T., Yamaguchi, S., Chida, K., & Shibuya, M. (2001). A single autophosphorylation site on KDR/Flk-1 is essential for VEGF-A-dependent activation of PLC-gamma and DNA synthesis in vascular endothelial cells. *The EMBO journal*, *20*(11), 2768–2778. https://doi.org/10.1093/emboj/20.11.2768

Tammela, T., Zarkada, G., Nurmi, H., Jakobsson, L., Heinolainen, K., Tvorogov, D., Zheng, W., Franco, C. A., Murtomäki, A., Aranda, E., Miura, N., Ylä-Herttuala, S., Fruttiger, M., Mäkinen, T., Eichmann, A., Pollard, J. W., Gerhardt, H., & Alitalo, K. (2011). VEGFR-3 controls tip to stalk conversion at vessel fusion sites by reinforcing Notch signalling. *Nature cell biology*, *13*(10), 1202–1213. https://doi.org/10.1038/ncb2331

Tarkowski, E., Issa, R., Sjögren, M., Wallin, A., Blennow, K., Tarkowski, A., & Kumar, P. (2002). Increased intrathecal levels of the angiogenic factors VEGF and TGF-beta in Alzheimer's disease and vascular dementia. *Neurobiology of aging*, *23*(2), 237–243. https://doi.org/10.1016/s0197-4580(01)00285-8

Torres-Vázquez, J., Gitler, A. D., Fraser, S. D., Berk, J. D., Van N Pham, Fishman, M. C., Childs, S., Epstein, J. A., & Weinstein, B. M. (2004). Semaphorin-plexin signaling guides patterning of the developing vasculature. *Developmental cell*, *7*(1), 117–123. https://doi.org/10.1016/j.devcel.2004.06.008

Torres-Vázquez, J., Kamei, M., & Weinstein, B. M. (2003). Molecular distinction between arteries and veins. *Cell and tissue research*, *314*(1), 43–59. https://doi.org/10.1007/s00441-003-0771-8

Tvorogov, D., Anisimov, A., Zheng, W., Leppänen, V. M., Tammela, T., Laurinavicius, S., Holnthoner, W., Heloterä, H., Holopainen, T., Jeltsch, M., Kalkkinen, N., Lankinen, H., Ojala, P. M., & Alitalo, K. (2010). Effective suppression of vascular network formation by combination of antibodies blocking VEGFR ligand binding and receptor dimerization. *Cancer cell*, *18*(6), 630–640. https://doi.org/10.1016/j.ccr.2010.11.001

Tzima, E., Irani-Tehrani, M., Kiosses, W. B., Dejana, E., Schultz, D. A., Engelhardt, B., Cao, G., DeLisser, H., & Schwartz, M. A. (2005). A mechanosensory complex that mediates the endothelial cell response to fluid shear stress. *Nature*, *437*(7057), 426–431. https://doi.org/10.1038/nature03952

Van Nostrand, W. E., Schmaier, A. H., Neiditch, B. R., Siegel, R. S., Raschke, W. C., Sisodia, S. S., & Wagner, S. L. (1994). Expression, purification, and characterization of the Kunitz-type proteinase inhibitor domain of the amyloid beta-protein precursor-like protein-2. *Biochimica et biophysica acta*, *1209*(2), 165–170. https://doi.org/10.1016/0167-4838(94)90180-5

Vander Kooi, C. W., Jusino, M. A., Perman, B., Neau, D. B., Bellamy, H. D., & Leahy, D. J. (2007). Structural basis for ligand and heparin binding to neuropilin B domains. *Proceedings of the National Academy of Sciences of the United States of America*, *104*(15), 6152–6157. https://doi.org/10.1073/pnas.0700043104

Villa, N., Walker, L., Lindsell, C. E., Gasson, J., Iruela-Arispe, M. L., & Weinmaster, G. (2001). Vascular expression of Notch pathway receptors and ligands is restricted to arterial vessels. *Mechanisms of development*, *108*(1-2), 161–164. https://doi.org/10.1016/s0925-4773(01)00469-5

Wang, Y., Nakayama, M., Pitulescu, M. E., Schmidt, T. S., Bochenek, M. L., Sakakibara, A., Adams, S., Davy, A., Deutsch, U., Lüthi, U., Barberis, A., Benjamin, L. E., Mäkinen, T., Nobes, C. D., & Adams, R. H. (2010). Ephrin-B2 controls VEGF-induced angiogenesis and lymphangiogenesis. *Nature*, *465*(7297), 483–486. https://doi.org/10.1038/nature09002

Wang, Q., Somwar, R., Bilan, P. J., Liu, Z., Jin, J., Woodgett, J. R., & Klip, A. (1999). Protein kinase B/Akt participates in GLUT4 translocation by insulin in L6 myoblasts. *Molecular and cellular biology*, *19*(6), 4008–4018. https://doi.org/10.1128/mcb.19.6.4008

West, X. Z., Meller, N., Malinin, N. L., Deshmukh, L., Meller, J., Mahabeleshwar, G. H., Weber, M. E., Kerr, B. A., Vinogradova, O., & Byzova, T. V. (2012). Integrin β3 crosstalk with VEGFR accommodating tyrosine phosphorylation as a regulatory switch. *PloS one*, *7*(2), e31071. https://doi.org/10.1371/journal.pone.0031071

Wietecha, M. S., Cerny, W. L., & DiPietro, L. A. (2013). Mechanisms of vessel regression: toward an understanding of the resolution of angiogenesis. *Current topics in microbiology and immunology*, *367*, 3–32. https://doi.org/10.1007/82_2012_287

Wythe, J. D., Dang, L. T., Devine, W. P., Boudreau, E., Artap, S. T., He, D., Schachterle, W., Stainier, D. Y., Oettgen, P., Black, B. L., Bruneau, B. G., & Fish, J. E. (2013). ETS factors regulate Vegf-dependent arterial specification. *Developmental cell*, *26*(1), 45–58. https://doi.org/10.1016/j.devcel.2013.06.007

Xu, D., Young, J., Song, D., & Esko, J. D. (2011). Heparan sulfate is essential for high mobility group protein 1 (HMGB1) signaling by the receptor for advanced glycation end products (RAGE). The Journal of biological chemistry, 286(48), 41736–41744. https://doi.org/10.1074/jbc.M111.299685

Xu, Y., Yuan, L., Mak, J., Pardanaud, L., Caunt, M., Kasman, I., Larrivée, B., Del Toro, R., Suchting, S., Medvinsky, A., Silva, J., Yang, J., Thomas, J. L., Koch, A. W., Alitalo, K., Eichmann, A., & Bagri, A. (2010). Neuropilin-2 mediates VEGF-C-induced lymphatic

sprouting together with VEGFR3. *The Journal of cell biology*, *188*(1), 115–130. https://doi.org/10.1083/jcb.200903137

Yamazaki, Y., Tokunaga, Y., Takani, K., & Morita, T. (2005). C-terminal heparin-binding peptide of snake venom VEGF specifically blocks VEGF-stimulated endothelial cell proliferation. *Pathophysiology of haemostasis and thrombosis*, *34*(4-5), 197–199. https://doi.org/10.1159/000092423

Yao, R., & Cooper, G. M. (1995). Requirement for phosphatidylinositol-3 kinase in the prevention of apoptosis by nerve growth factor. *Science (New York, N.Y.)*, *267*(5206), 2003–2006. https://doi.org/10.1126/science.7701324

You, L. R., Lin, F. J., Lee, C. T., DeMayo, F. J., Tsai, M. J., & Tsai, S. Y. (2005). Suppression of Notch signalling by the COUP-TFII transcription factor regulates vein identity. *Nature*, *435*(7038), 98–104. https://doi.org/10.1038/nature03511

Zhu, X., & Zhou, W. (2015). The Emerging Regulation of VEGFR-2 in Triple-Negative Breast Cancer. *Frontiers in endocrinology*, *6*, 159. https://doi.org/10.3389/fendo.2015.00159